

Multi-Messenger Data Analysis - Part II

Markus Ahlers
Niels Bohr Institute, Copenhagen

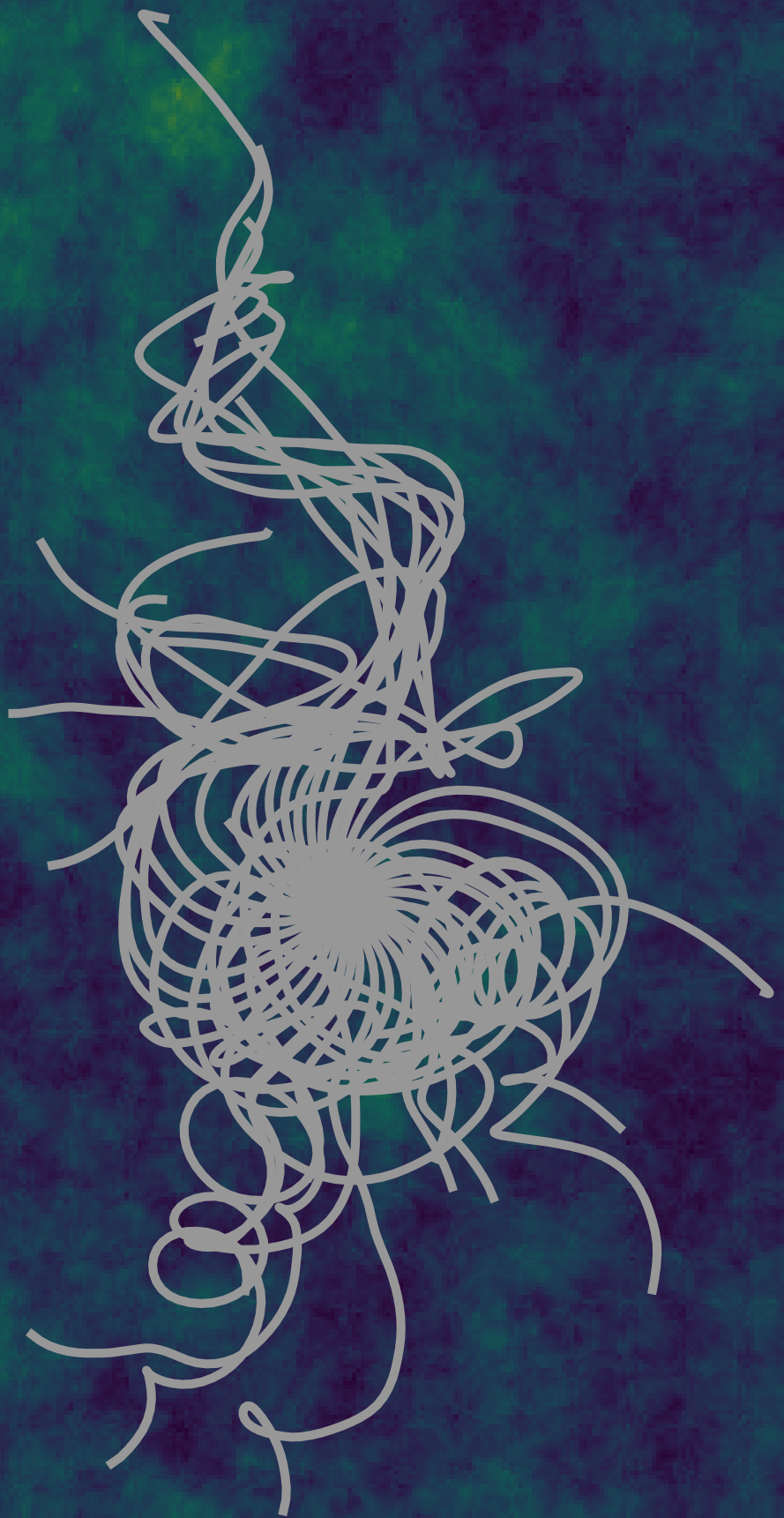
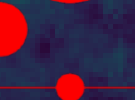
KSETA Topical Course

Karlsruhe, March 9, 2023

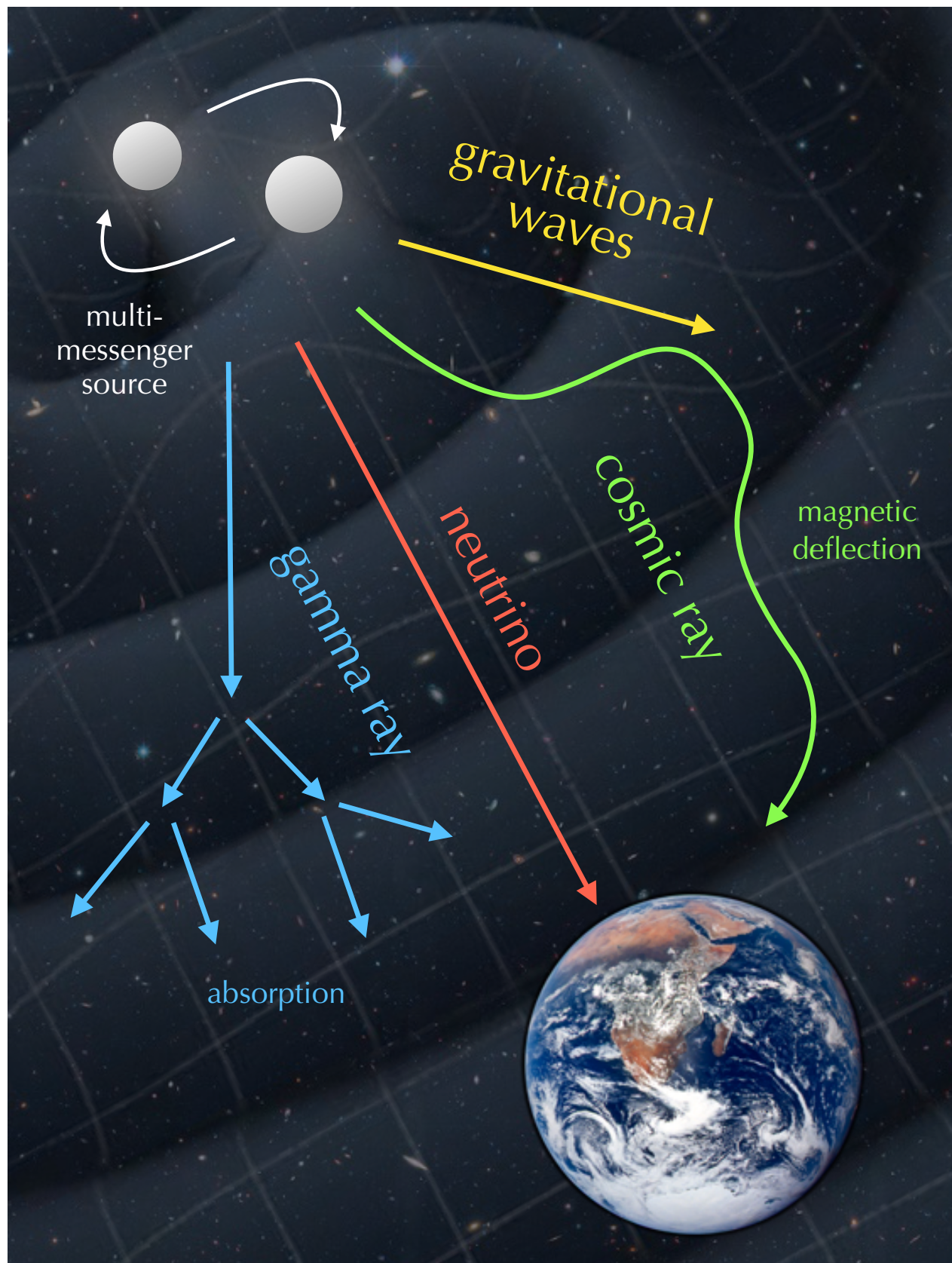
VILLUM FONDEN



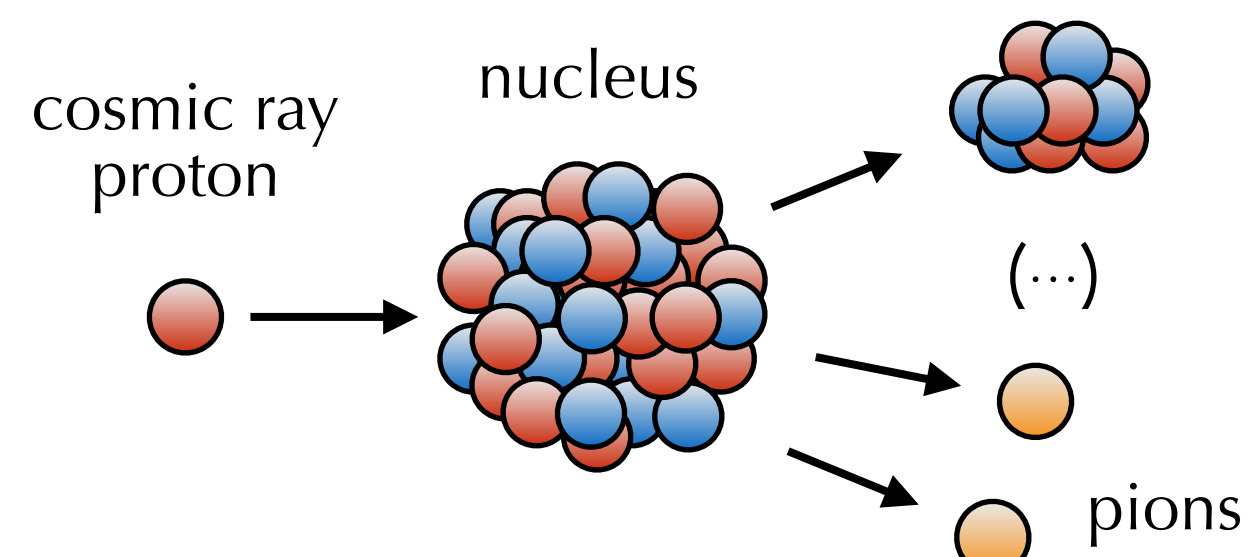
KØBENHAVNS
UNIVERSITET



Multi-Messenger Paradigm



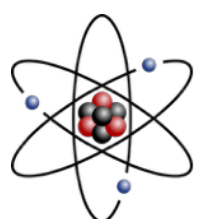
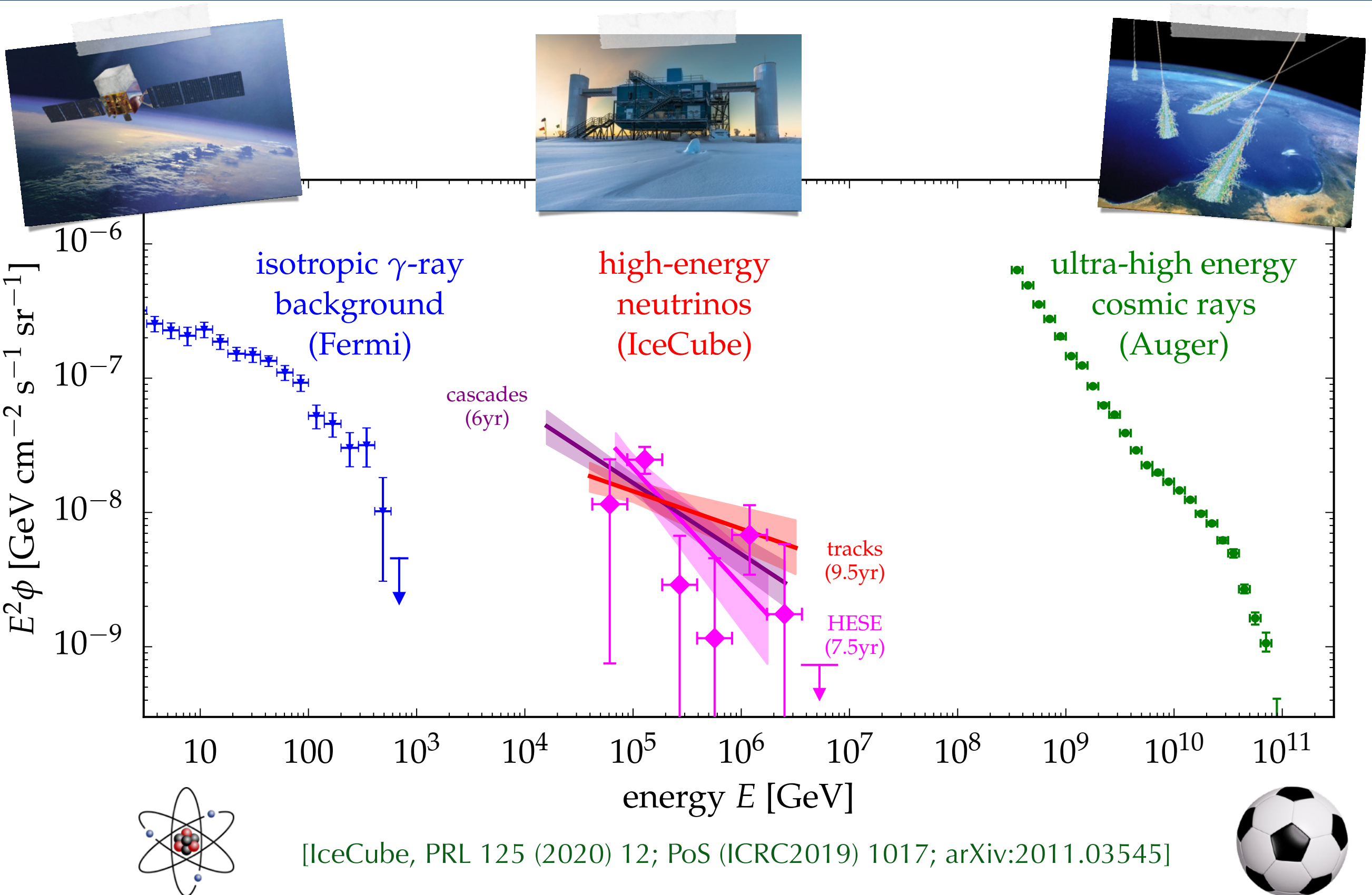
Acceleration of **cosmic rays** - especially in the aftermath of cataclysmic events, sometimes visible in **gravitational waves**.



Secondary **neutrinos** and **gamma-rays** from pion decays:

$$\begin{aligned}\pi^+ &\rightarrow \mu^+ + \nu_\mu & \pi^0 &\rightarrow \gamma + \gamma \\ && \downarrow & e^+ + \nu_e + \bar{\nu}_\mu\end{aligned}$$

Diffuse TeV-PeV Neutrinos



Point Source vs. Diffuse Flux

Populations of extragalactic neutrino sources can be visible

individual sources

or by the

combined isotropic emission.

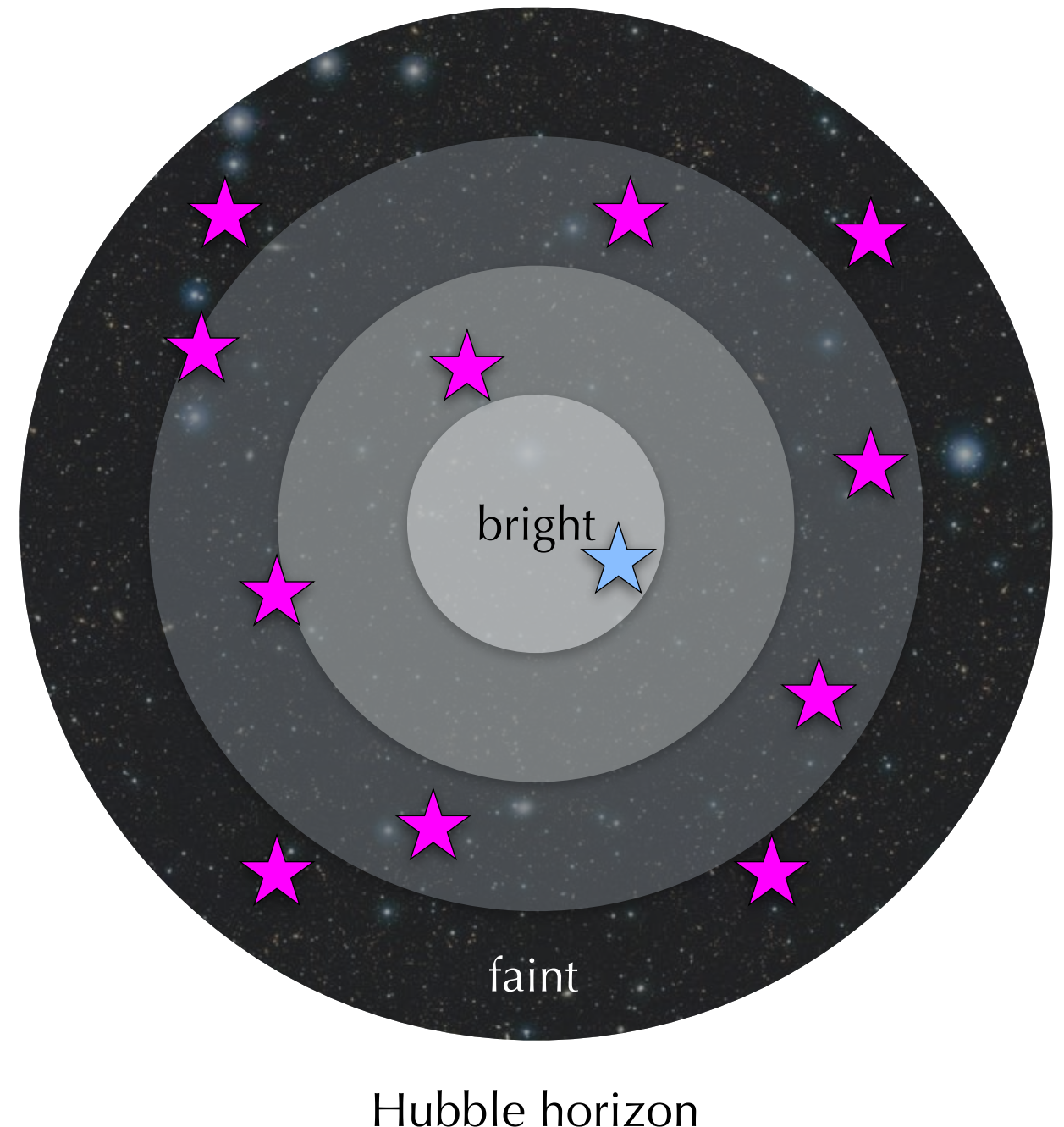
The relative contribution can
be parametrized (*to first order*)
by the average

local source density

and

source luminosity.

“Observable Universe”
with far (faint) and near (bright) sources.

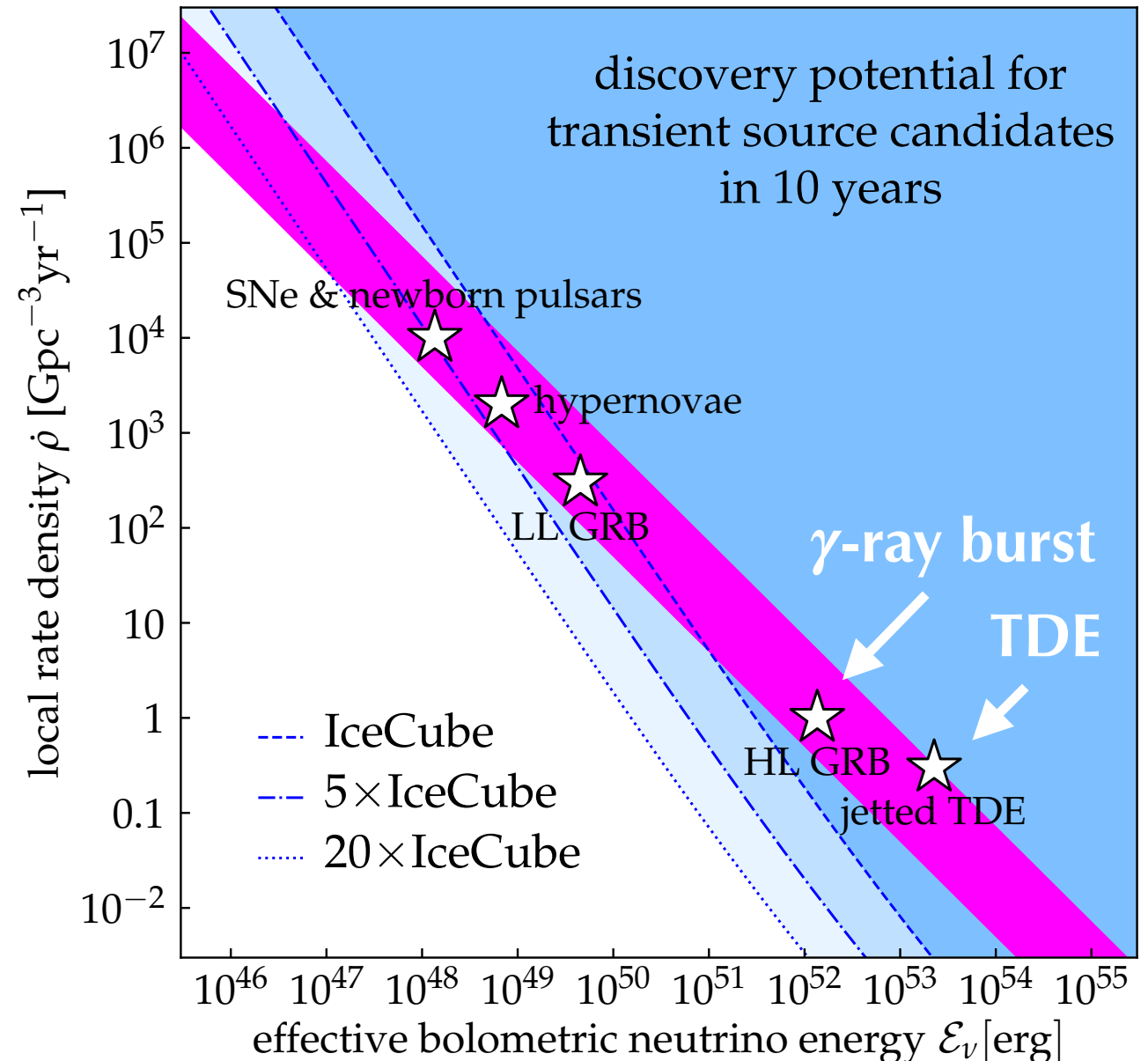
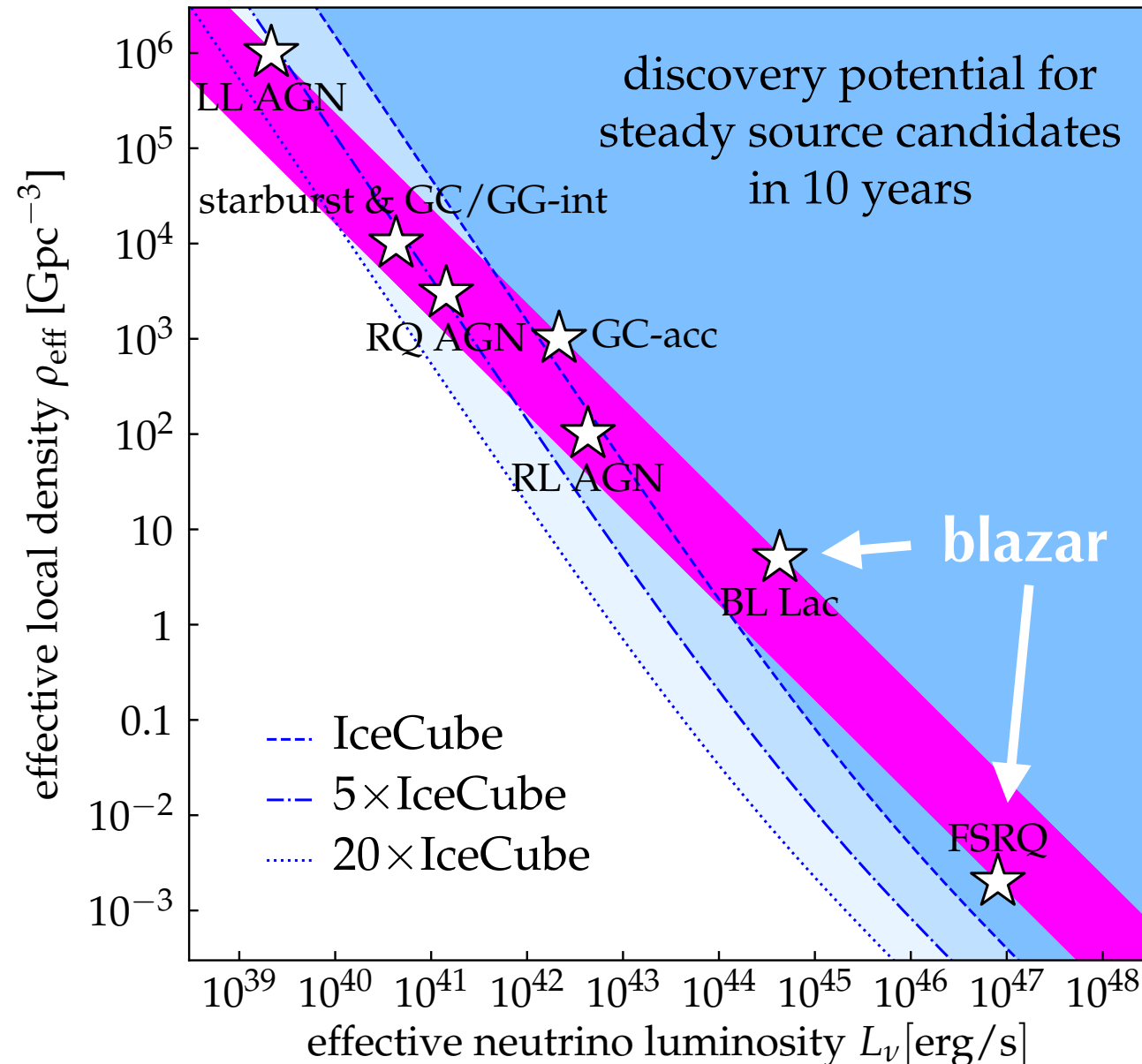


Point Source vs. Diffuse Flux

Neutrino sources are hiding in plain sight.



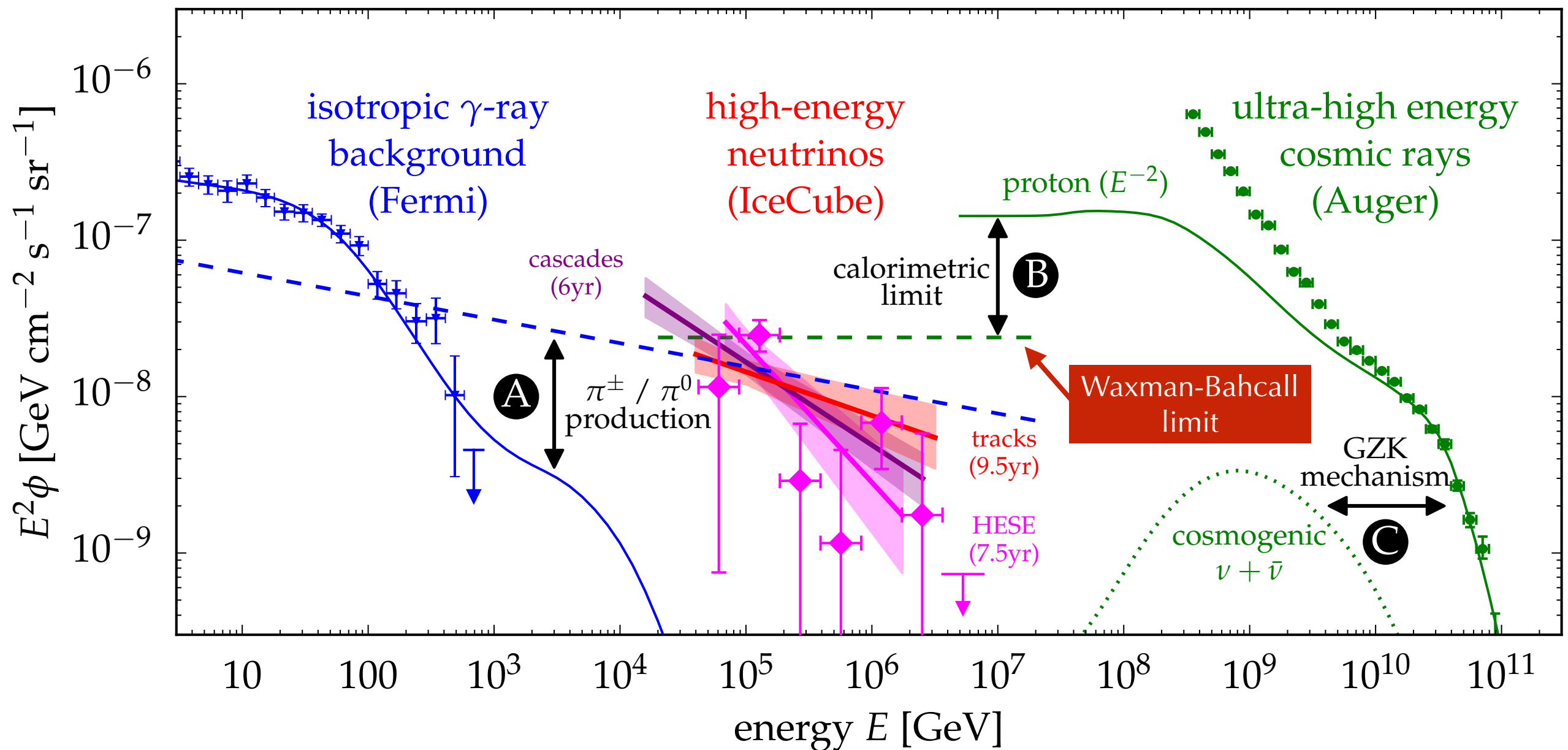
Point Source vs. Diffuse Flux



[Murase & Waxman'16; Ackermann *et al.*'19]

Rare sources, like blazars or gamma-ray bursts, can not be the dominant sources of TeV-PeV neutrino emission (magenta band).

Multi-Messenger Interfaces



The high intensity of the neutrino flux compared to that of γ -rays and cosmic rays offers many interesting multi-messenger interfaces.

Waxman-Bahcall Limit

- UHE CR **proton emission rate density**: [e.g. MA & Halzen'12]

$$[E_p^2 Q_p(E_p)]_{10^{19.5}\text{eV}} \simeq 8 \times 10^{43} \text{erg Mpc}^{-3} \text{yr}^{-1}$$

- Neutrino flux can be estimated as (ξ_z : redshift evolution factor) :

$$E_\nu^2 \phi_\nu(E_\nu) \simeq f_\pi \underbrace{\frac{\xi_z K_\pi}{1 + K_\pi}}_{\mathcal{O}(1)} \underbrace{1.5 \times 10^{-8} \text{GeV cm}^{-2} \text{s}^{-1} \text{sr}^{-1}}_{\text{IceCube diffuse level}}$$

- Limited by **pion production efficiency**: $f_\pi \lesssim 1$ [Waxman & Bahcall'98]

- Similar UHE **nucleon emission rate density** (local minimum at $\Gamma \simeq 2.04$) :

$$[E_N^2 Q_N(E_N)]_{10^{19.5}\text{eV}} \simeq 2.2 \times 10^{43} \text{erg Mpc}^{-3} \text{yr}^{-1}$$

[Auger'16; see also Jiang, Zhang & Murase'20]

- **Competition** between pion production efficiency (*dense target*) and CR acceleration efficiency (*thin target*).

UHE CR-Neutrino Correlations?

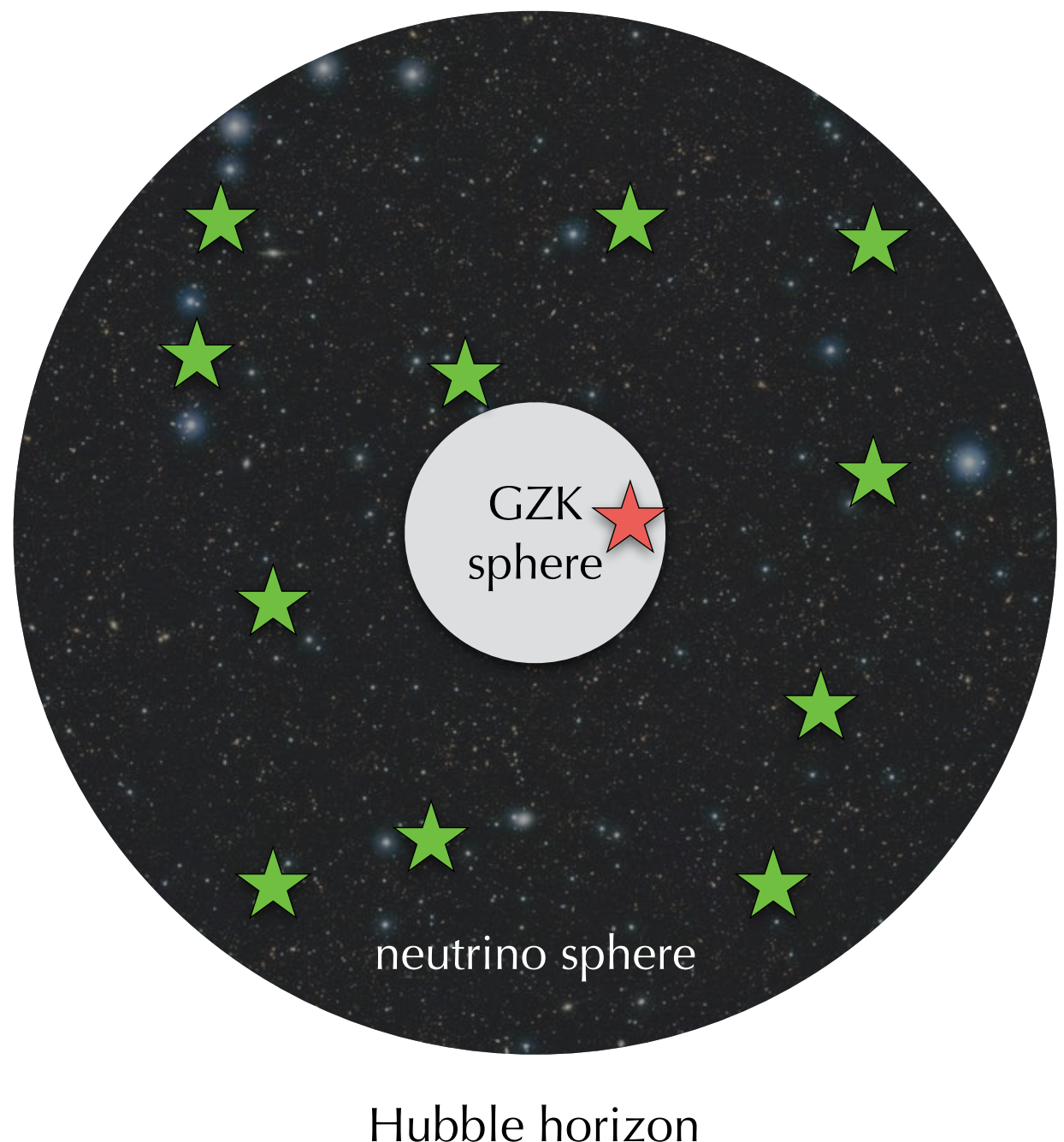
- Unified source models are tested by joint neutrino & CR analyses by **ANTARES, Auger, IceCube & TA**.

[PoS (ICRC2019) 842]

- So far, no significant correlations have been identified.
- Principal challenge:*** Only 5% of observed TeV-PeV neutrinos are expected to correlate with UHE CRs.

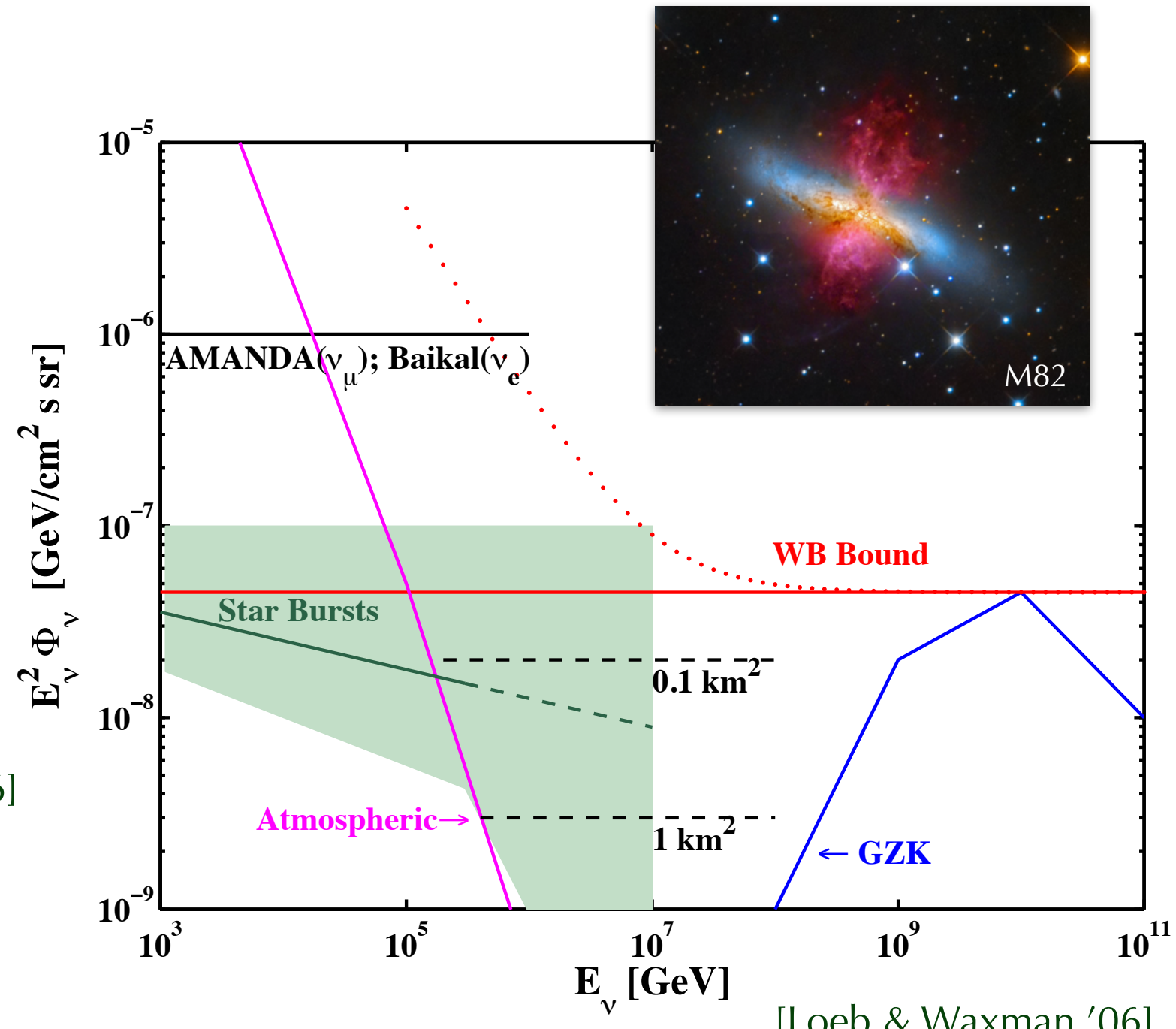
$$\frac{\lambda_{\text{GZK}}}{\lambda_{\text{Hubble}}} \sim 5 \%$$

“Observable Universe”
in **neutrinos** and **UHE CRs**



Starburst Galaxies

- High rate of **star formation** and SN explosions enhances (UHE) CR production.
- Low-energy cosmic rays remain magnetically confined and eventually collide in **dense environment**.
- In time, efficient **conversion of CR energy density into γ -rays and neutrinos**. [Loeb & Waxman '06]
- Power-law neutrino spectra with high-energy softening from CR leakage and/or acceleration.

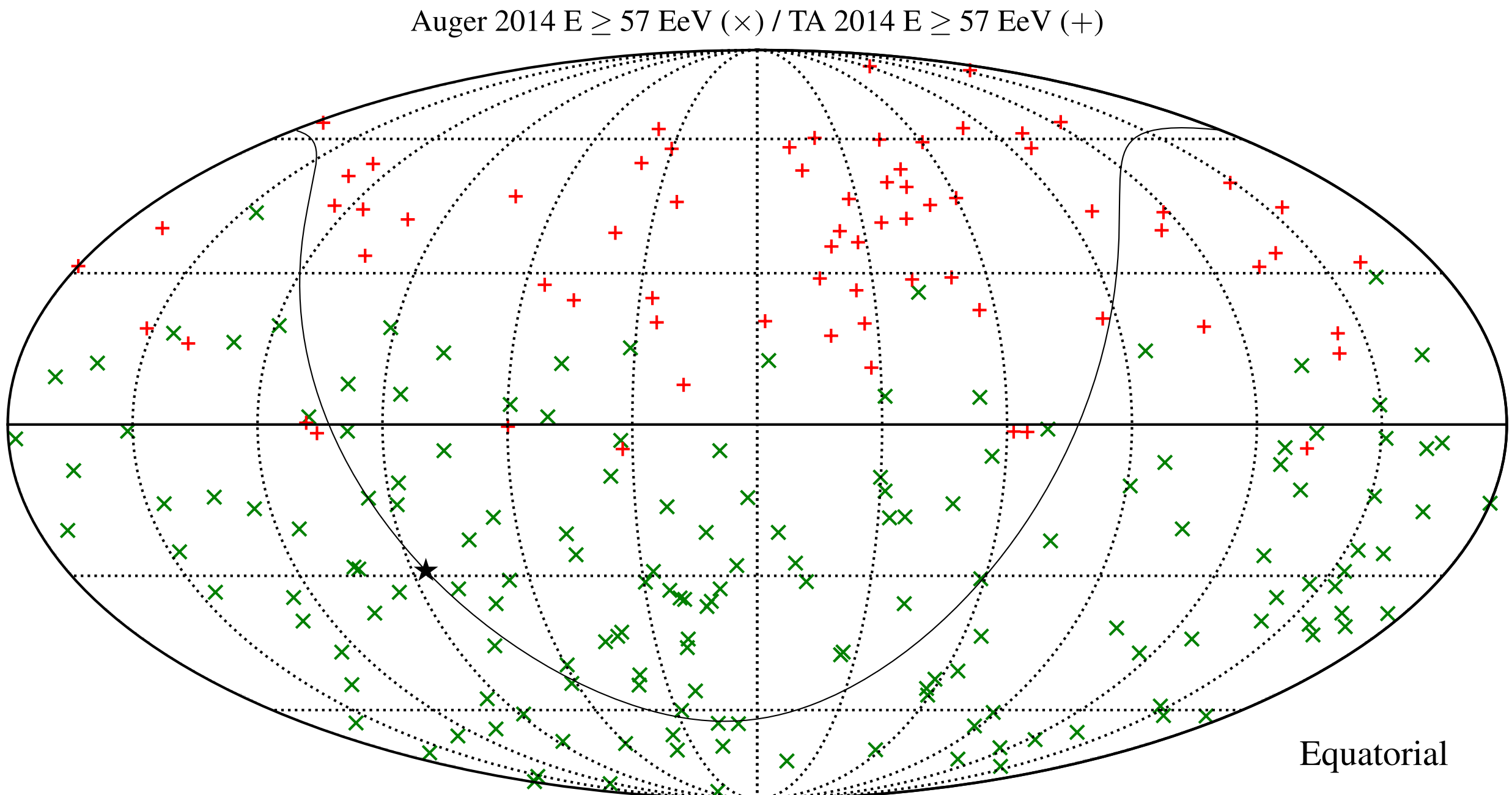


[Romero & Torres'03; Liu, Wang, Inoue, Crocker & Aharonian'14; Tamborra, Ando & Murase'14]

[Palladino, Fedynitch, Rasmussen & Taylor'19; Peretti, Blasi, Aharonian, Morlino & Cristofari'19]

[Ambrosone, Chianese, Fiorillo, Marinelli, Miele & Pisanti'20]

Example : UHE CRs



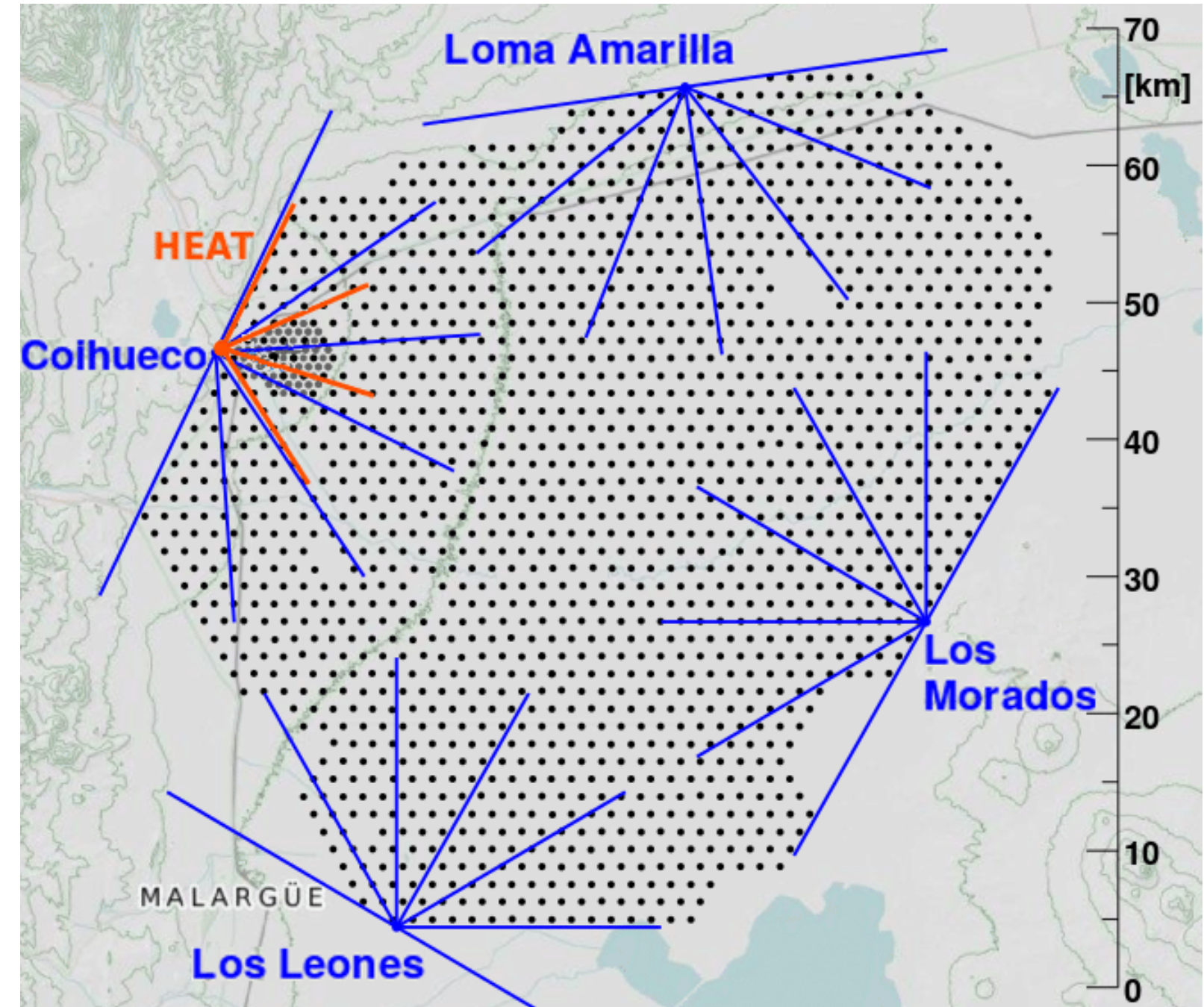
Ultra-High Energy (UHE) Cosmic Rays (CRs) observed
by Pierre Auger Observatory and Telescope Array

Example : Auger Observatory

fluorescence detector

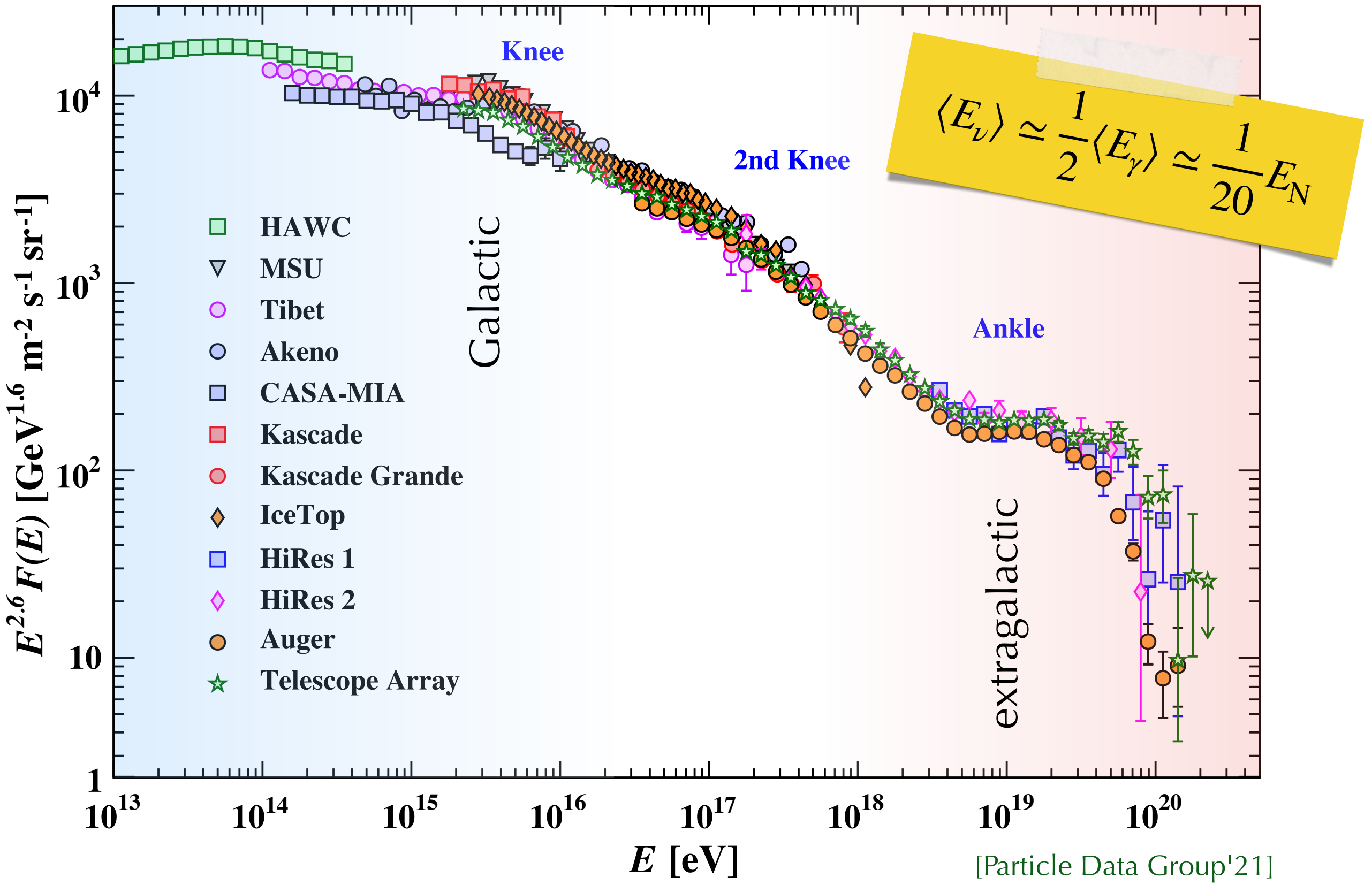


water Cherenkov detector



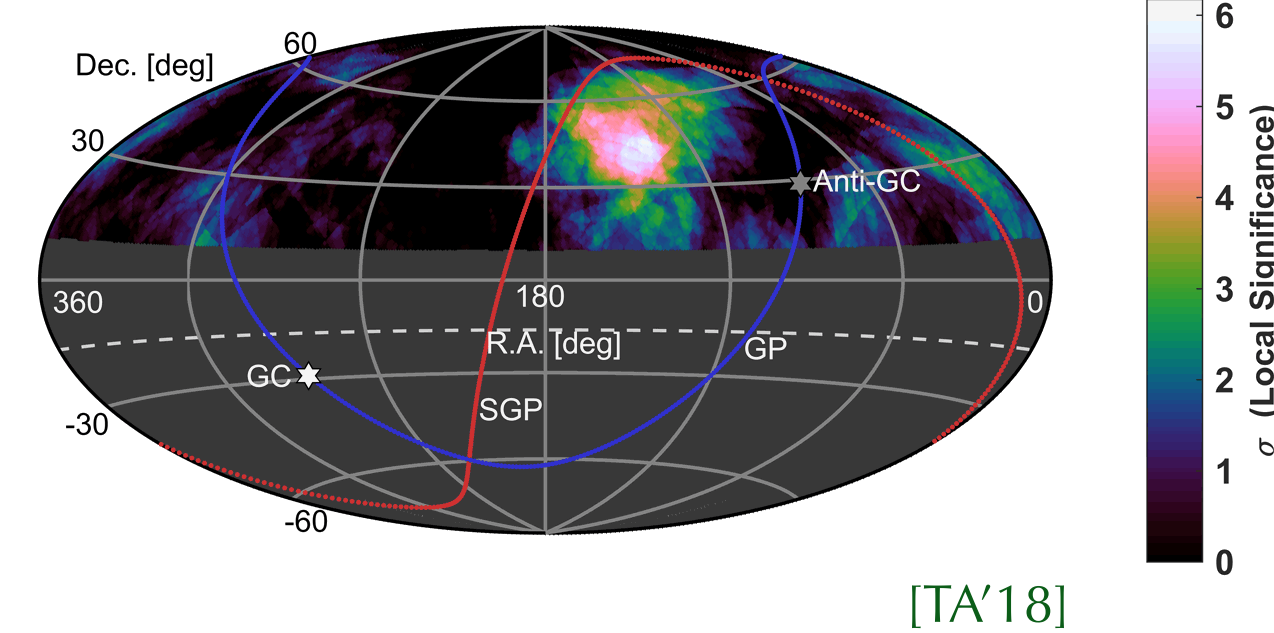
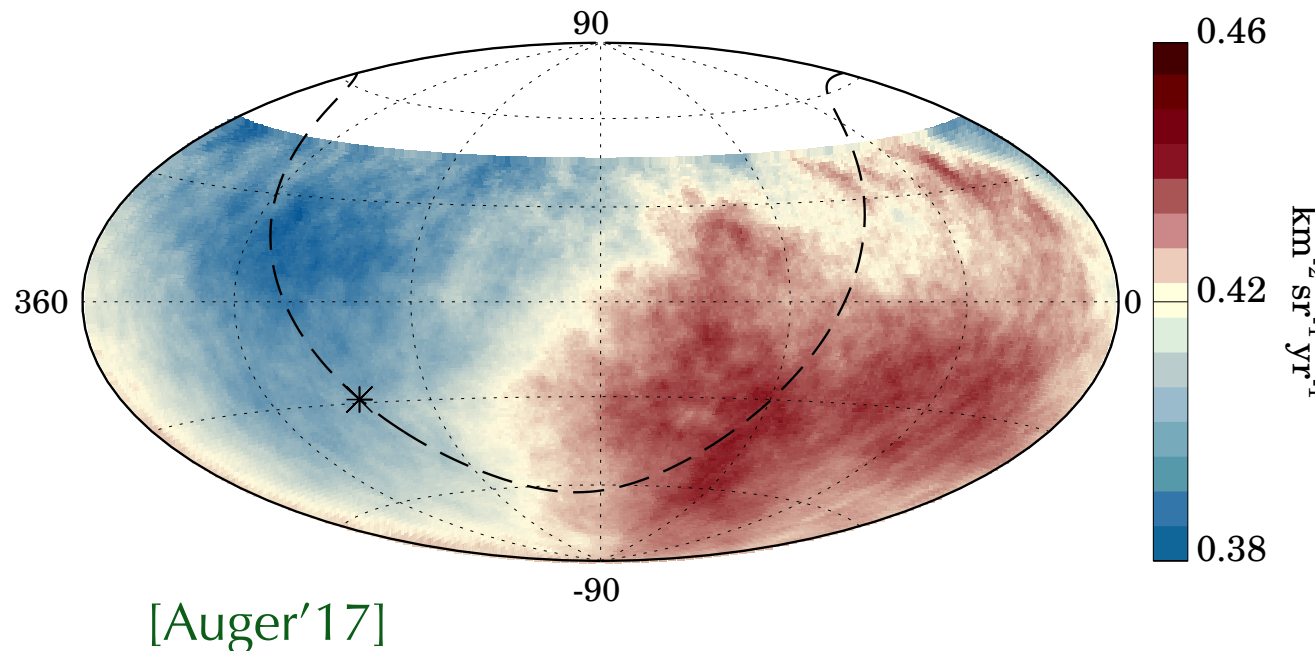
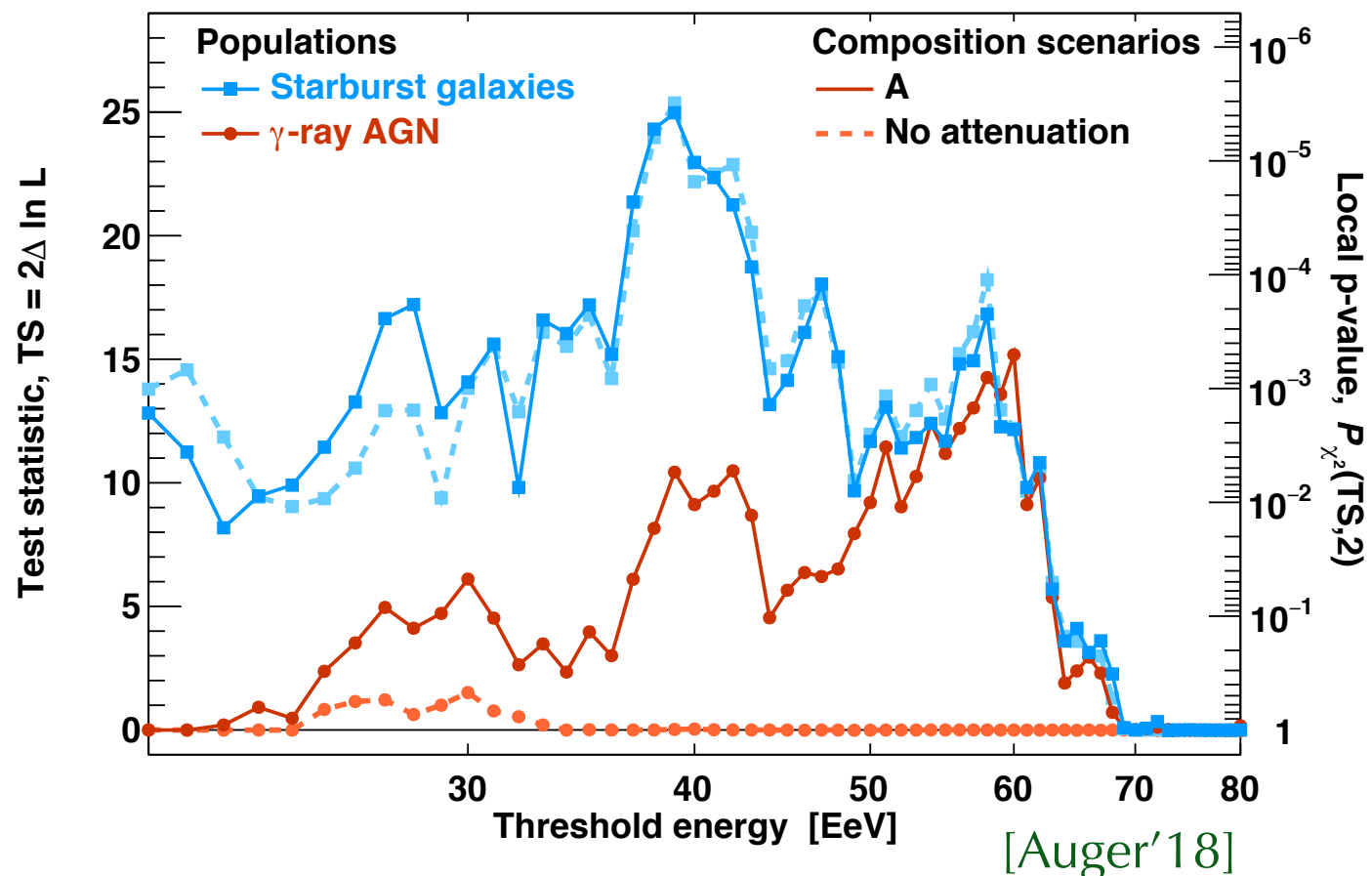
Auger Observatory covering 3000 km^2 with 1660 surface detectors and 4 fluorescence detectors

The Cosmic Ray Monopole



UHE CR Anisotropies

- UHE CR arrival direction above 8EeV show strong (6.5%) **dipole anisotropy** (5.2σ). [Auger'17]
- Arrival directions of UHE CRs above 40 EeV show **correlation with local starburst galaxies** (4σ).
- Indications for **medium-scale anisotropy** above 16 EeV in Northern Hemisphere (3.7σ) [TA'18]



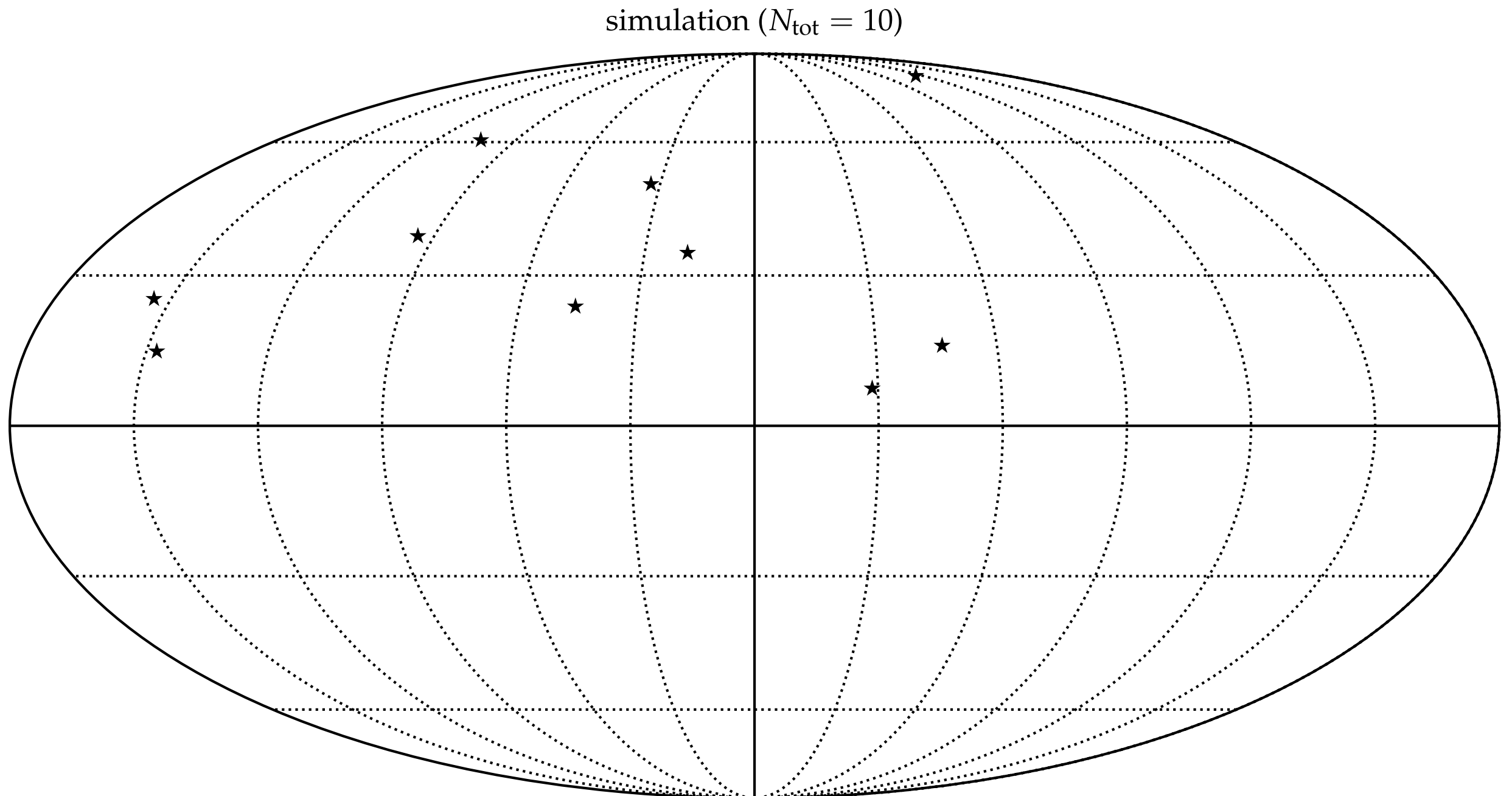
Autocorrelation

- So far, we have only looked into local excesses in individual bins.
- This method was not sensitive to the correlation between events, e.g. in neighbouring bins or in small clusters.
- Consider N_{tot} events distributed on a sphere with position \mathbf{n}_i (unit vector).
- For two events with label i and j ($i \neq j$) we can define an angular distance:
- The **cumulative two-point autocorrelation function** counts the number of pairs with angular distance less than an angle φ :

$$\mathcal{C}(\{\mathbf{n}_i\}, \varphi) = \frac{2}{N_{\text{tot}}(N_{\text{tot}} - 1)} \sum_{i=1}^{N_{\text{tot}}} \sum_{j=1}^{i-1} \Theta(\cos \varphi_{ij} - \cos \varphi)$$

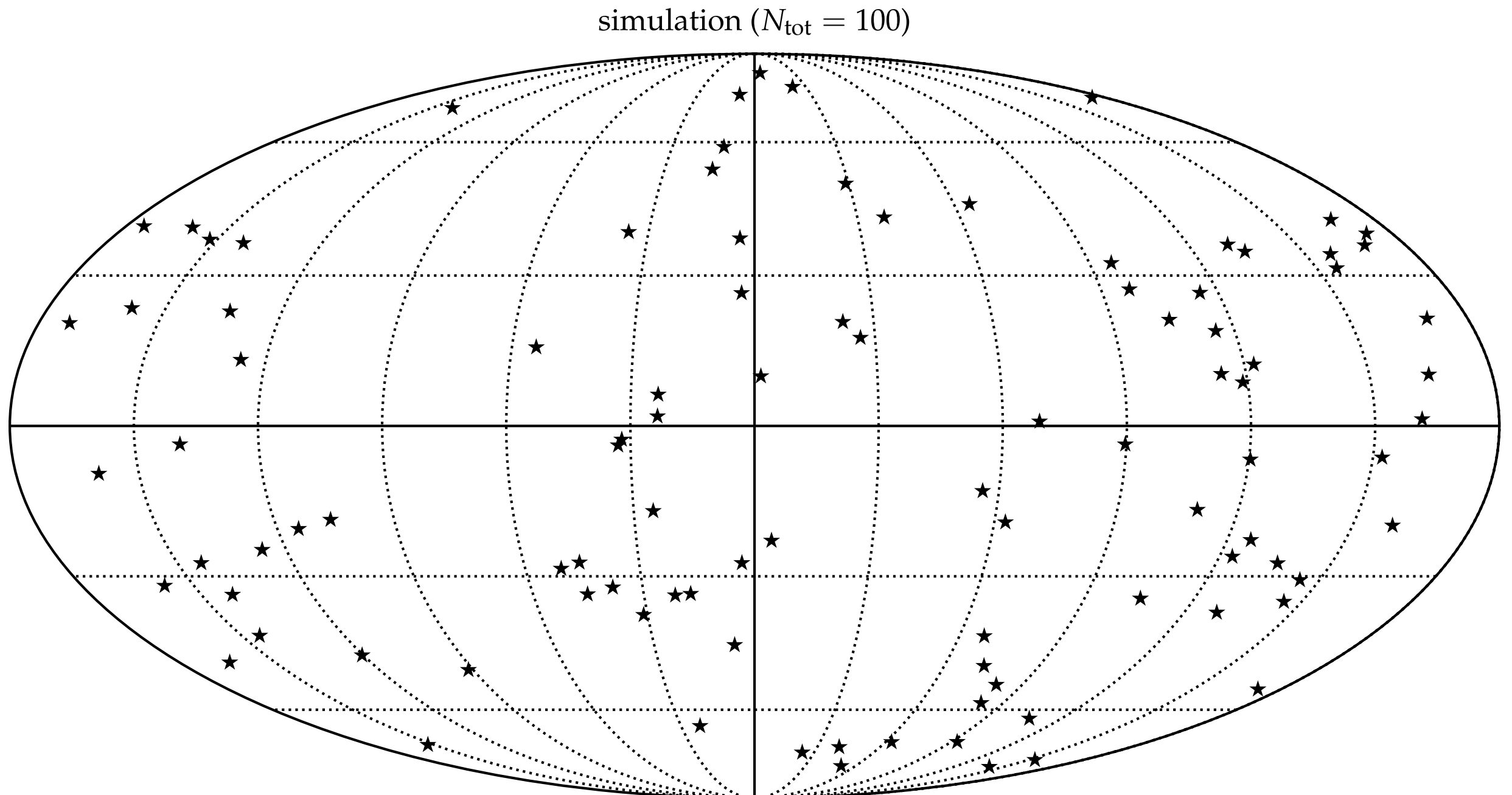
(step function $\Theta(x) = 1$ for $x \geq 0$ and $\Theta(x) = 0$ for $x < 0$)

Autocorrelation



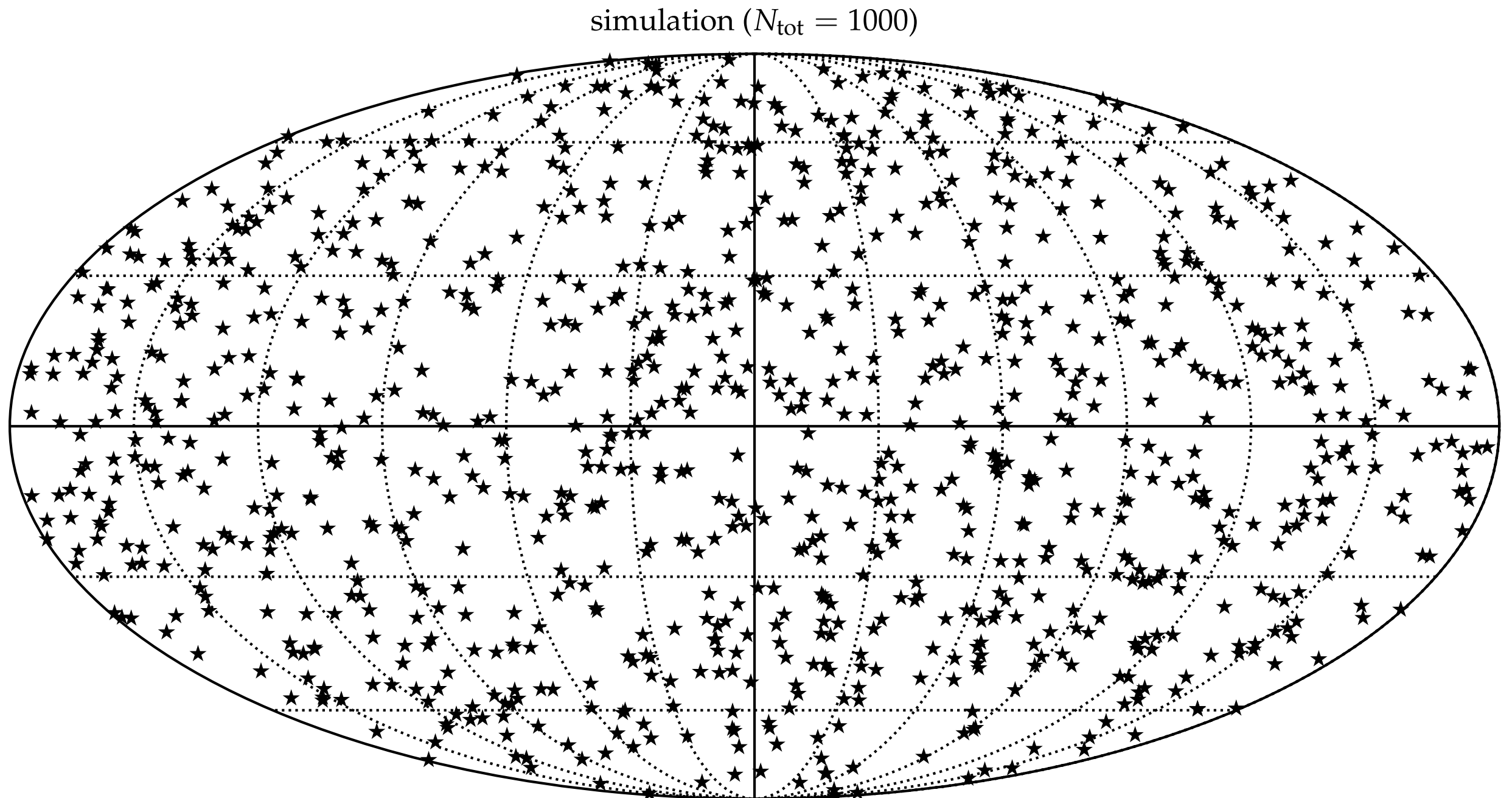
autocorrelation_example.ipynb

Autocorrelation



autocorrelation_example.ipynb

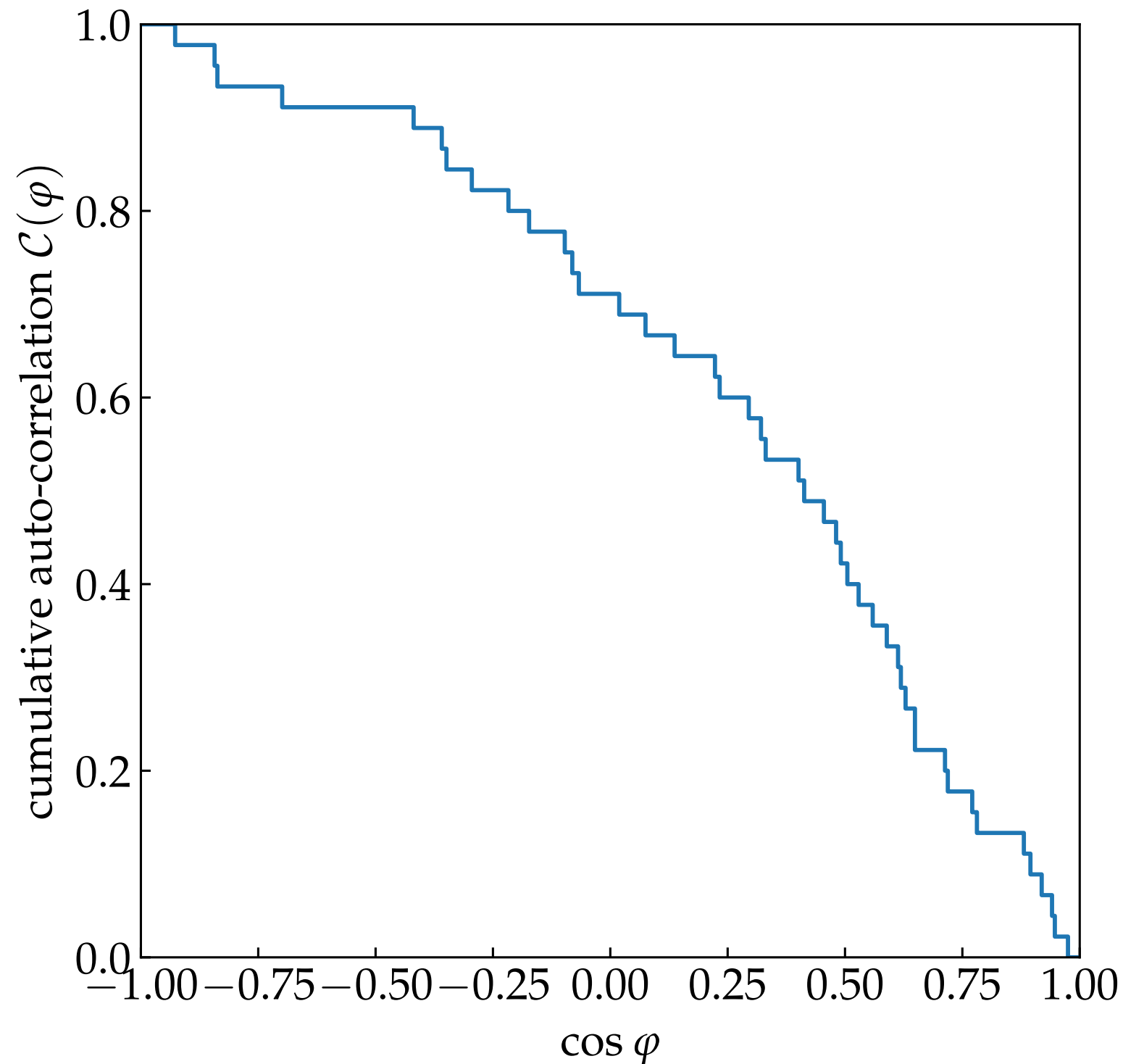
Autocorrelation



autocorrelation_example.ipynb

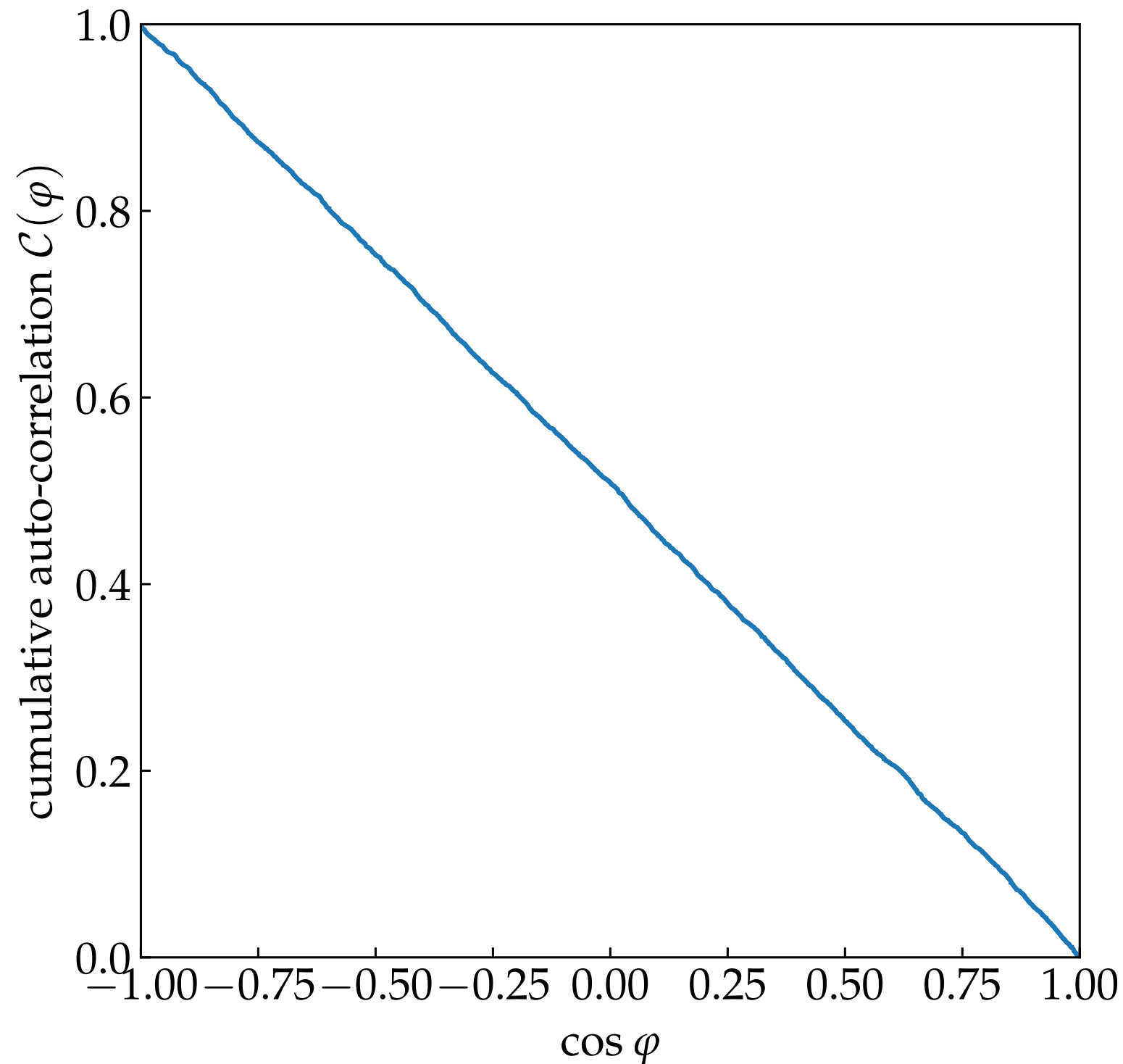
Autocorrelation

simulation (10 events)



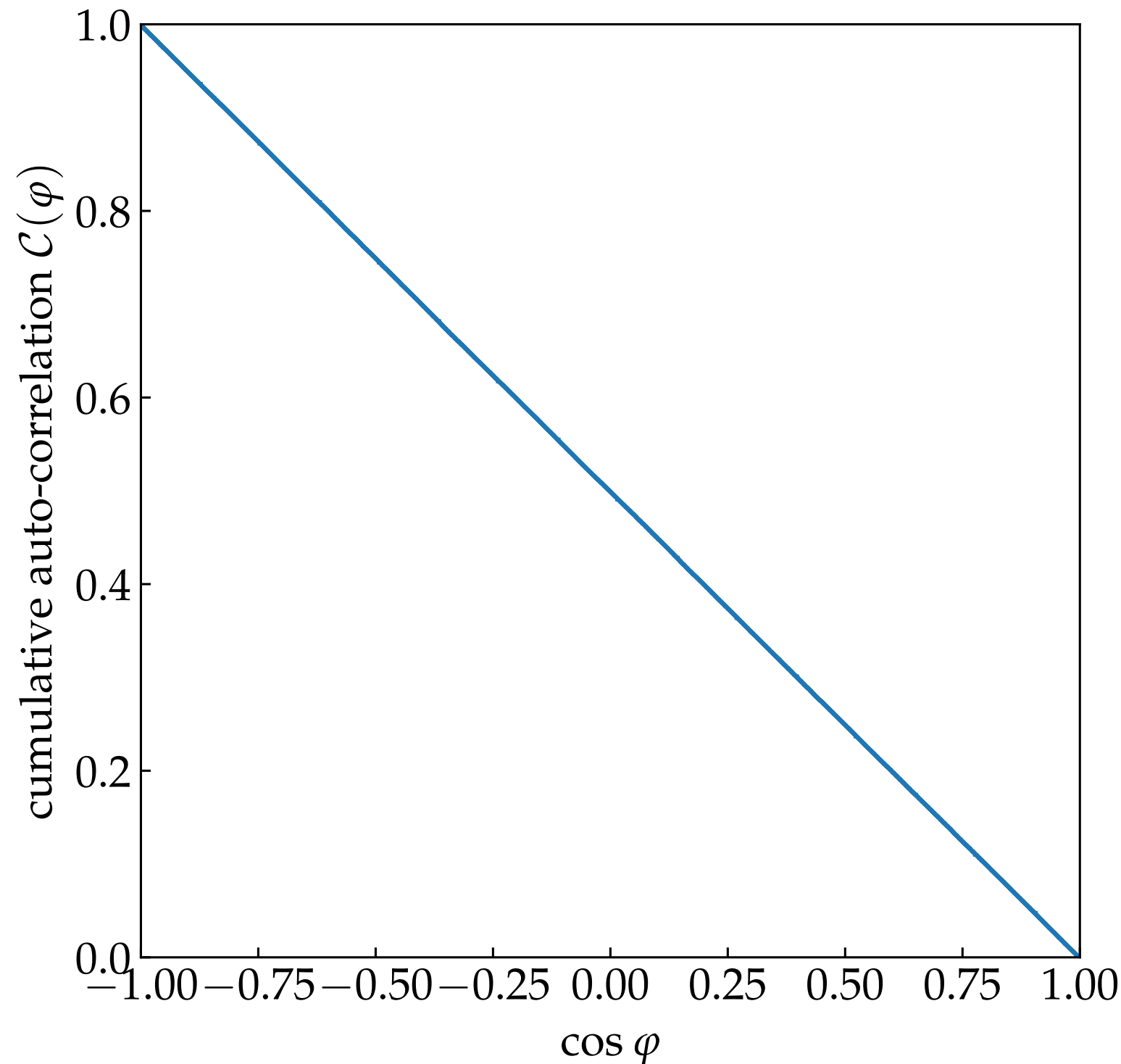
Autocorrelation

simulation (100 events)



Autocorrelation

simulation (1000 events)



Autocorrelation

- In the limit of a large number of events, N_{tot} , the cumulative distribution is just given by the relative size of the solid angle $\Delta\Omega$ with half-opening angle φ :

$$\lim_{N_{\text{tot}} \rightarrow \infty} \mathcal{C}(\{\mathbf{n}_i\}, \varphi) \rightarrow \mathcal{C}_{\text{iso}}(\varphi) = \frac{\Delta\Omega}{4\pi}$$

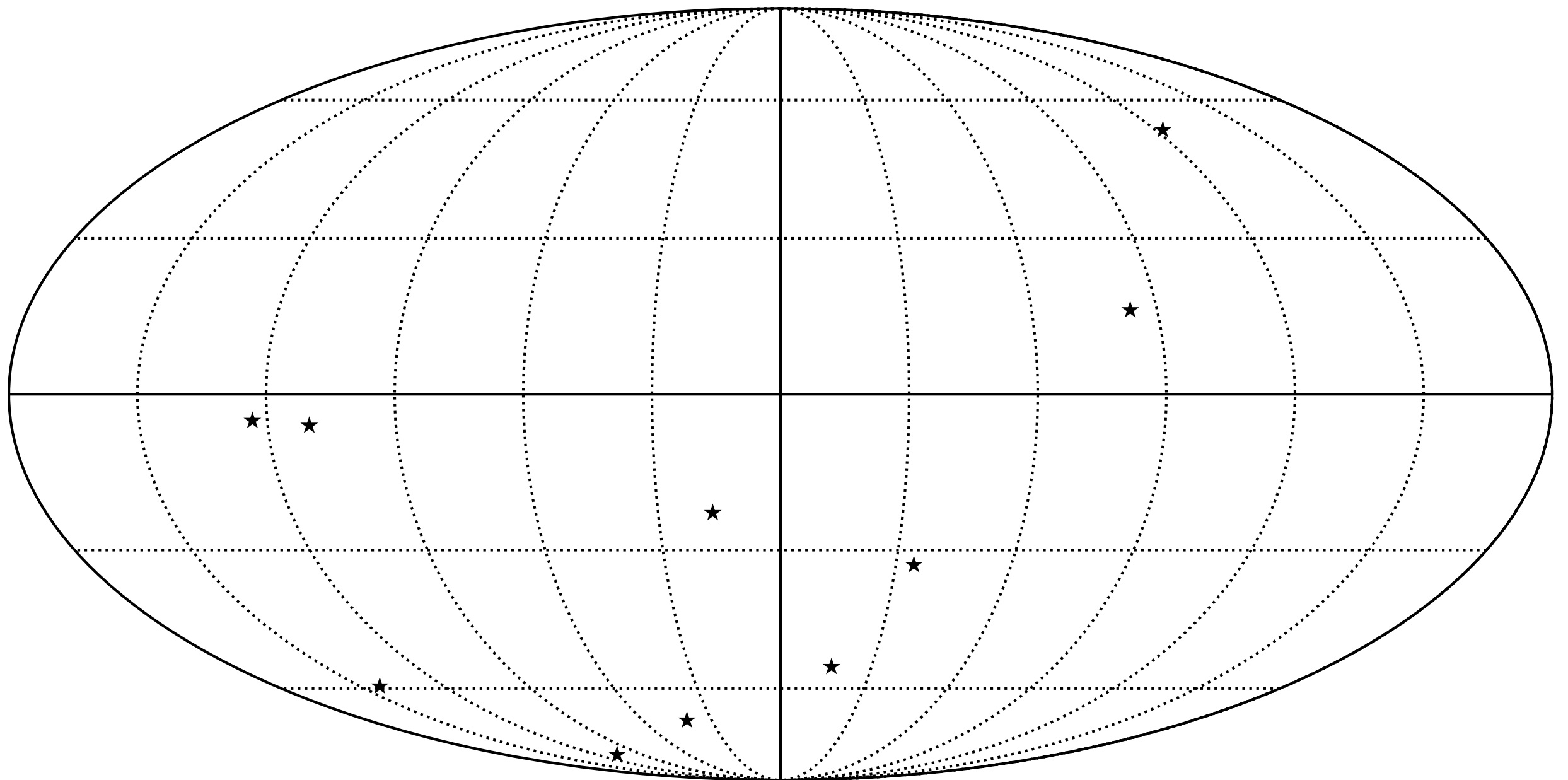
- solid angle is $\Delta\Omega = 2\pi(1 - \cos \varphi)$:
- isotropic distribution:

$$\mathcal{C}_{\text{iso}}(\varphi) = \frac{1}{2}(1 - \cos \varphi)$$

- **Note:** an isotropic distribution of a finite number of events will always show deviations from \mathcal{C}_{iso} .

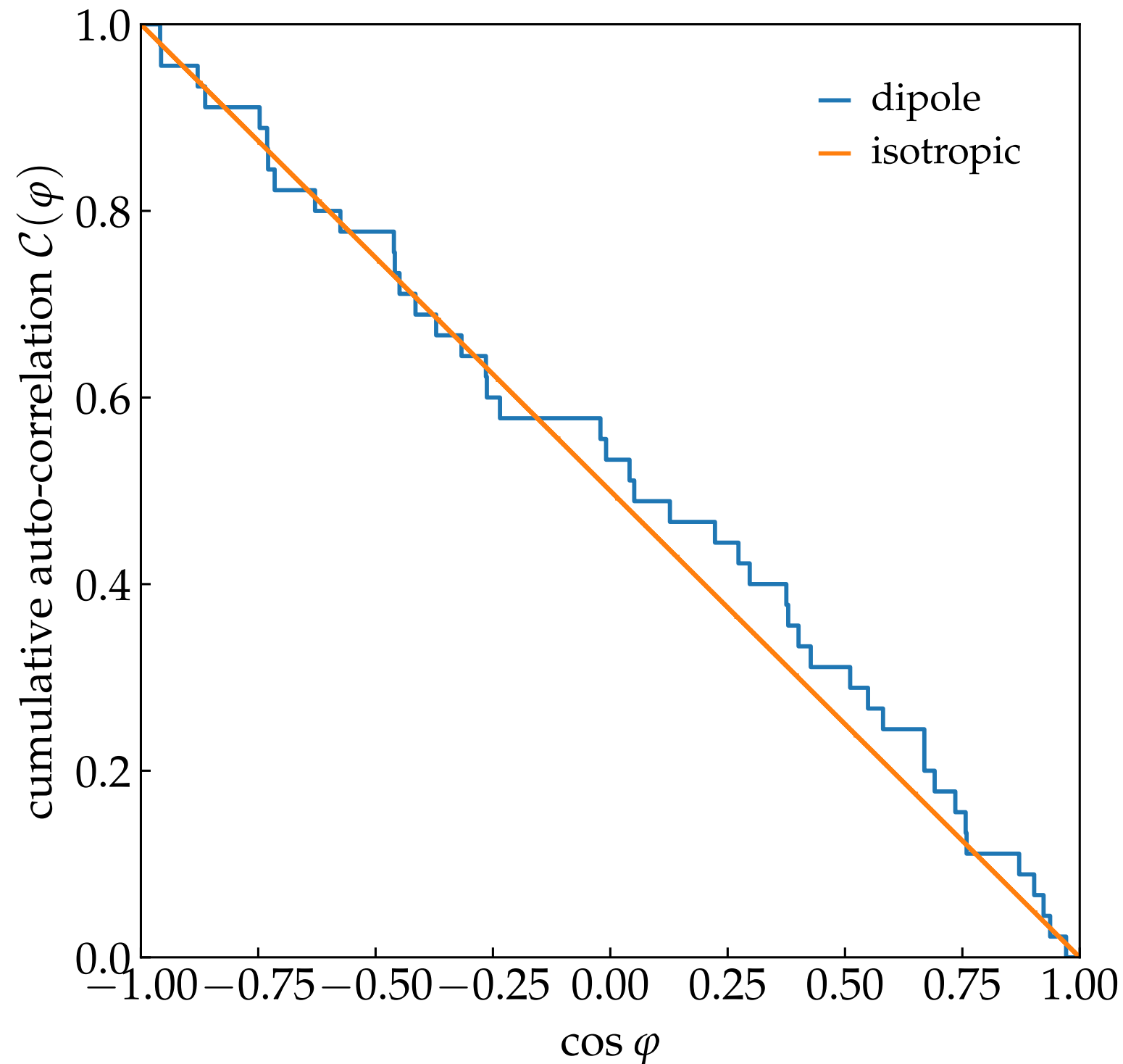
Autocorrelation

simulation with dipole anisotropy (10 events)



Autocorrelation

simulation (10 events)



Kolmogorov-Smirnov Test

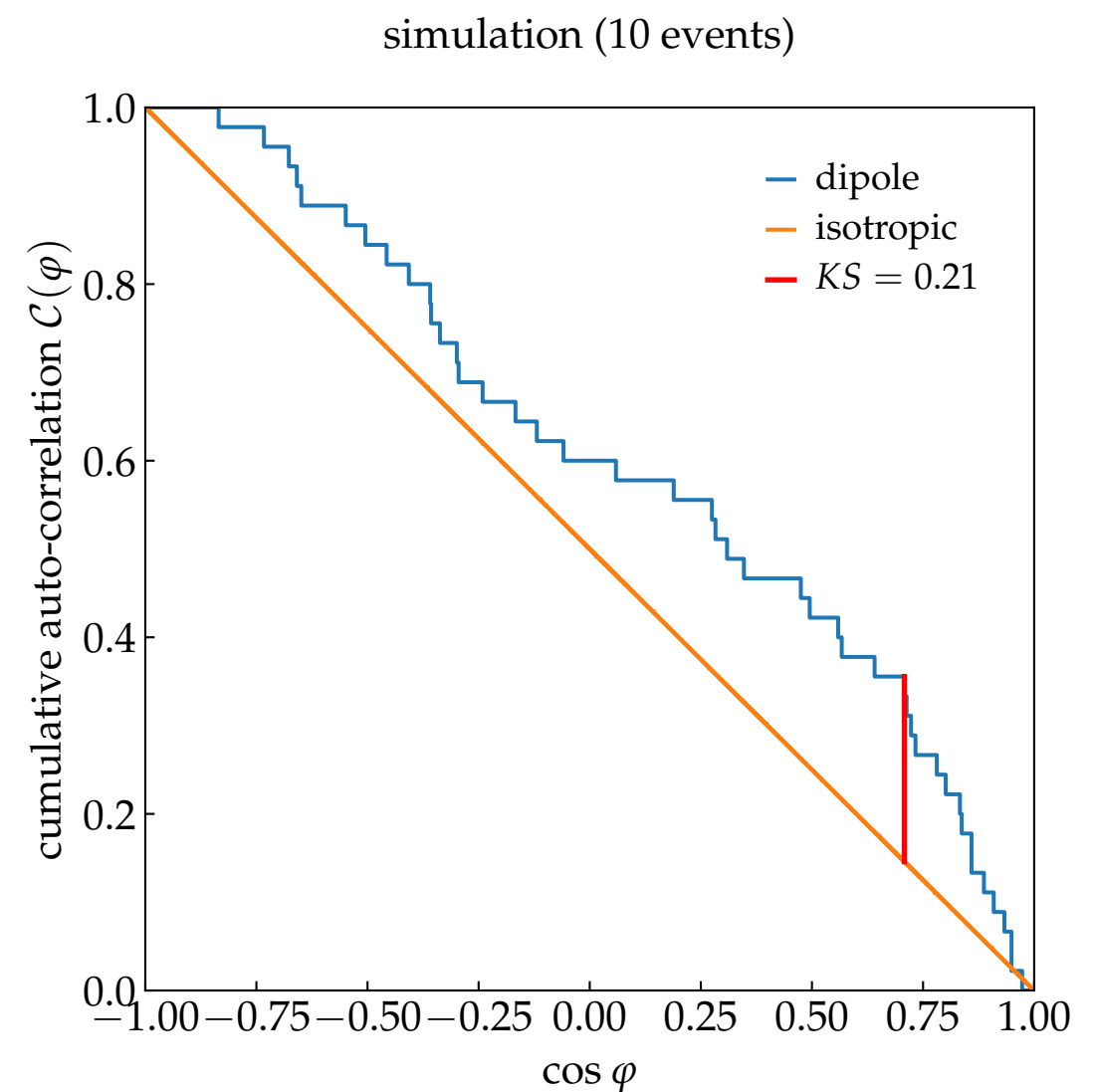
- We want to define a quantity that is a statistical measure for the difference between the empirical distribution and background distribution.

- Area between two curves (L^1 norm)?

$$\int d\cos\varphi |\mathcal{C}(\{\mathbf{n}_i\}, \varphi) - \mathcal{C}_{\text{iso}}(\varphi)|$$

- Or, more general (L^p norm)?

$$\left[\int d\cos\varphi \left| \mathcal{C}(\{\mathbf{n}_i\}, \varphi) - \mathcal{C}_{\text{iso}}(\varphi) \right|^p \right]^{\frac{1}{p}}$$



Kolmogorov-Smirnov:
 $p \rightarrow \infty$.

Kolmogorov-Smirnov Test

- In general, given two cumulative probability distributions, $0 \leq A(x) \leq 1$ and $0 \leq B(x) \leq 1$, we can define the **Kolmogorov-Smirnov test** as:

$$KS = \sup_x |A(x) - B(x)|$$

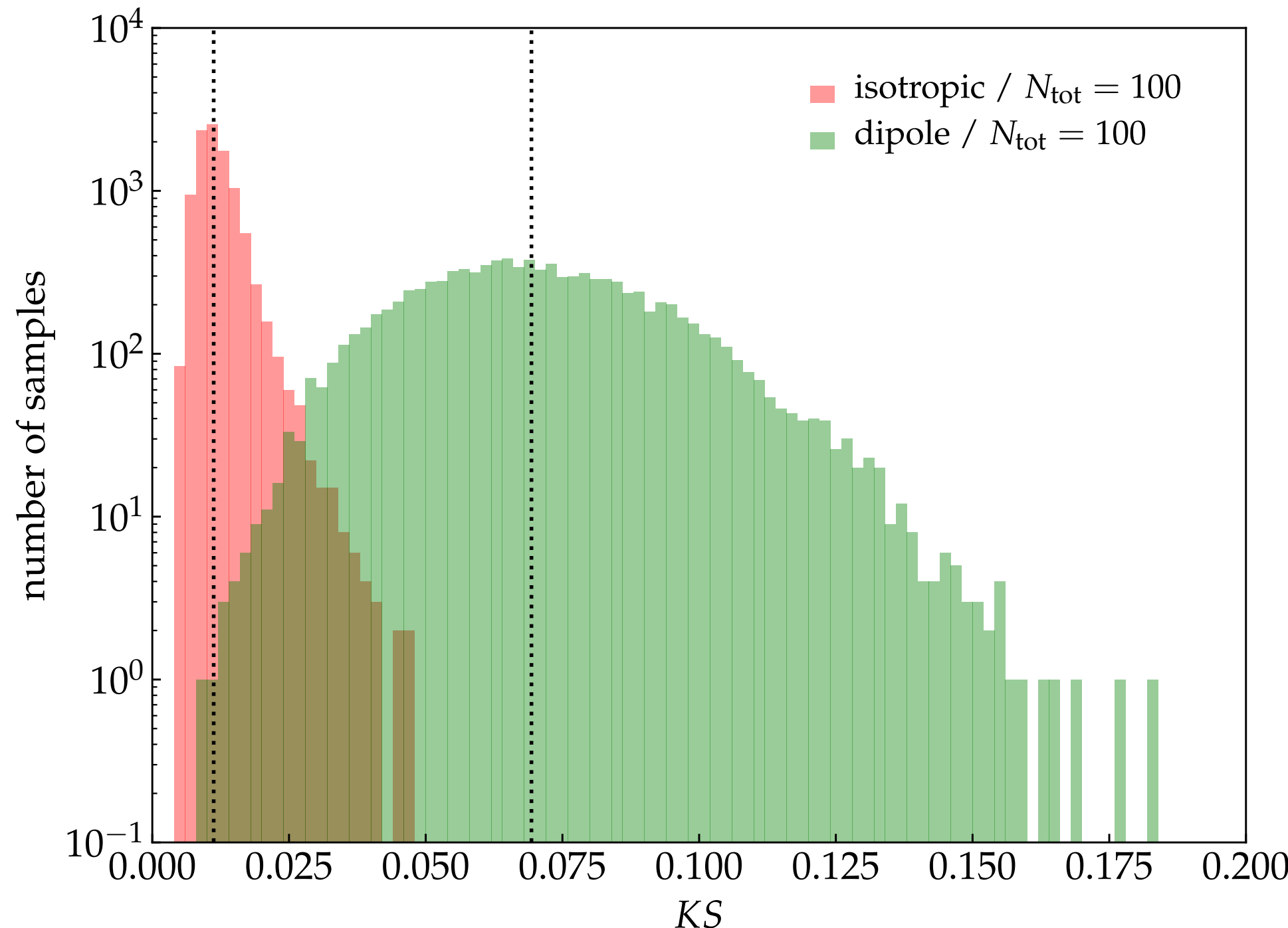
- Cumulative auto-correlation function $\mathcal{C}(\{\mathbf{n}_i\}, \varphi)$ follows the probability distributions to find a pair of events within an angular distance φ .
- We will use this in the following to define a test statistic, that describes **deviation from an isotropic background distribution**:

$$KS(\{\mathbf{n}_i\}) = \sup_{\varphi} |\mathcal{C}(\{\mathbf{n}_i\}, \varphi) - \mathcal{C}_{\text{iso}}(\varphi)|$$

KS_example.ipynb

Kolmogorov Smirnov Test

simulation (10^4 samples)



KS_example.ipynb

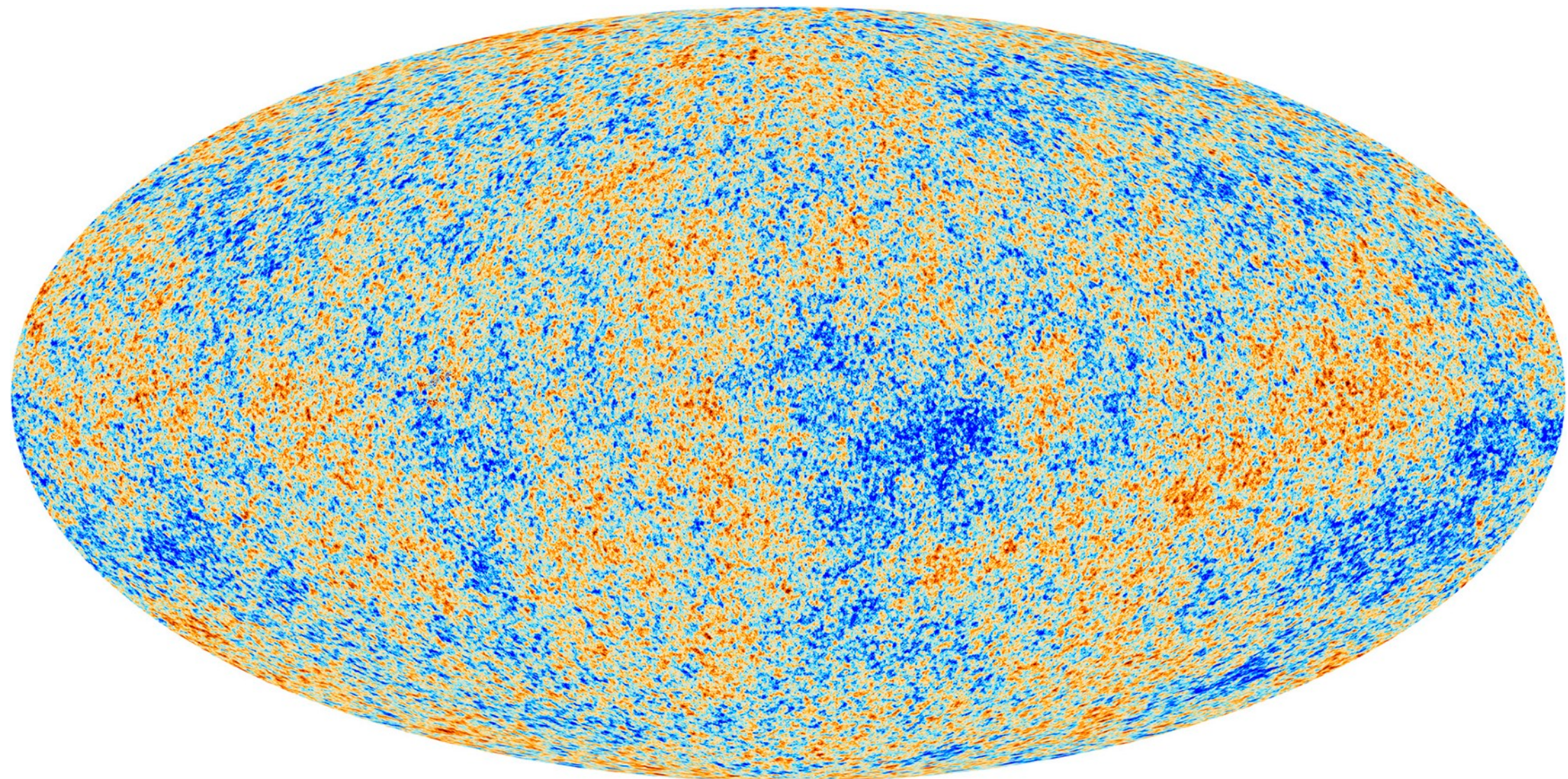
Kolmogorov-Smirnov Test

- For a fixed number of events N_{tot} we can simulate isotropic event distributions (null hypothesis) and their KS values (test statistic).
- Separation of KS for observed data from background distribution allows to **estimate significance of an excess**.
- Similar to Wilks' theorem the background distribution approaches a **predictive asymptotic behaviour** for large number of events, but we will not cover this here.
- number of event pairs increases as:

$$N_{\text{pair}} = \frac{1}{2}N_{\text{tot}}(N_{\text{tot}} - 1) \propto N_{\text{tot}}^2$$

- Cumulative auto-correlation function becomes **numerically inefficient**.

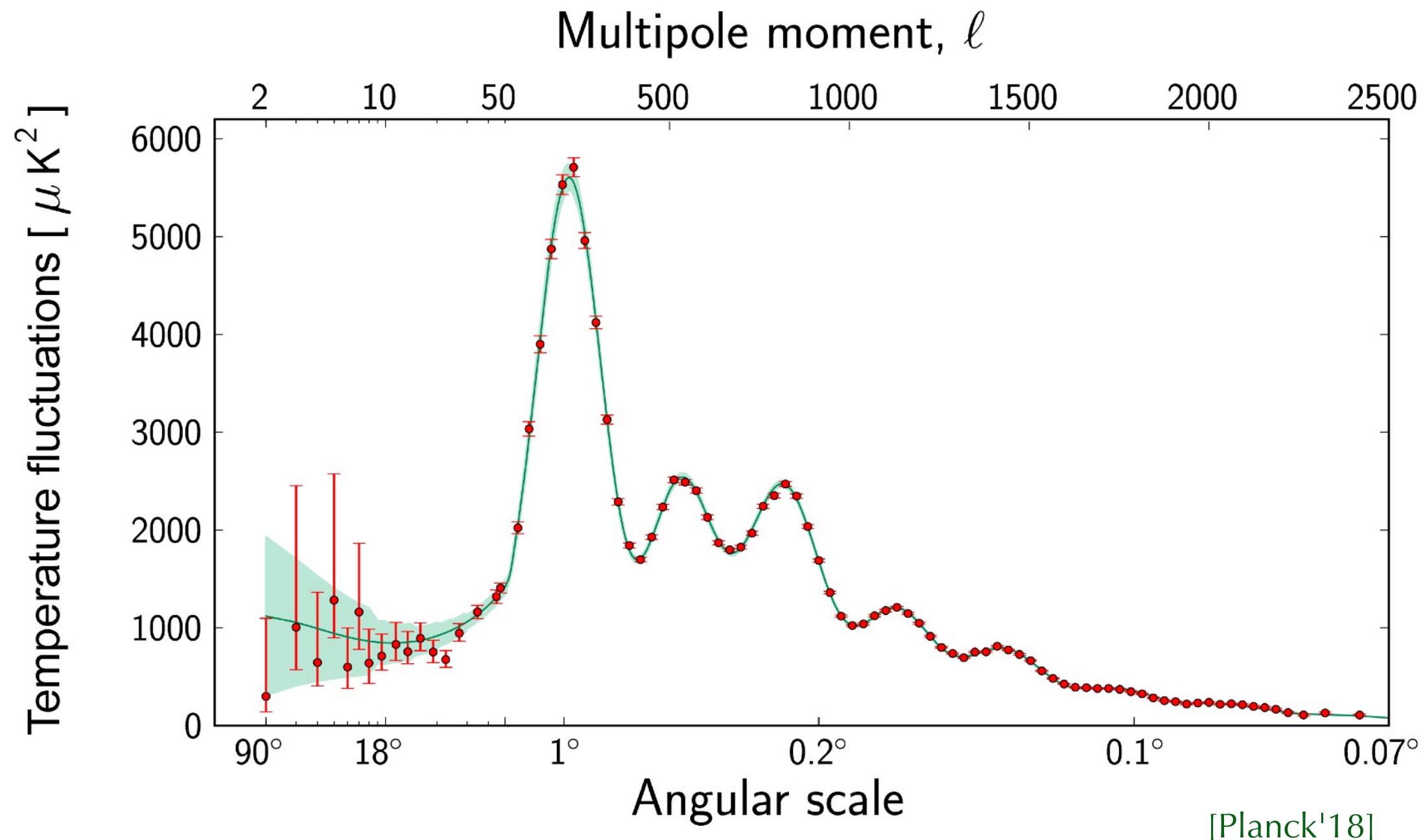
Example: CMB



[Planck'18]

Temperature anisotropies of the cosmic microwave background (CMB) observed by the Planck satellite.

Angular Power Spectrum



The angular power spectrum C_ℓ of the temperature fluctuations.

Autocorrelation

- In the Kolmogorov-Smirnov test we observed that for large N_{tot} the number of pairs increase as N_{tot}^2 and the calculation can become very inefficient.
- In **large- N_{tot} limit** we can approximate the event distribution by a smooth function:

$$g(\Omega) = \lim_{N_{\text{bins}} \rightarrow \infty} \frac{\Delta n(\Omega)}{N_{\text{tot}} \Delta \Omega}$$

- On a smooth distribution we can define the **two-point autocorrelation function** as:

$$\xi(\varphi) = \int d\Omega_1 \int d\Omega_2 \delta(\mathbf{n}(\Omega_1)\mathbf{n}(\Omega_2) - \cos \varphi) g(\Omega_1) g(\Omega_2)$$

- **Note:** This is the differential version of cumulative autocorrelation function.

Autocorrelation

- **comment 1:** *cumulative* two-point autocorrelation function:

$$\mathcal{C}(\varphi) = \int_{\cos \varphi}^1 d \cos \varphi' \xi(\varphi')$$

- **comment 2:** isotropic distribution $g(\Omega) = 1/(4\pi)$:

$$\xi(\varphi) = {}^\dagger \frac{1}{2} \quad \rightarrow \quad \mathcal{C}_{\text{iso}}(\varphi) = \int_{\cos \varphi}^1 d \cos \varphi' \frac{1}{2} = \frac{1}{2}(1 - \cos \varphi)$$

† follows from:

$$\delta(\mathbf{n}(\Omega_1)\mathbf{n}(\Omega_2) - \cos \varphi) = 2\pi \sum_{\ell=0}^{\infty} \sum_{m=-\ell}^{\ell} P_\ell(\cos \varphi) Y_{\ell m}^*(\Omega_1) Y_{\ell m}(\Omega_2)$$

Spherical Harmonics

- Every smooth function $g(\theta, \phi)$ on a sphere can be decomposed in terms of spherical harmonics $Y_{\ell m}$:

$$g(\theta, \phi) = \sum_{\ell=0}^{\infty} \sum_{m=-\ell}^{\ell} a_{\ell m} Y_{\ell m}(\theta, \phi)$$

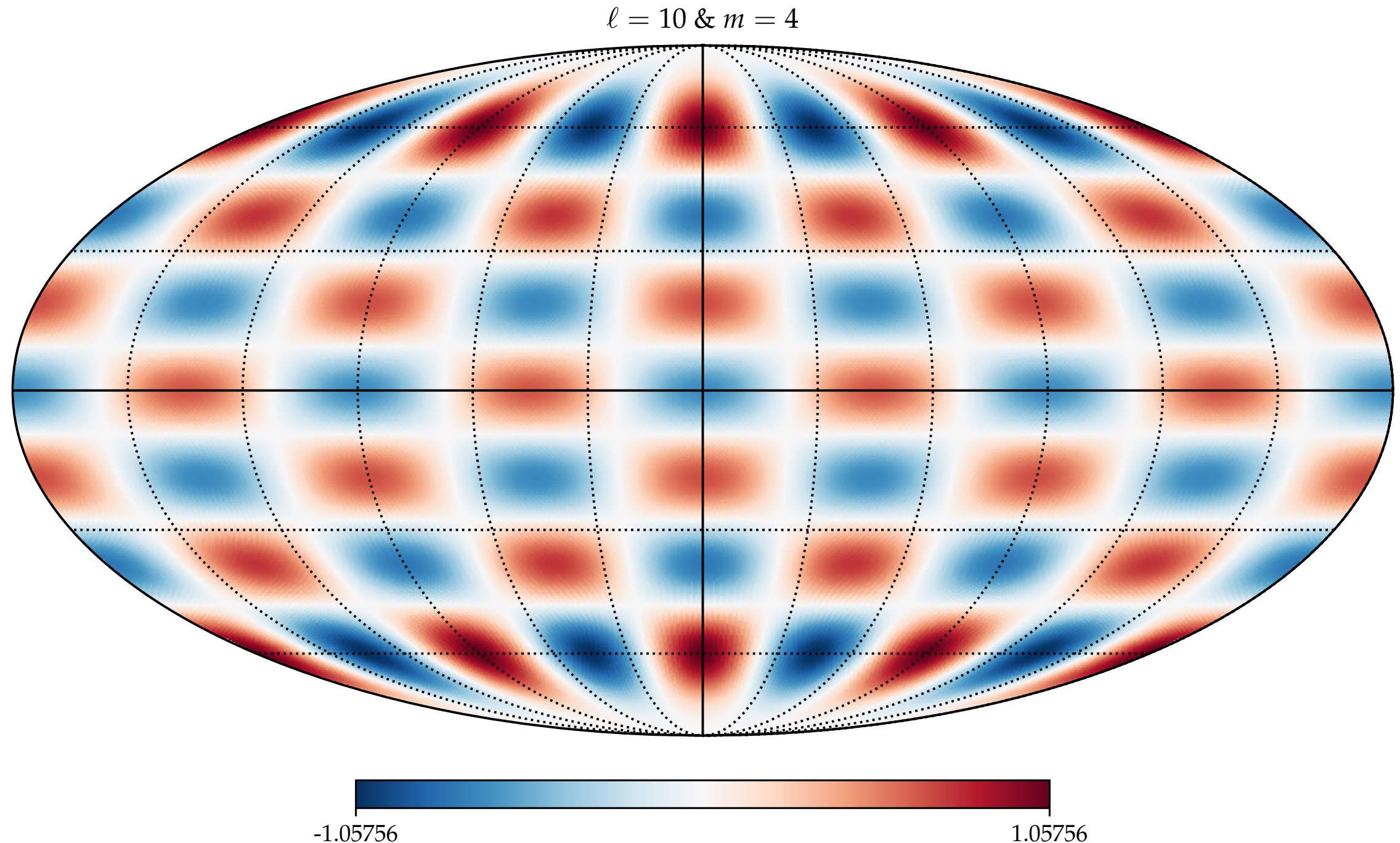
- coefficients given by:

$$a_{\ell m} = \int d\Omega Y_{\ell m}^*(\theta, \phi) g(\theta, \phi)$$

- for real-valued functions:

$$a_{\ell m}^* = (-1)^m a_{\ell -m}$$

Spherical Harmonics



Spherical Harmonics

- The low- ℓ components are:

- $\ell = 0$: **monopole**: $Y_{00} = \sqrt{\frac{1}{4\pi}}$

- $\ell = 1$: **dipole**:

$$Y_{10} = \sqrt{\frac{3}{4\pi}} \cos \theta \quad Y_{1-1} = \sqrt{\frac{3}{8\pi}} \sin \theta e^{-i\varphi} \quad Y_{11} = -\sqrt{\frac{3}{8\pi}} \sin \theta e^{i\varphi}$$

- $\ell = 2$: **quadrupole**, $\ell = 3$: **octupole**, etc.

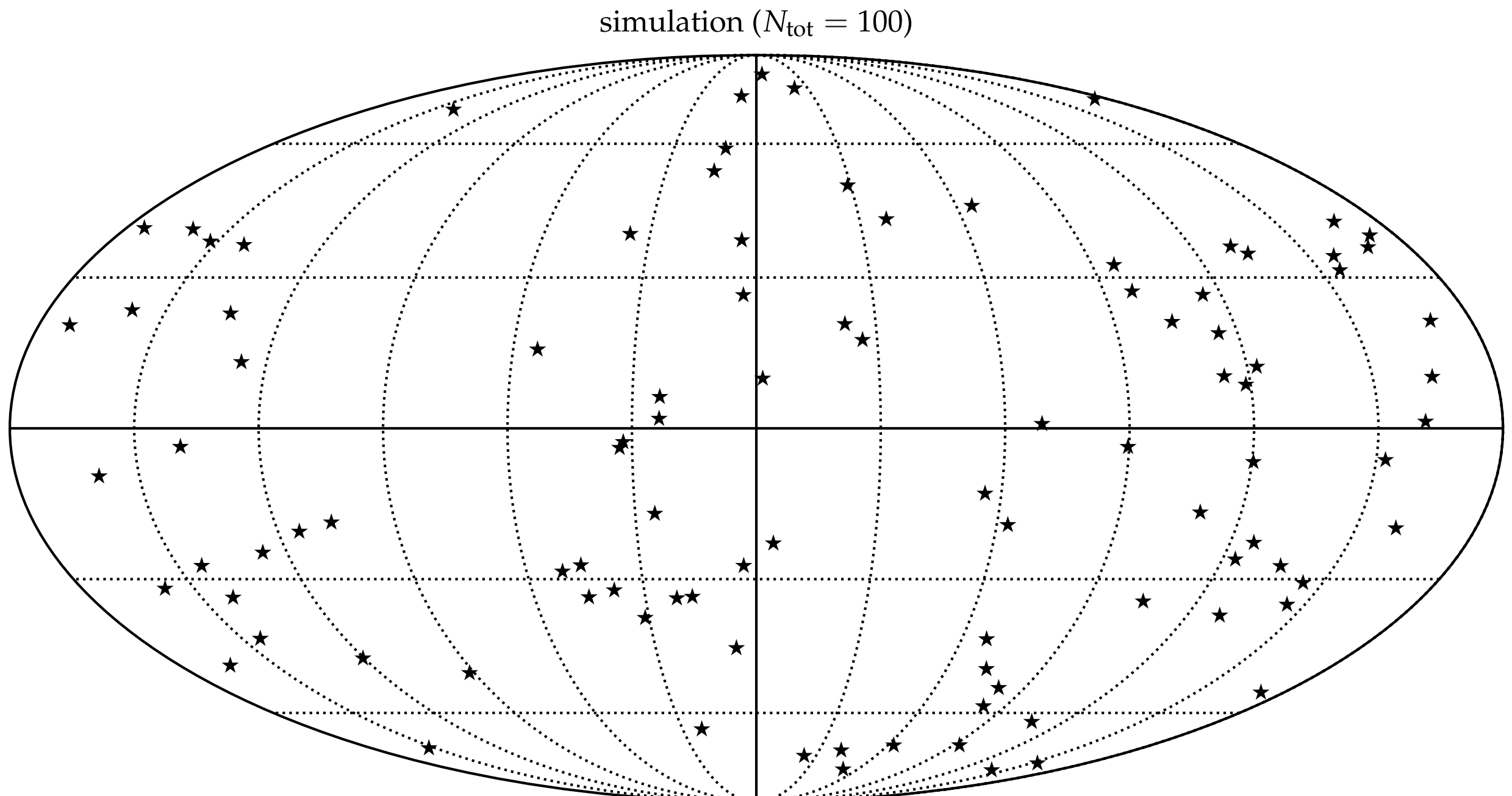
- **angular power spectrum**:

$$C_\ell = \frac{1}{2\ell + 1} \sum_{m=-\ell}^{\ell} |a_{\ell m}|^2$$

- simple relation to ξ via Legendre polynomials P_ℓ :

$$\xi(\varphi) = 2\pi \sum_{\ell} (2\ell + 1) C_\ell P_\ell(\cos \varphi)$$

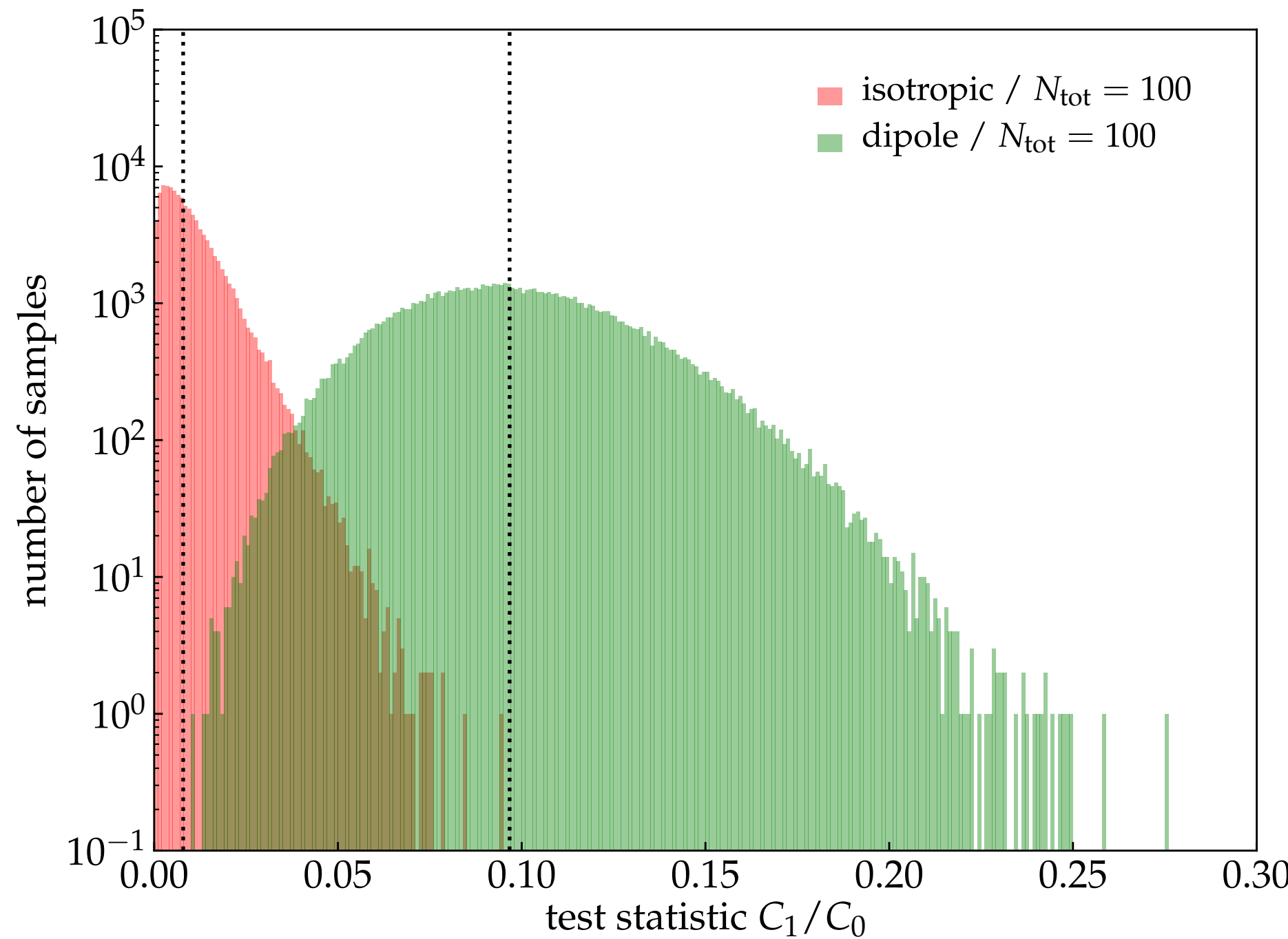
Angular Power Spectrum



dipole_power_example.ipynb

Angular Power Spectrum

simulation (10^5 samples)



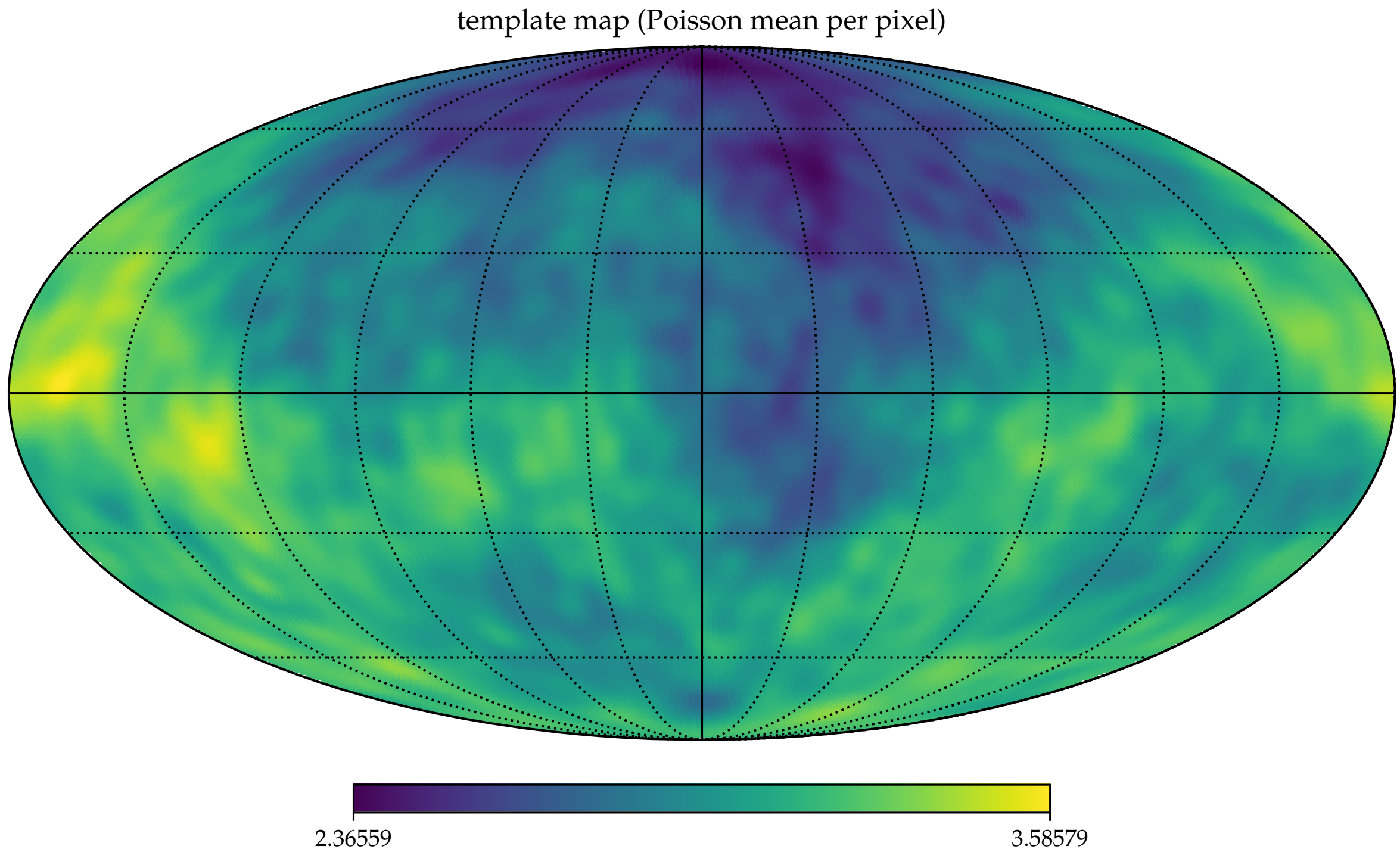
`dipole_power_example.ipynb`

Angular Power Spectrum

- In general, we want to judge if a distribution of events shows evidence for an excess in the power spectrum compared to background expectations.
- **Strategy:** Generate background maps from data via scrambling:
 - A. choose two random bins i and j
 - B. interchange the events in the two bins
 - C. repeat from A. until $N_{\text{scramble}} \gg N_{\text{bins}}$
- The distribution of the power spectrum of these maps gives an estimate of the median and variance of the background power.
- Expected median noise level:

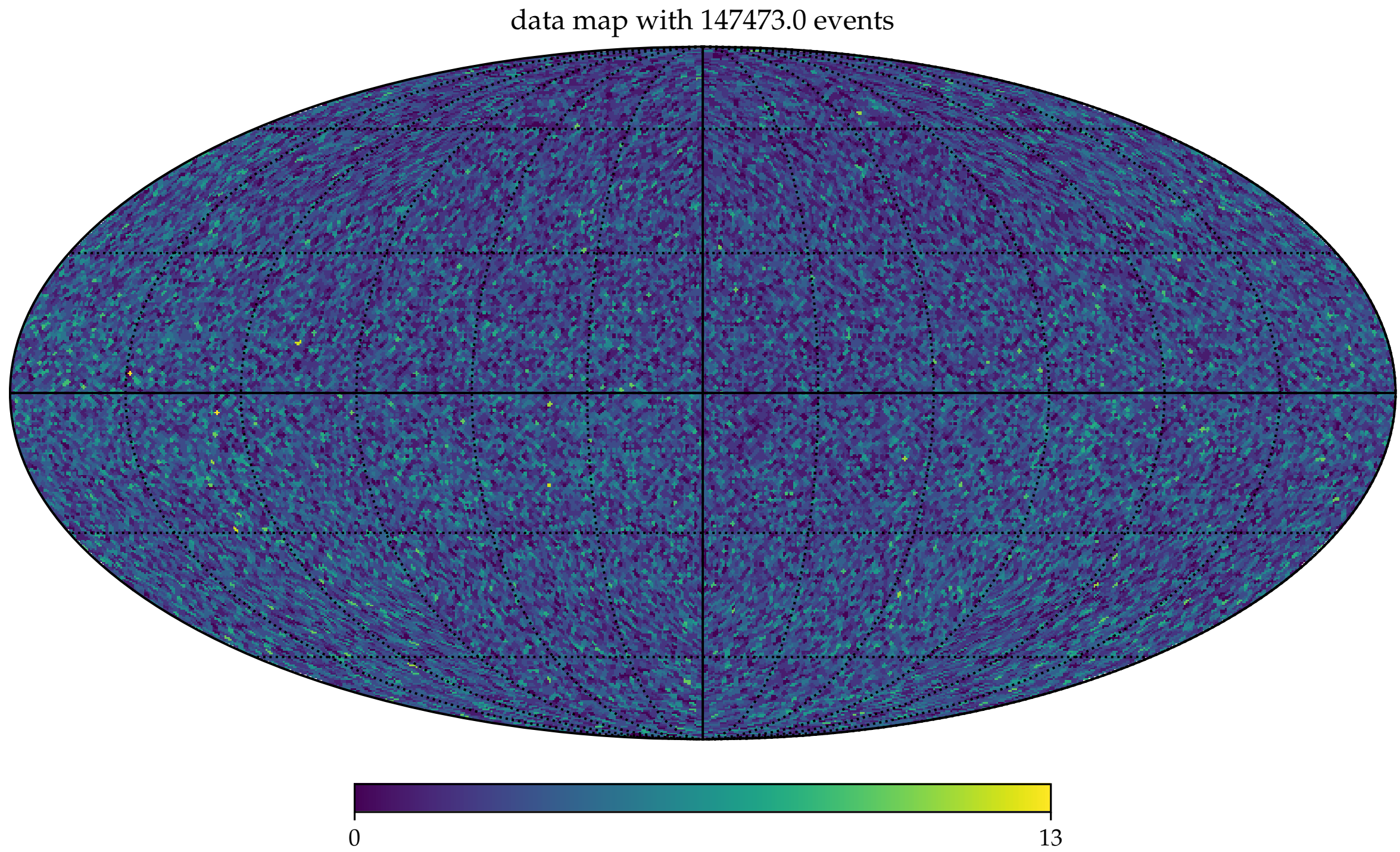
$$\mathcal{N} = \frac{1}{N_{\text{tot}}}$$

Angular Power Spectrum



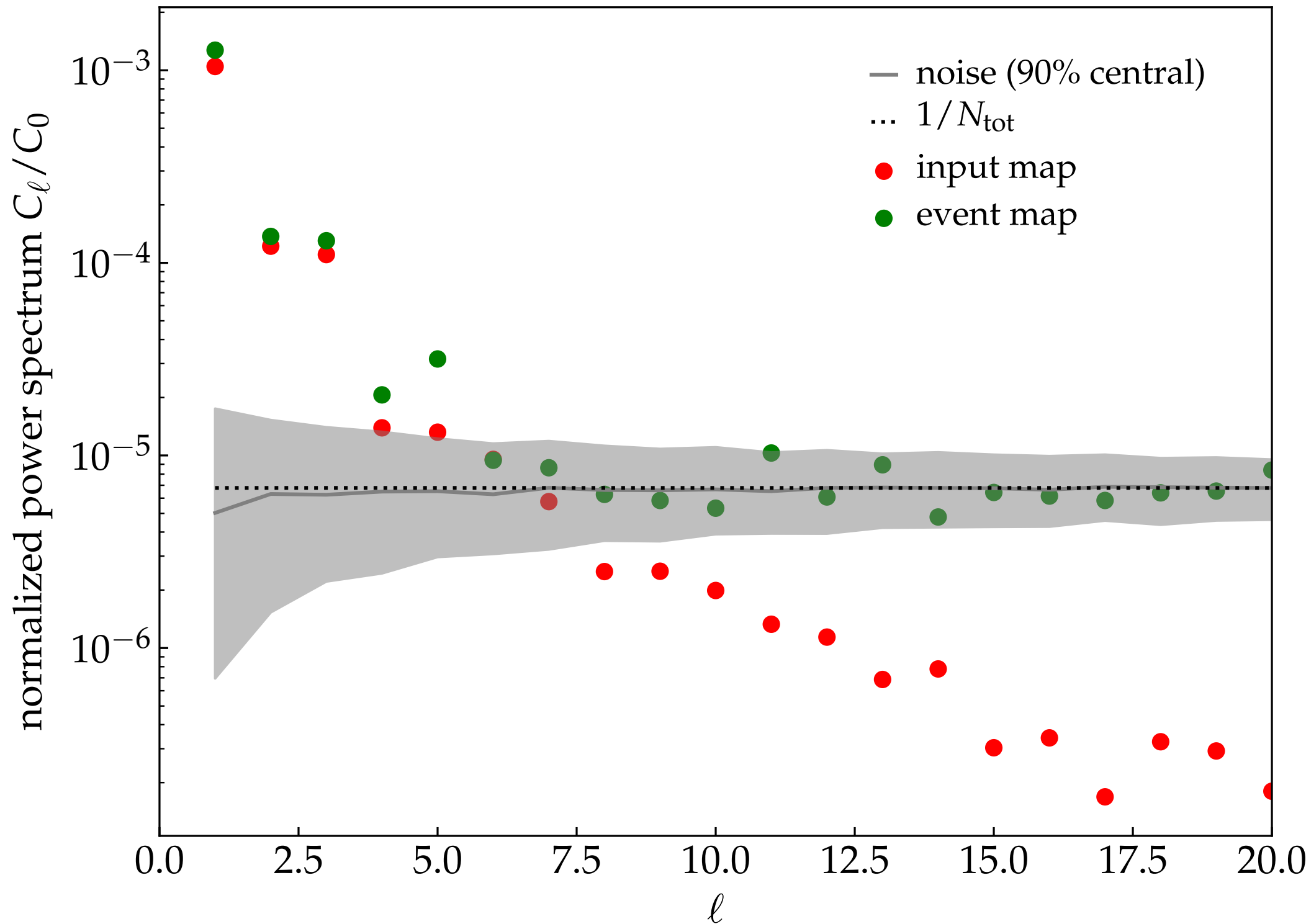
powerspectrum_example.ipynb

Angular Power Spectrum



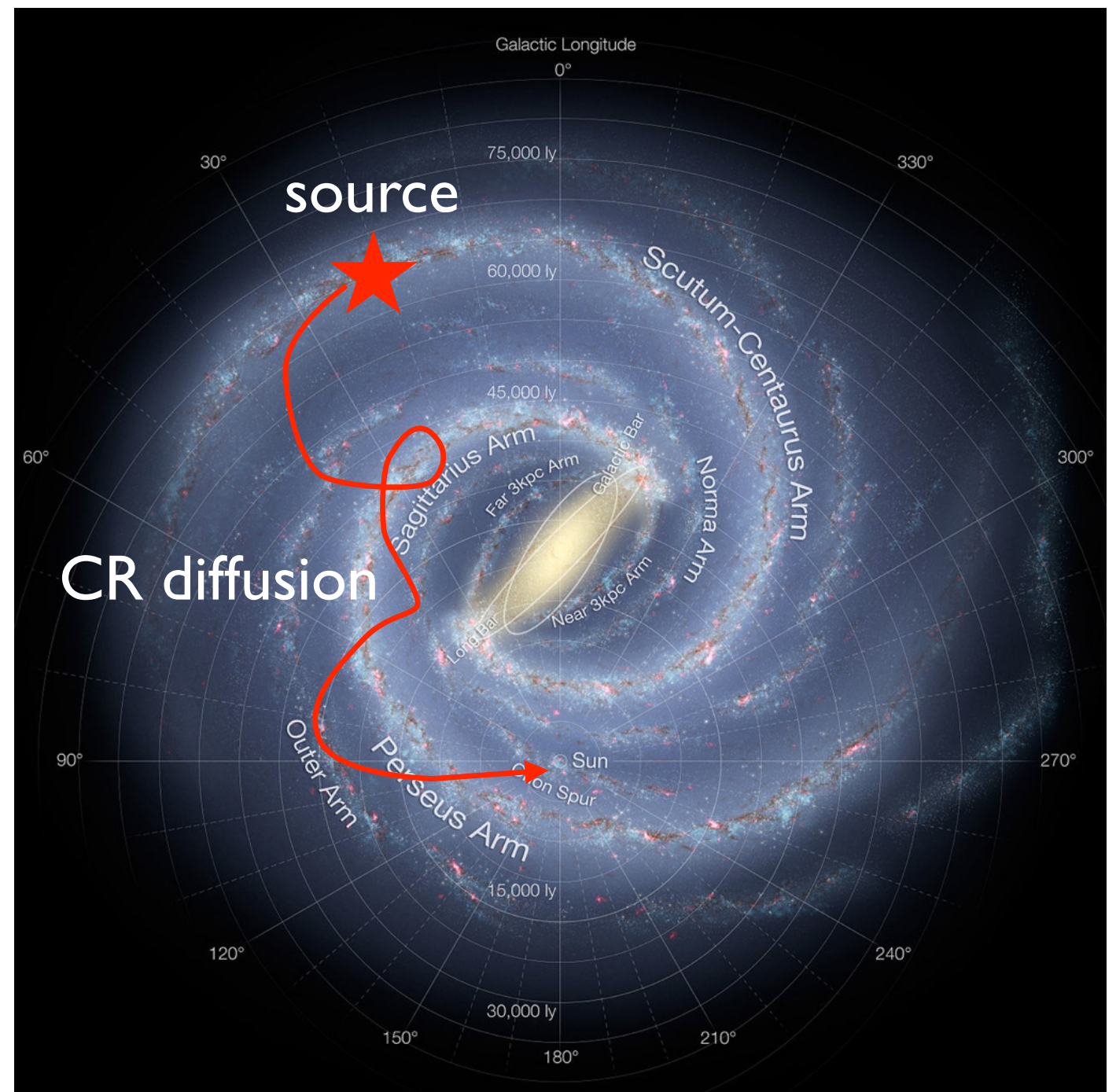
powerspectrum_example.ipynb

Angular Power Spectrum



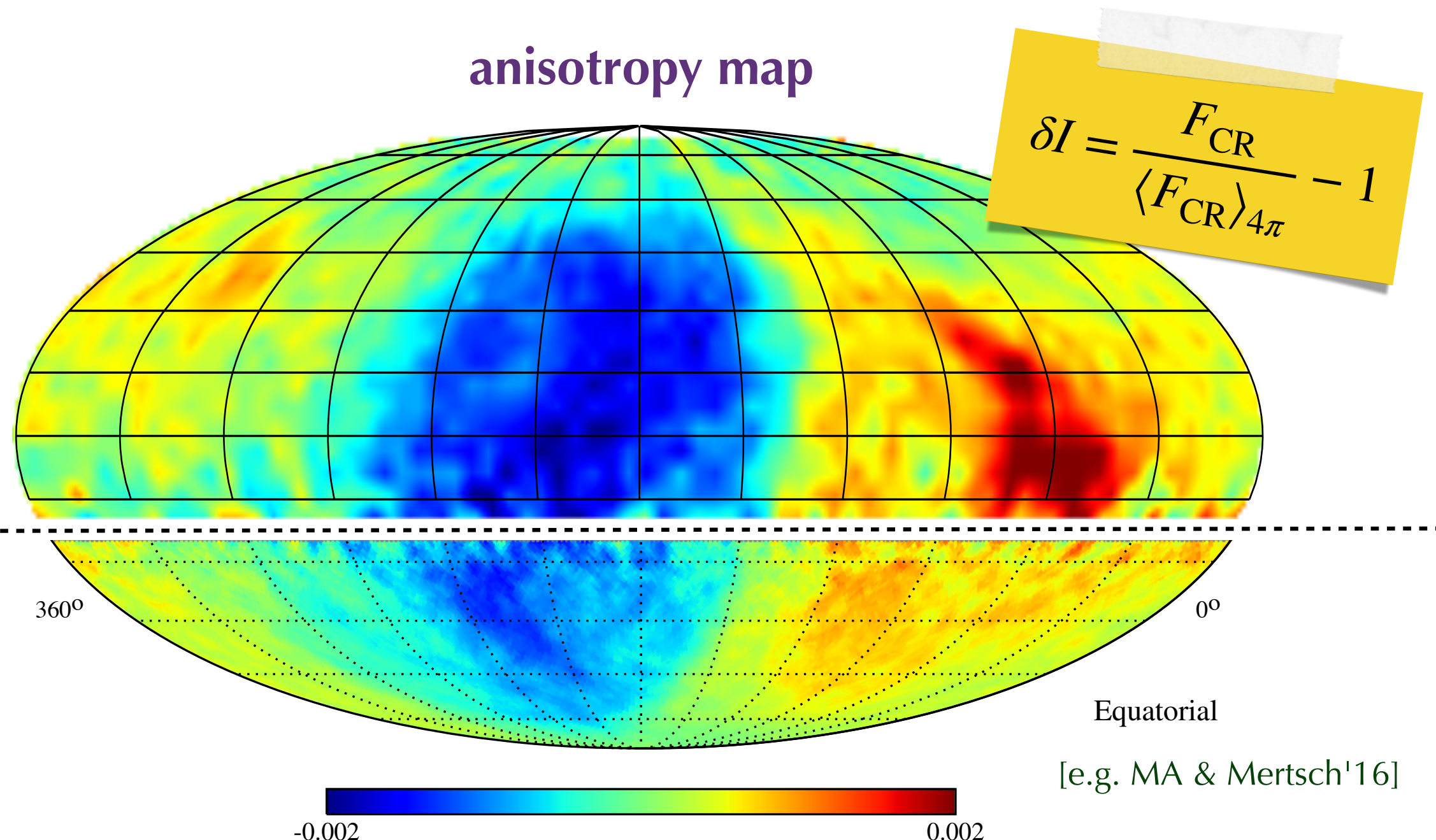
Galactic Cosmic Rays

- *Standard paradigm:*
Galactic CRs accelerated in supernova remnants
- sufficient power: $\sim 10^{-3} M_{\odot}$ per 3 SNe per century
[Baade & Zwicky'34]
- diffusive shock acceleration:
 $n_{\text{CR}} \propto E^{-\Gamma}$
- rigidity-dependent escape from Galaxy:
 $n_{\text{CR}} \propto E^{-\Gamma-\delta}$
- mostly isotropic CR arrival directions



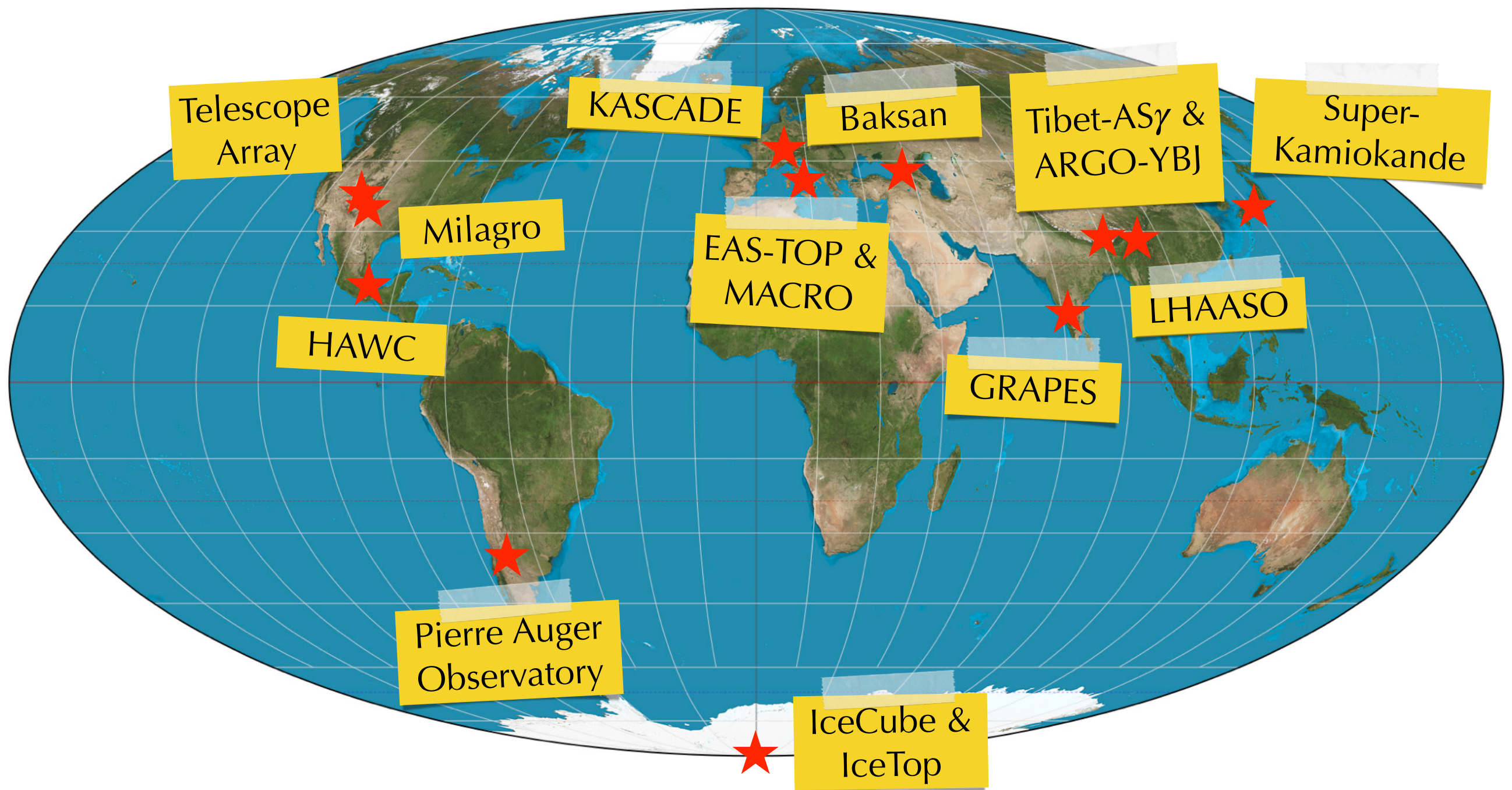
Galactic Cosmic Rays Anisotropy

Cosmic ray anisotropies up to the level of **one-per-mille** at various energies
(Super-Kamiokande, Milagro, ARGO-YBJ, EAS-TOP, Tibet AS γ , IceCube, HAWC)

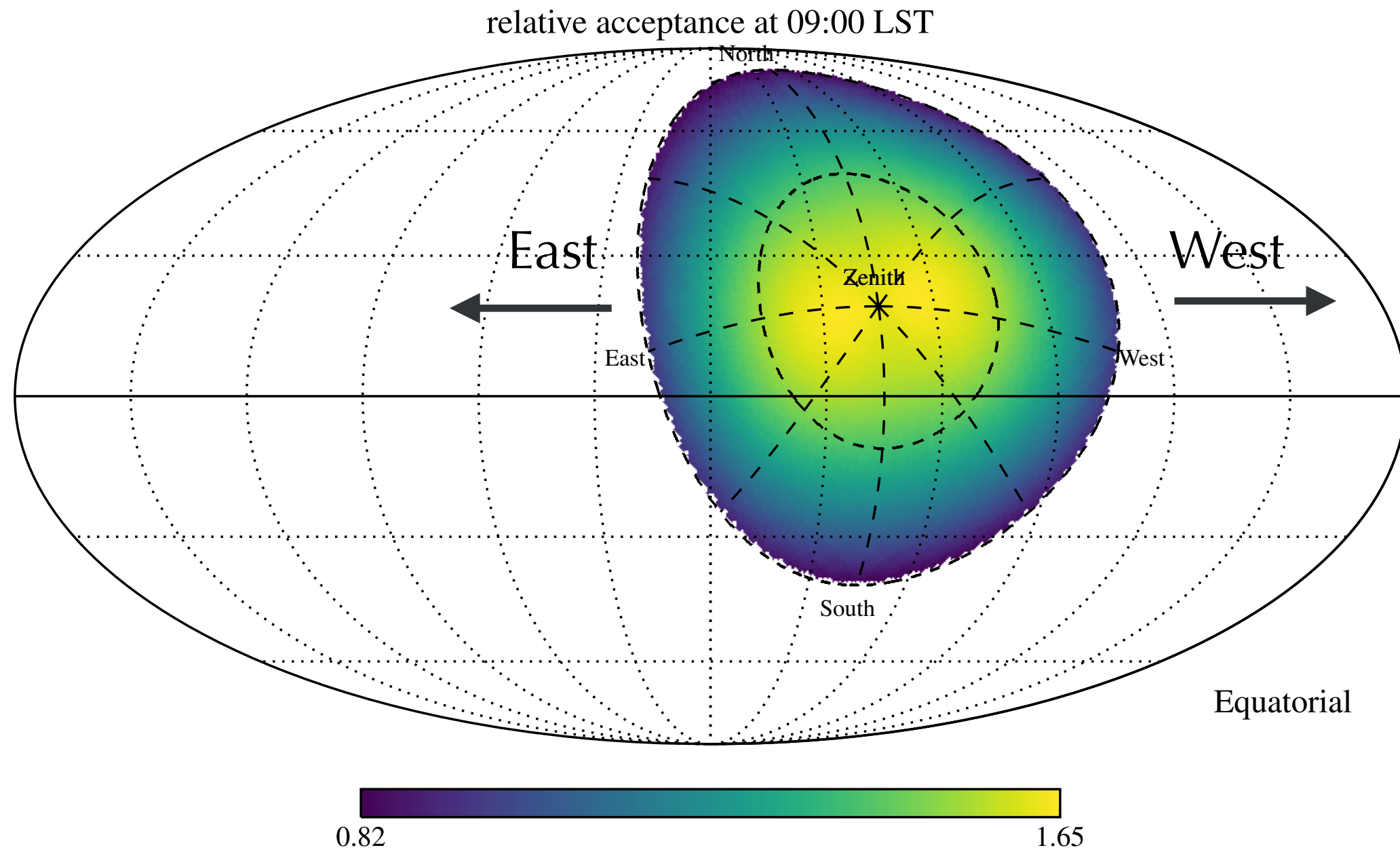


Galactic Cosmic Rays Anisotropy

Cosmic ray anisotropies up to the level of **one-per-mille** at various energies
(Super-Kamiokande, Milagro, ARGO-YBJ, EAS-TOP, Tibet AS γ , IceCube, HAWC)

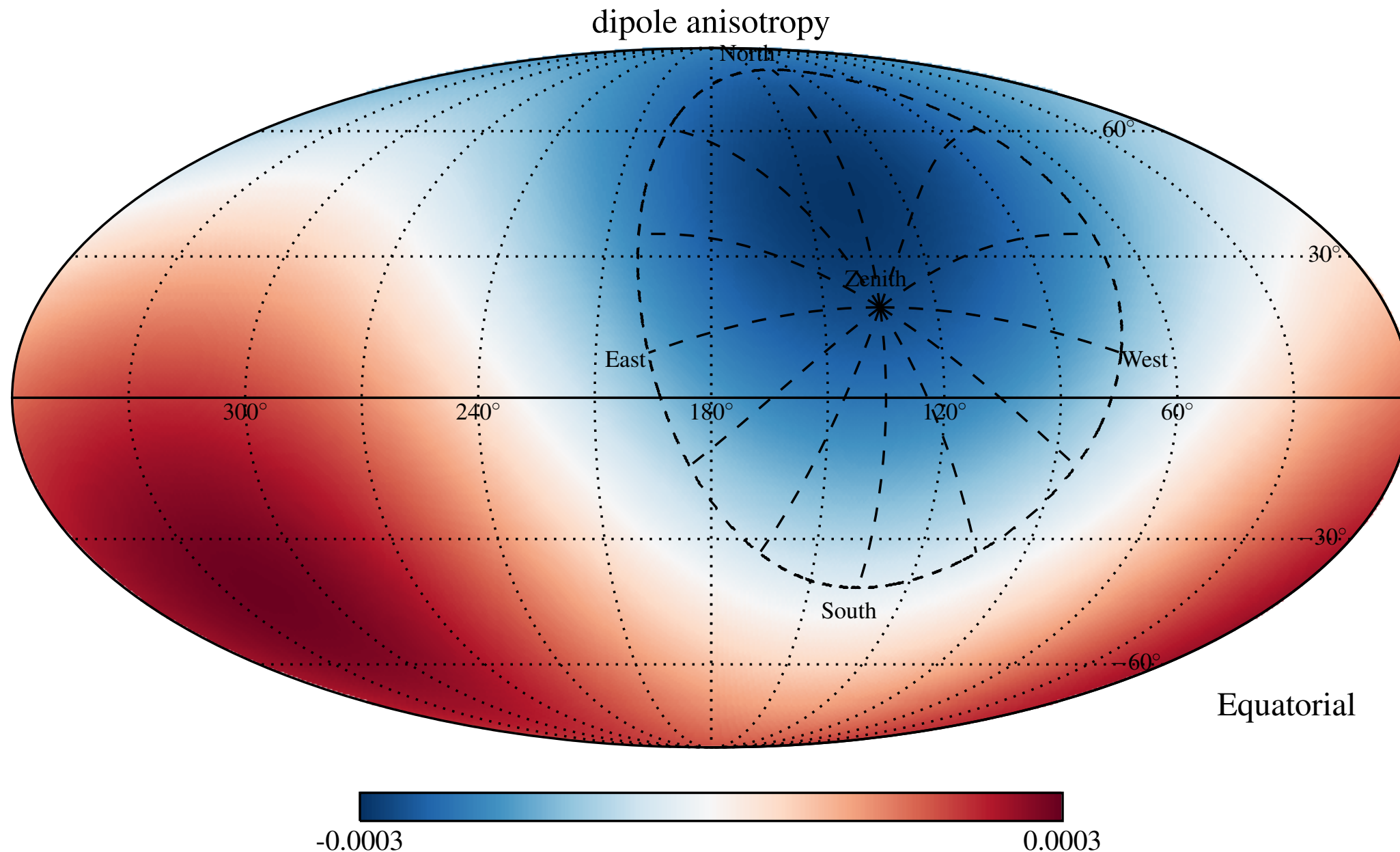


Ground-Based Observations



Field of View (FoV) of ground-based detector (e.g. HAWC at geographic latitude 19°) sweeps across the Sky over 24h.

Issues with Reconstructions

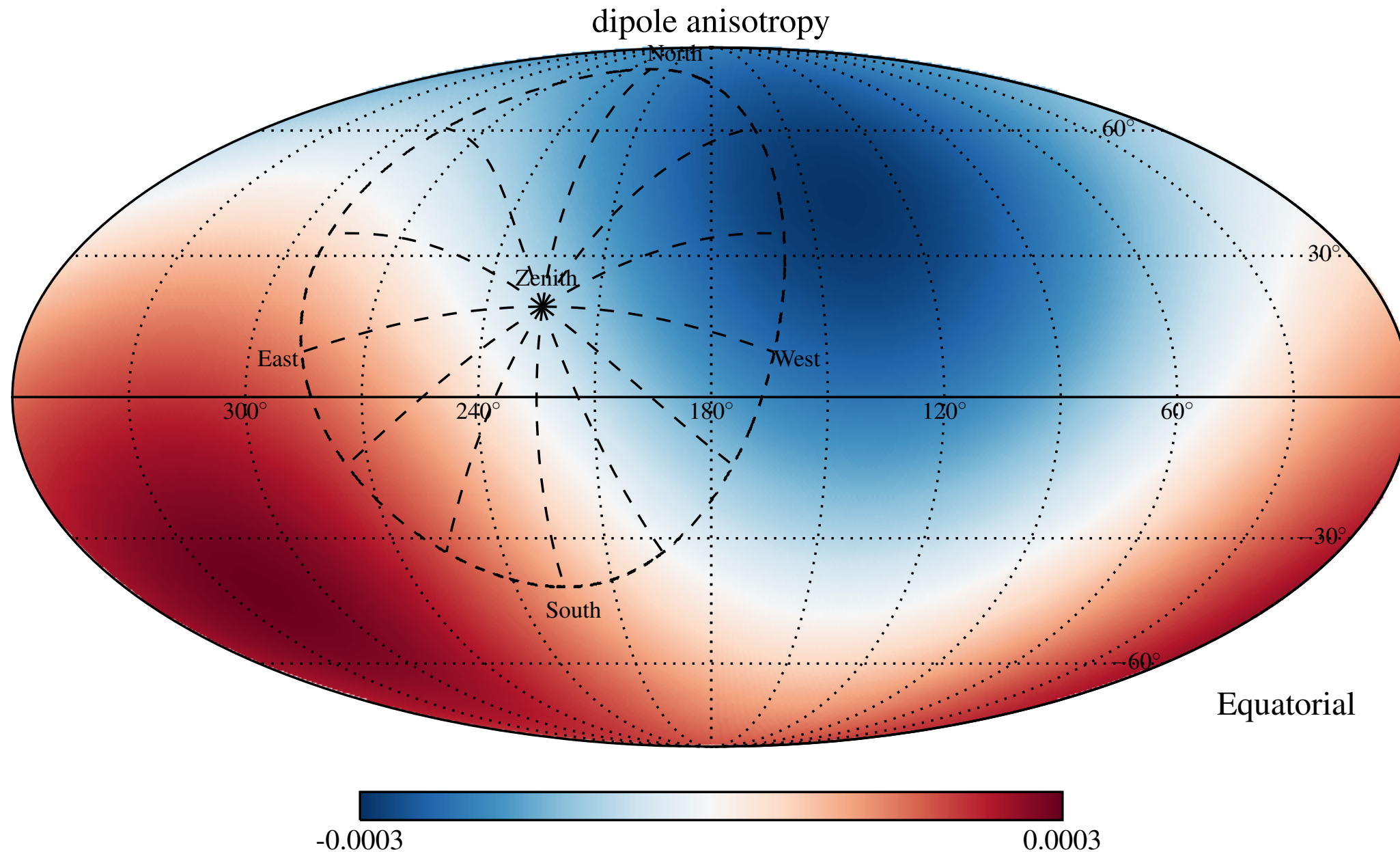


True CR dipole is defined by amplitude A and direction (α, δ) .

Observable dipole is projected onto equatorial plane: $A' = A \cos \delta$

[Iuppa & Di Sciascio'13; MA et al.'15]

Issues with Reconstructions

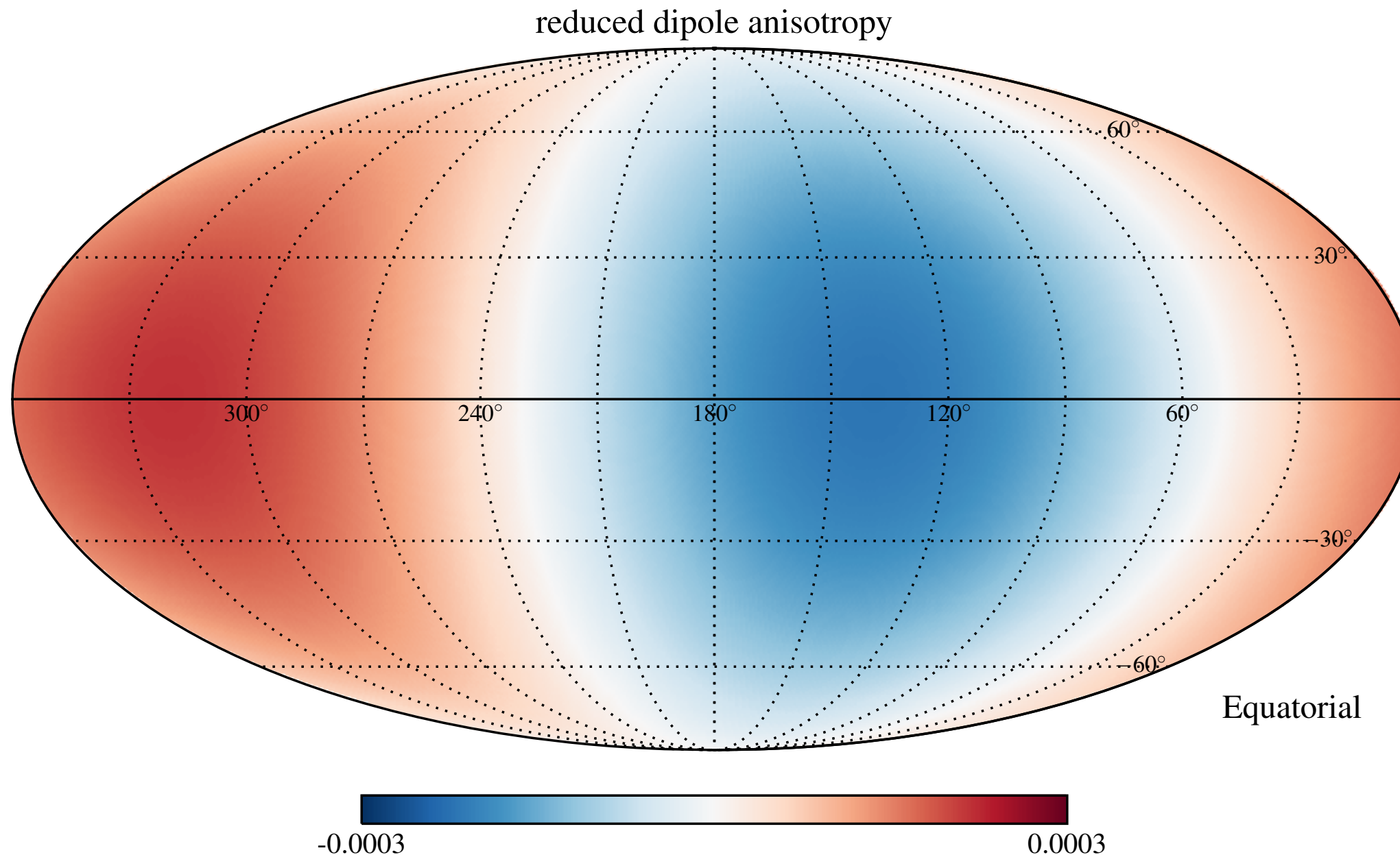


True CR dipole is defined by amplitude A and direction (α, δ) .

Observable dipole is projected onto equatorial plane: $A' = A \cos \delta$

[Iuppa & Di Sciascio'13; MA et al.'15]

Issues with Reconstructions

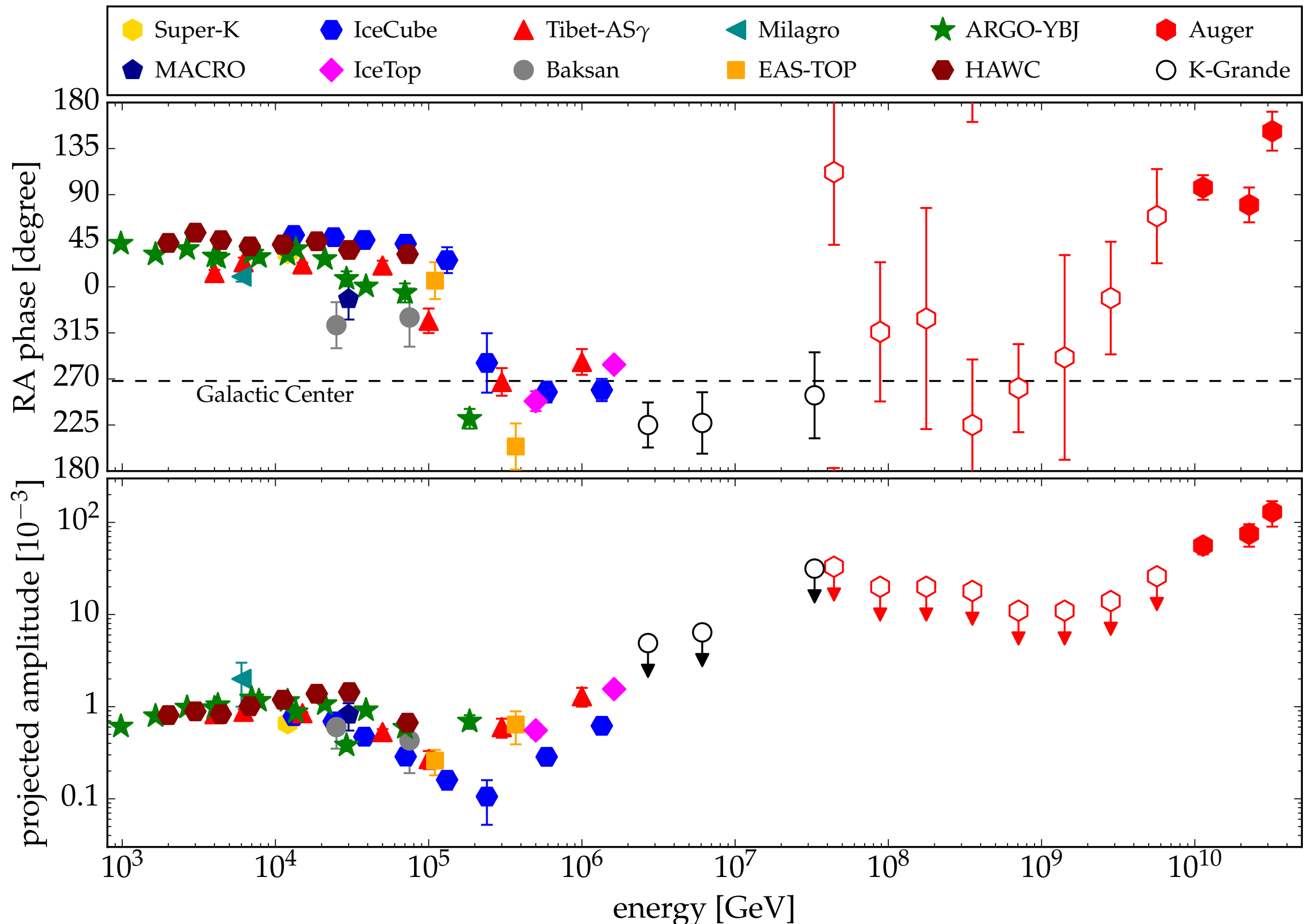


True CR dipole is defined by amplitude A and direction (α, δ) .

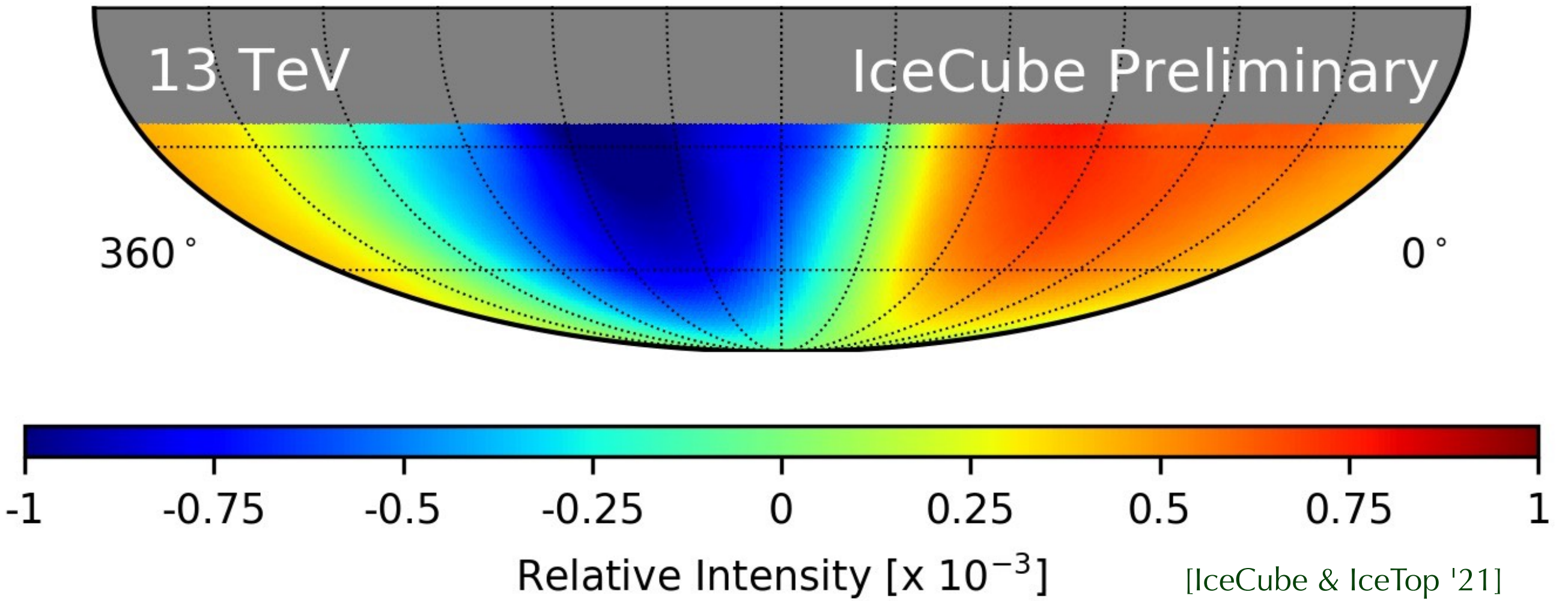
Observable dipole is projected onto equatorial plane: $A' = A \cos \delta$

[Iuppa & Di Sciascio'13; MA et al.'15]

Dipole Anisotropy

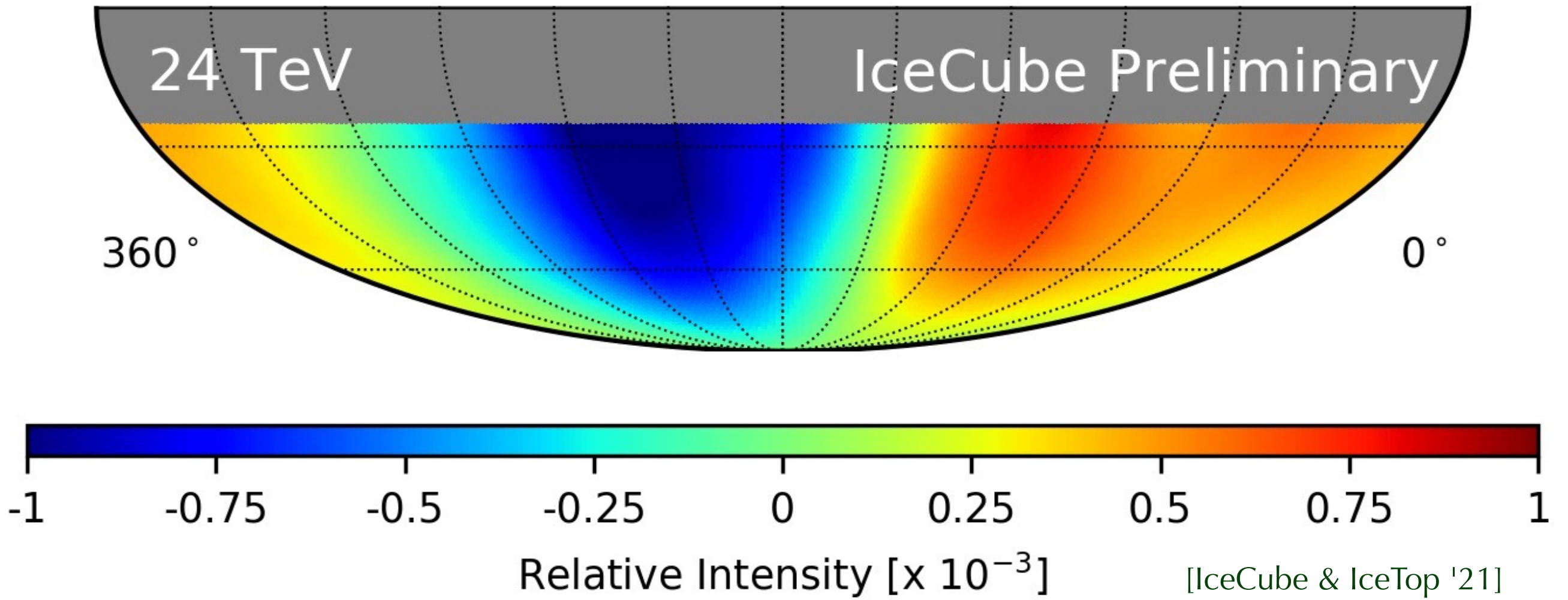


Large-Scale Anisotropy



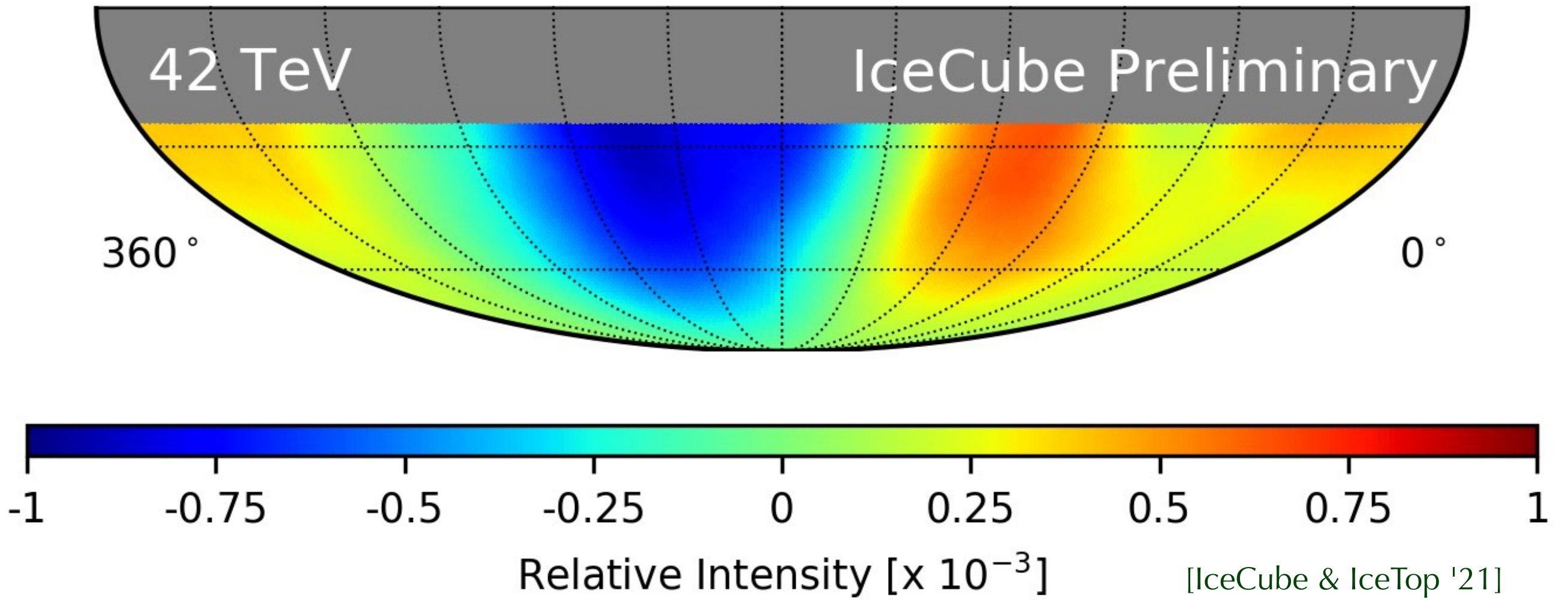
Amplitude of large-scale dipole anisotropy has strong energy dependence with a phase flip around 100 TeV.

Large-Scale Anisotropy



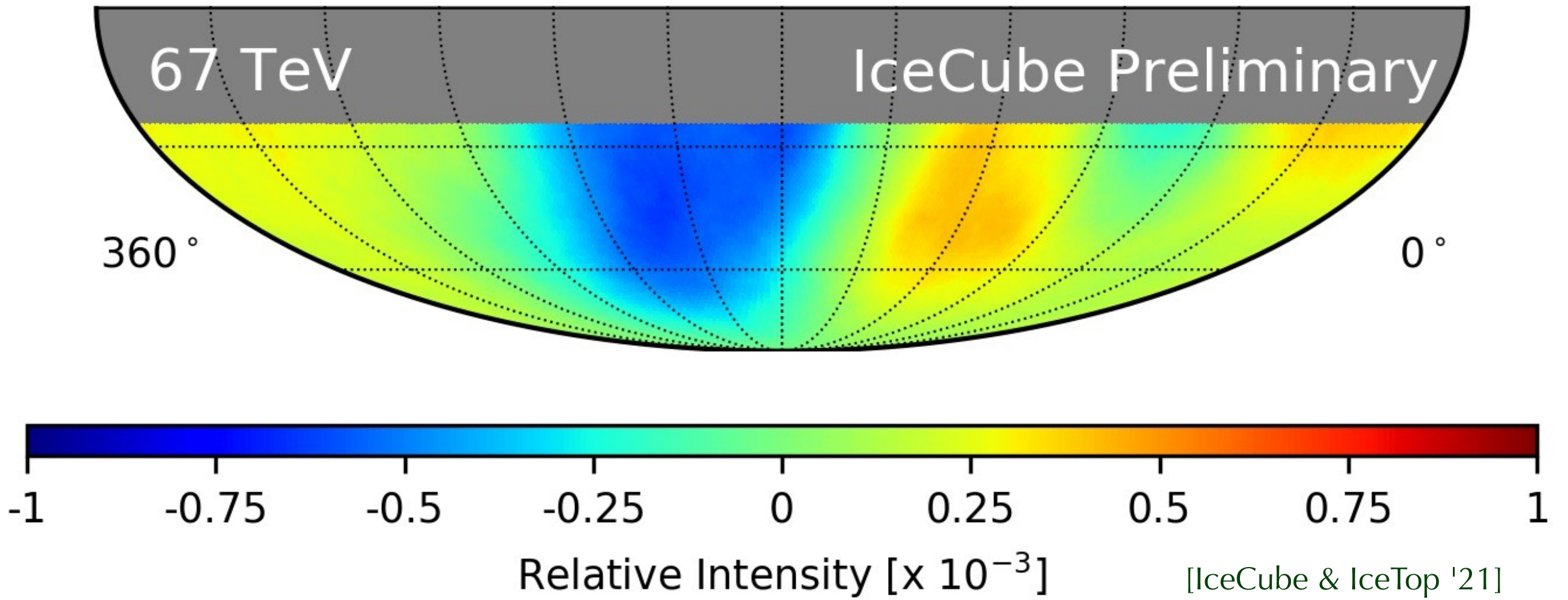
Amplitude of large-scale dipole anisotropy has strong energy dependence with a phase flip around 100 TeV.

Large-Scale Anisotropy



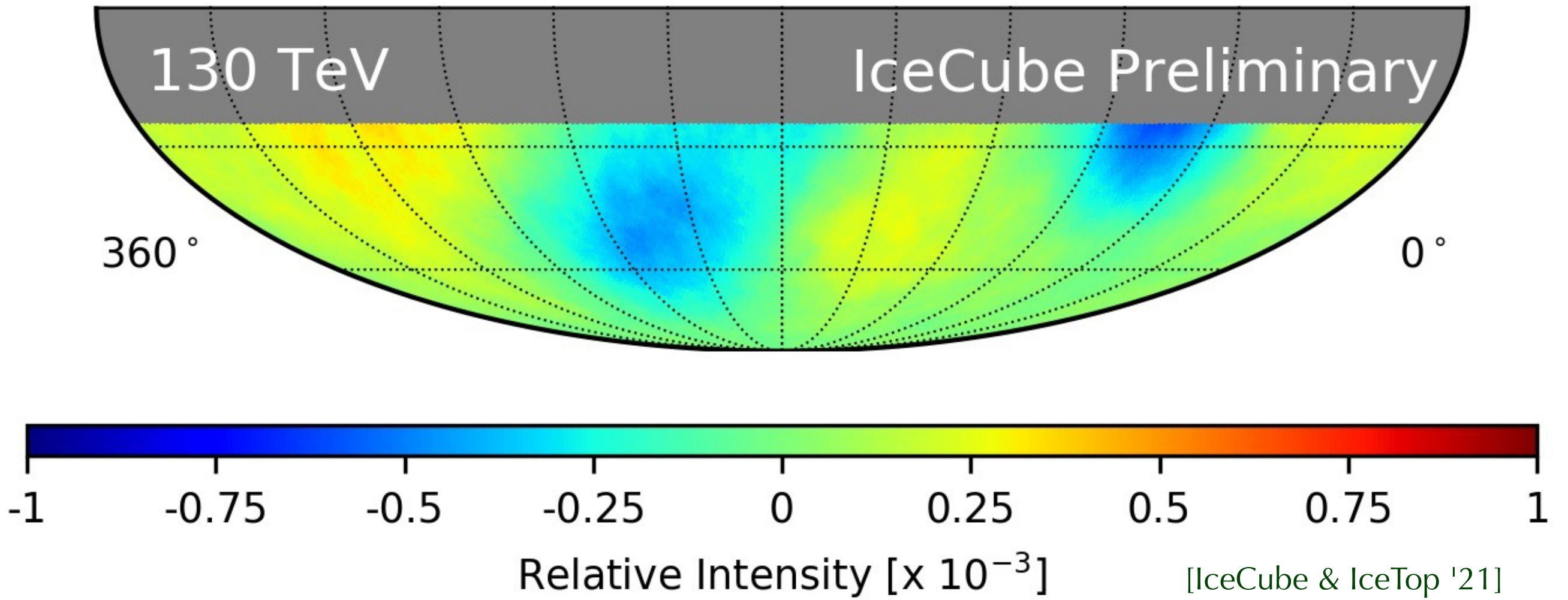
Amplitude of large-scale dipole anisotropy has strong energy dependence with a phase flip around 100 TeV.

Large-Scale Anisotropy



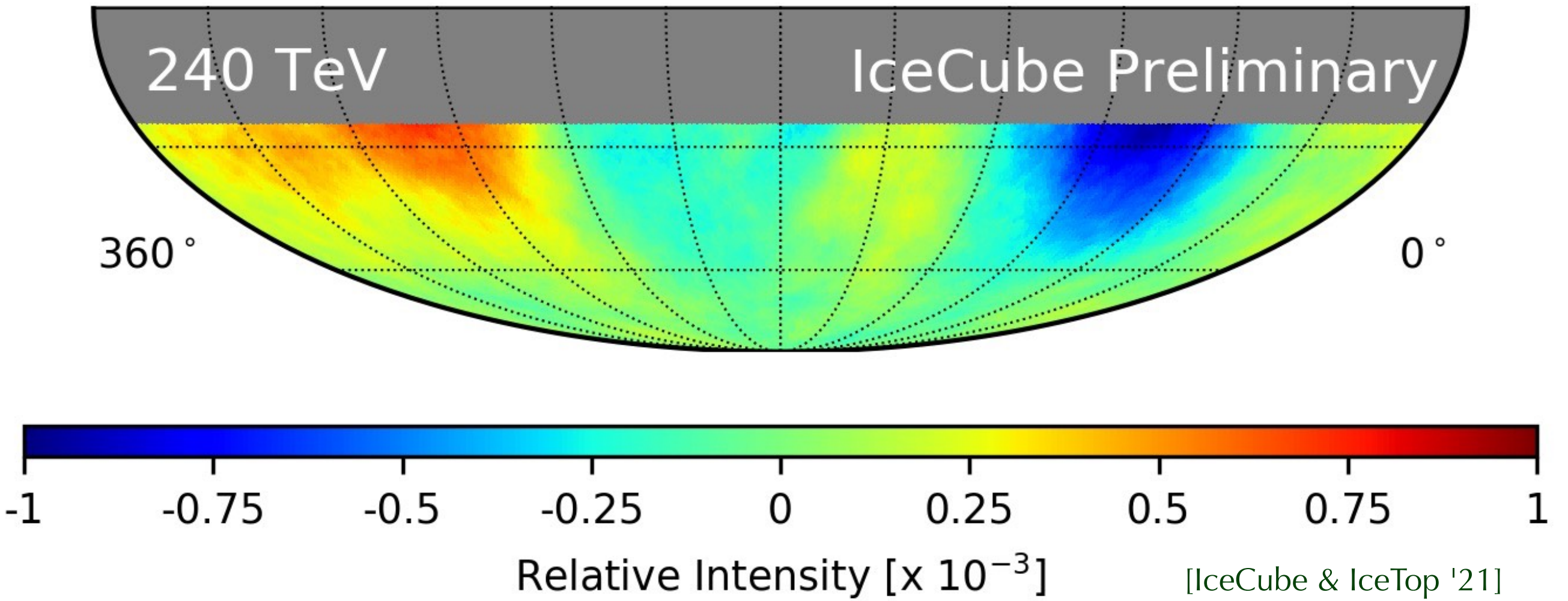
Amplitude of large-scale dipole anisotropy has strong energy dependence with a phase flip around 100 TeV.

Large-Scale Anisotropy



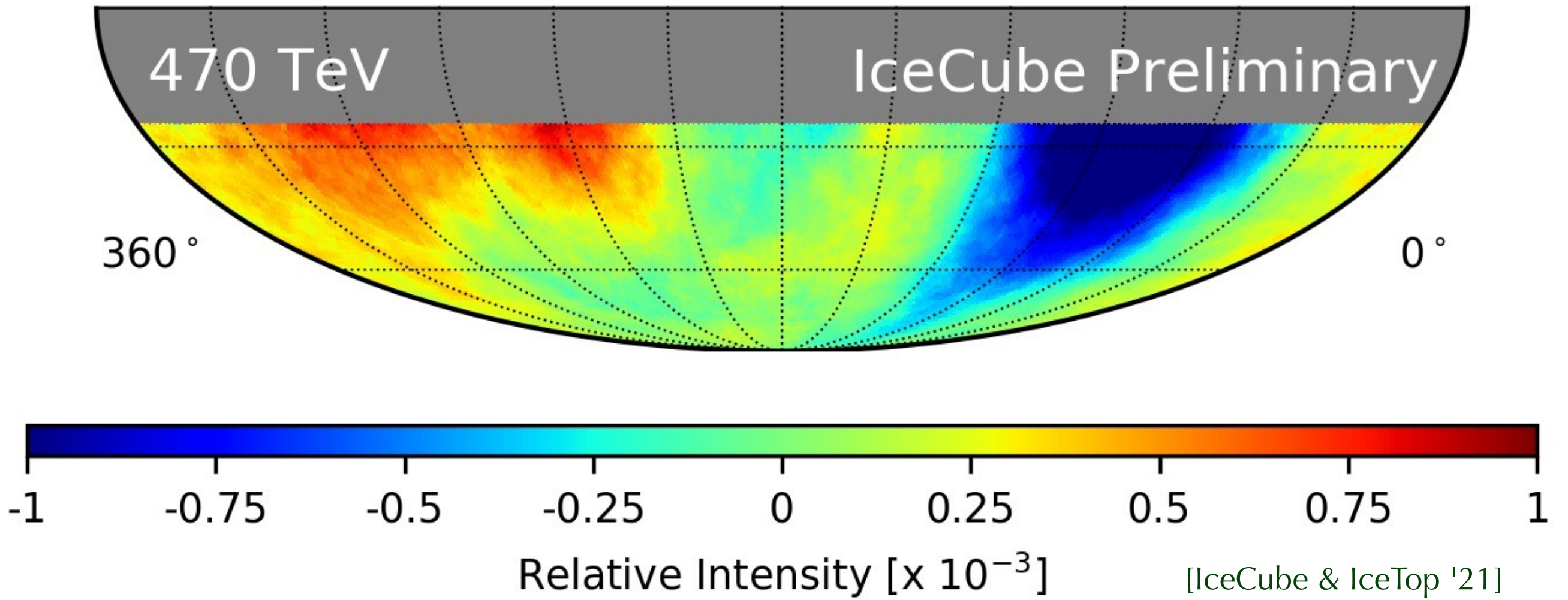
Amplitude of large-scale dipole anisotropy has strong energy dependence with a phase flip around 100 TeV.

Large-Scale Anisotropy



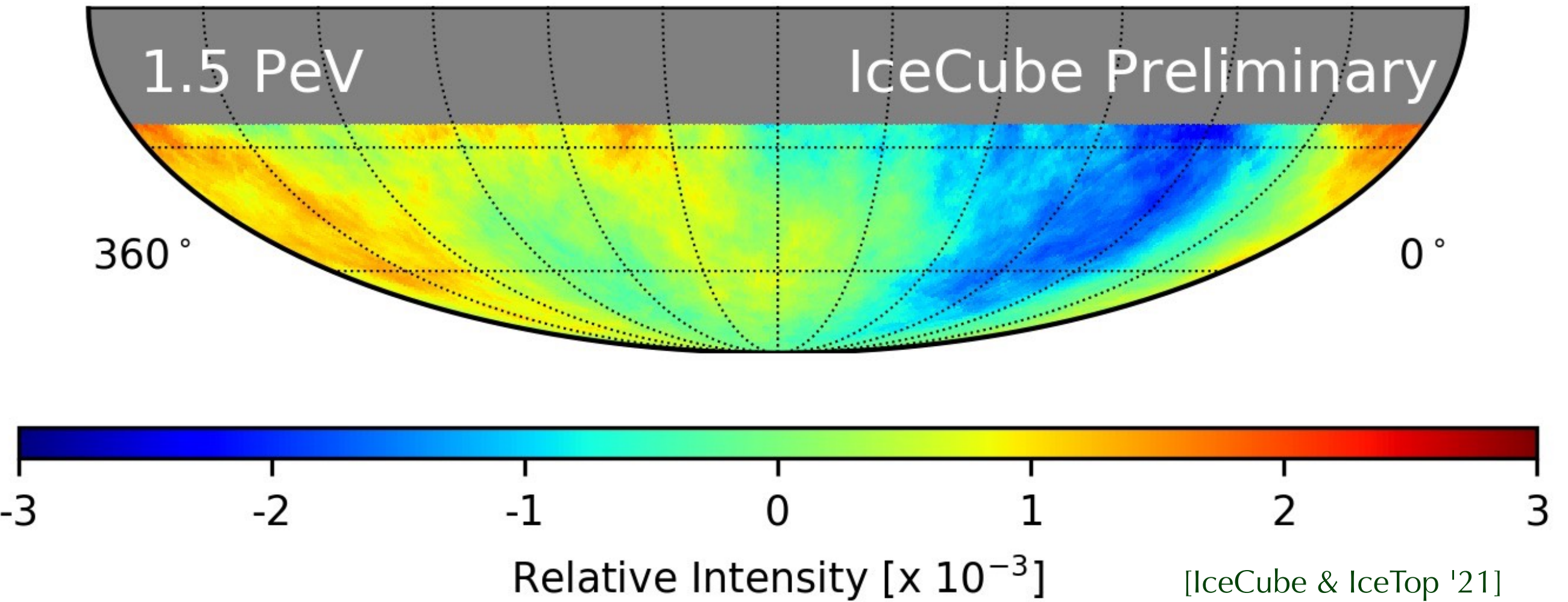
Amplitude of large-scale dipole anisotropy has strong energy dependence with a phase flip around 100 TeV.

Large-Scale Anisotropy



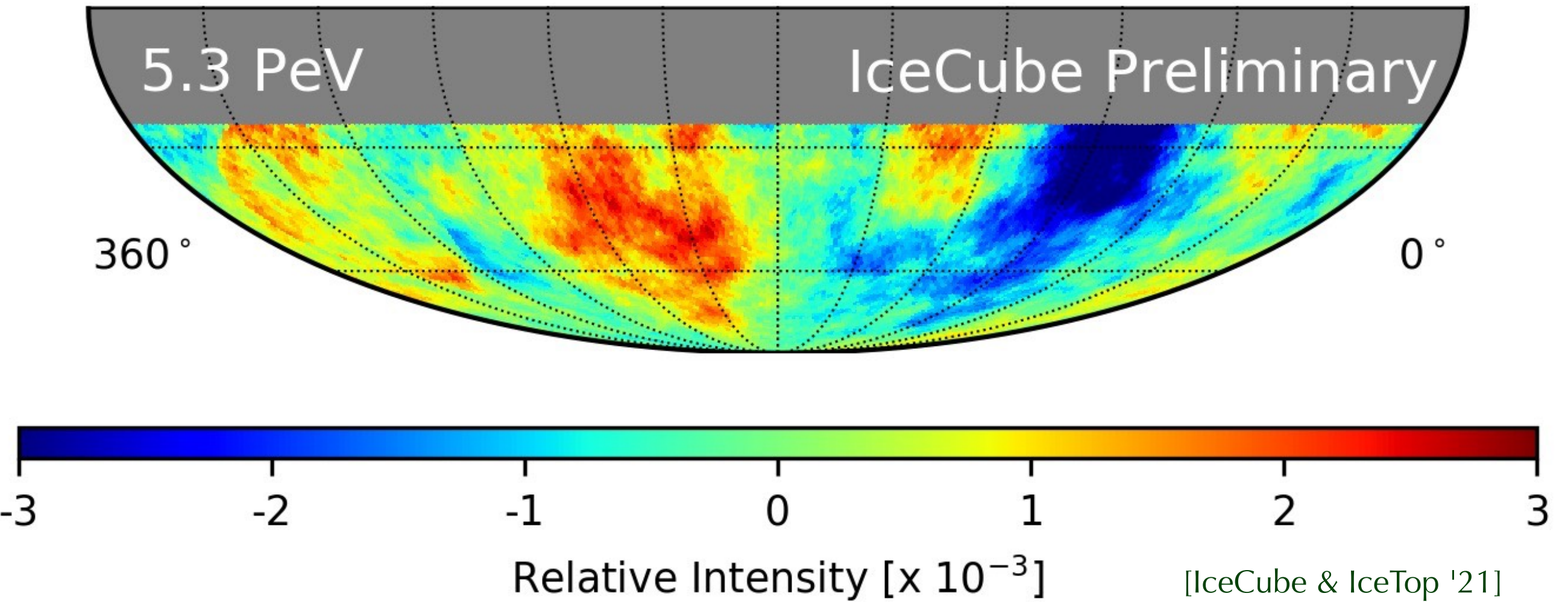
Amplitude of large-scale dipole anisotropy has strong energy dependence with a phase flip around 100 TeV.

Large-Scale Anisotropy



Amplitude of large-scale dipole anisotropy has strong energy dependence with a phase flip around 100 TeV.

Large-Scale Anisotropy



Amplitude of large-scale dipole anisotropy has strong energy dependence with a phase flip around 100 TeV.

Example: Pierre Auger >8 EeV

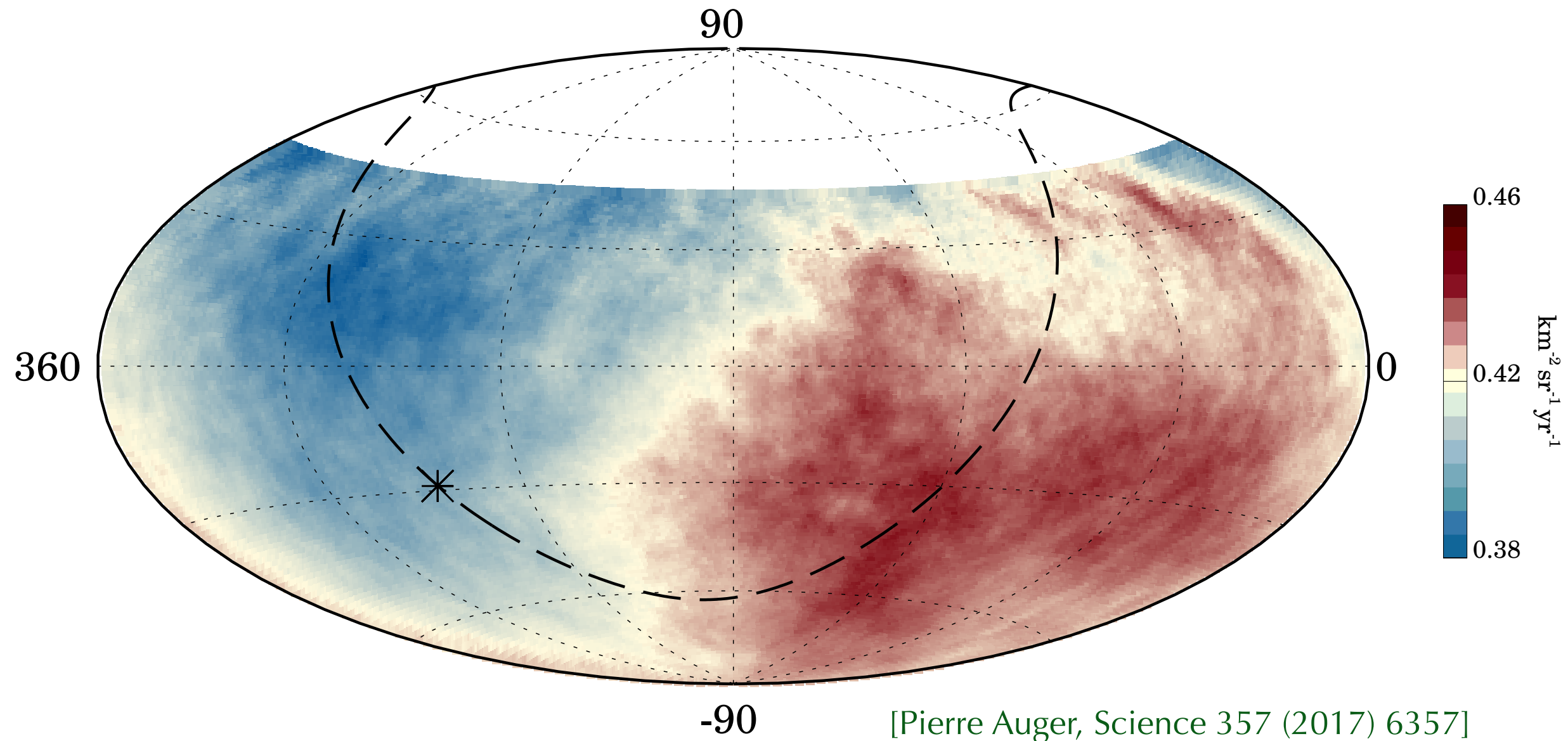
Observation of a large-scale anisotropy in the arrival directions of cosmic rays above 8×10^{18} eV

The Pierre Auger Collaboration*†

Cosmic rays are atomic nuclei arriving from outer space that reach the highest energies observed in nature. Clues to their origin come from studying the distribution of their arrival directions. Using 3×10^4 cosmic rays with energies above 8×10^{18} electron volts, recorded with the Pierre Auger Observatory from a total exposure of $76,800 \text{ km}^2 \text{ sr year}$, we determined the existence of anisotropy in arrival directions. The anisotropy, detected at more than a 5.2σ level of significance, can be described by a dipole with an amplitude of $6.5_{-0.9}^{+1.3}$ percent toward right ascension $\alpha_d = 100 \pm 10$ degrees and declination $\delta_d = -24_{-13}^{+12}$ degrees. That direction indicates an extragalactic origin for these ultrahigh-energy particles.

[Pierre Auger, Science 357 (2017) 6357]

Example: Pierre Auger >8 EeV

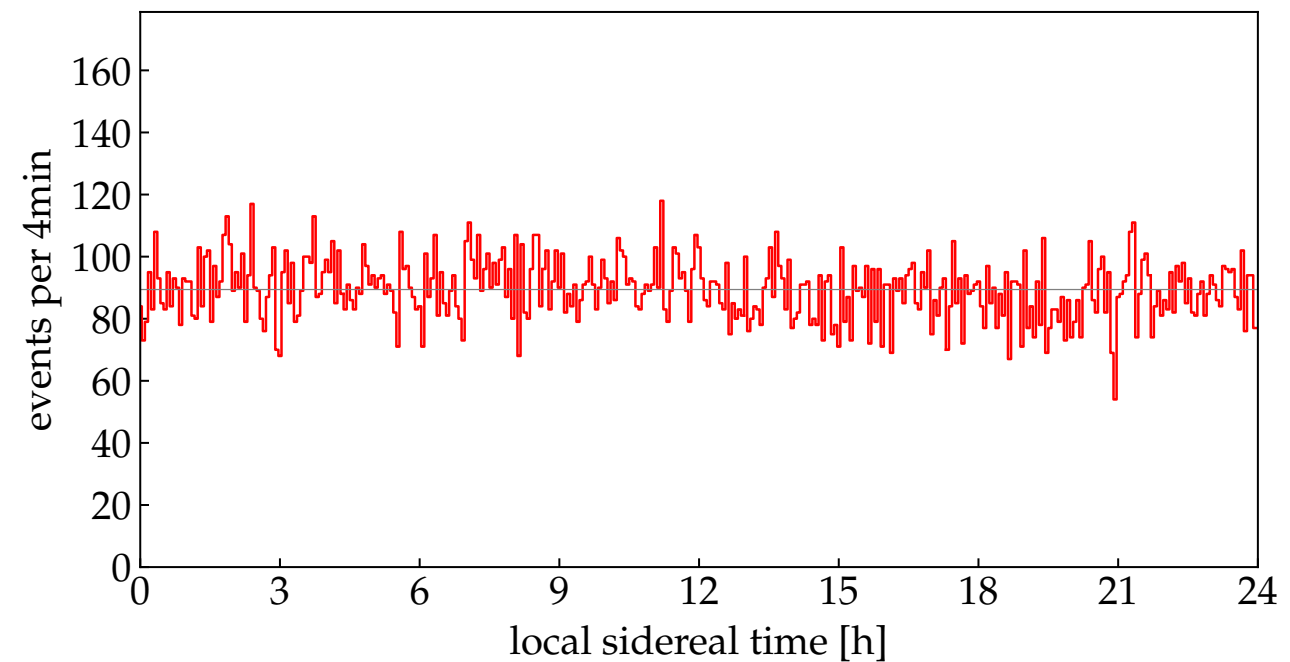
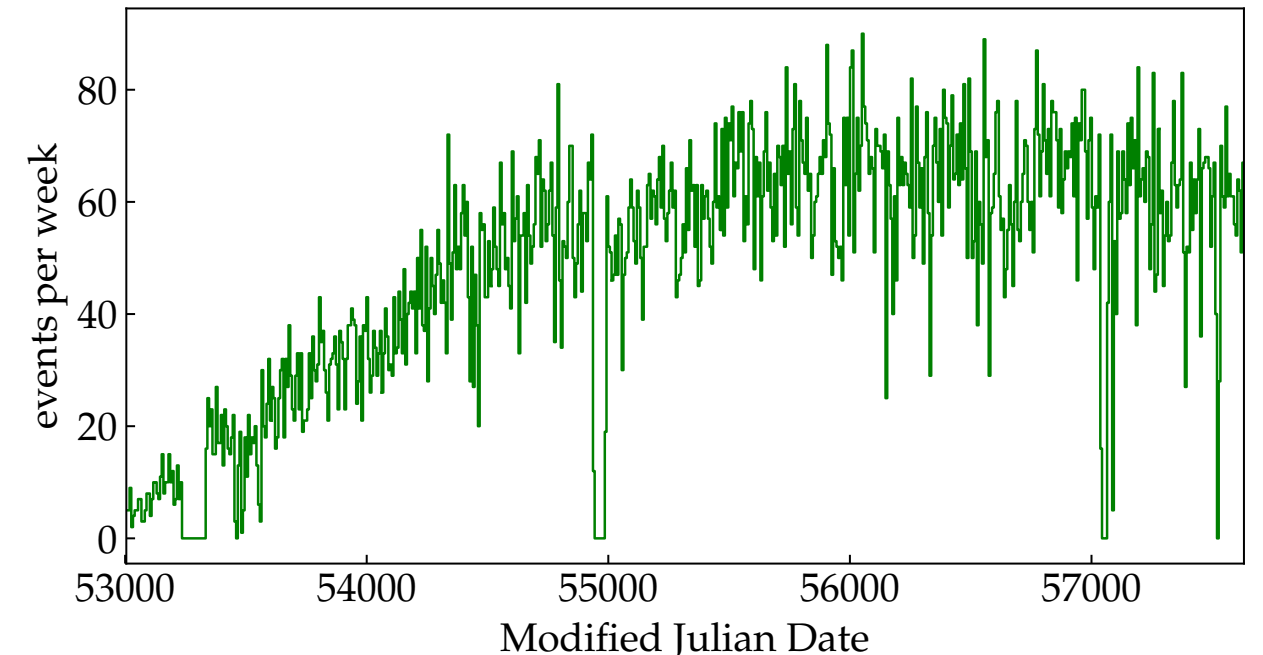


Energy [EeV]	Dipole component d_z	Dipole component d_{\perp}	Dipole amplitude d	Dipole declination δ_d [°]	Dipole right ascension α_d [°]
4 to 8	-0.024 ± 0.009	$0.006^{+0.007}_{-0.003}$	$0.025^{+0.010}_{-0.007}$	-75^{+17}_{-8}	80 ± 60
8	-0.026 ± 0.015	$0.060^{+0.011}_{-0.010}$	$0.065^{+0.013}_{-0.009}$	-24^{+12}_{-13}	100 ± 10

Reconstruction

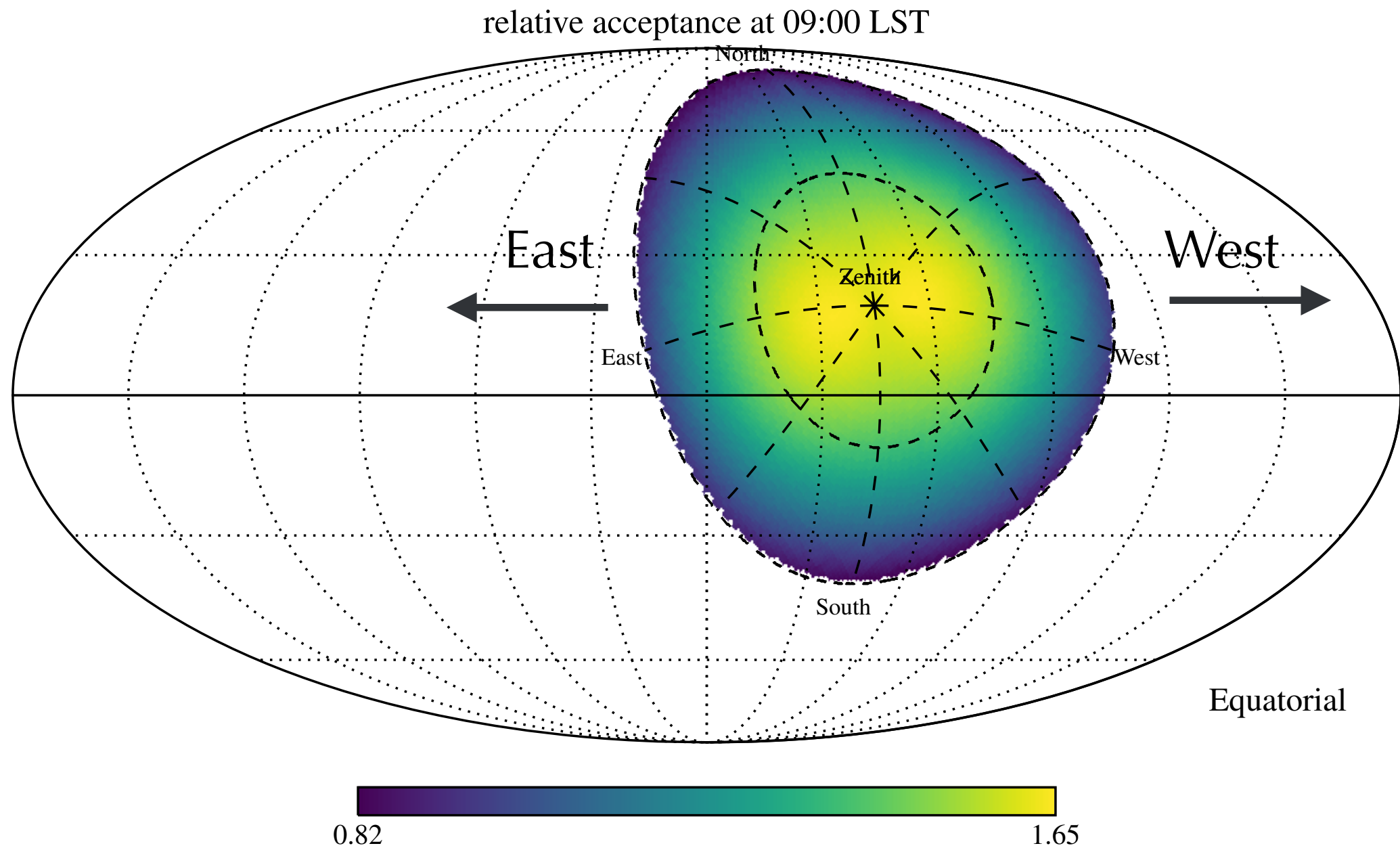
- data has **strong time dependence**
 - detector deployment/maintenance
 - atmospheric conditions (day/night, seasons)
 - power outages, etc.
- **local anisotropy** of detector:
 - non-uniform geometry
- two analysis strategies:
 - **Monte-Carlo & monitoring**
(systematic limited)
 - **data-driven LH methods**
(statistics limited)

Example: Auger data $> 8 \text{ EeV}$



[Pierre Auger Observatory'17; MA'18]

East-West Method



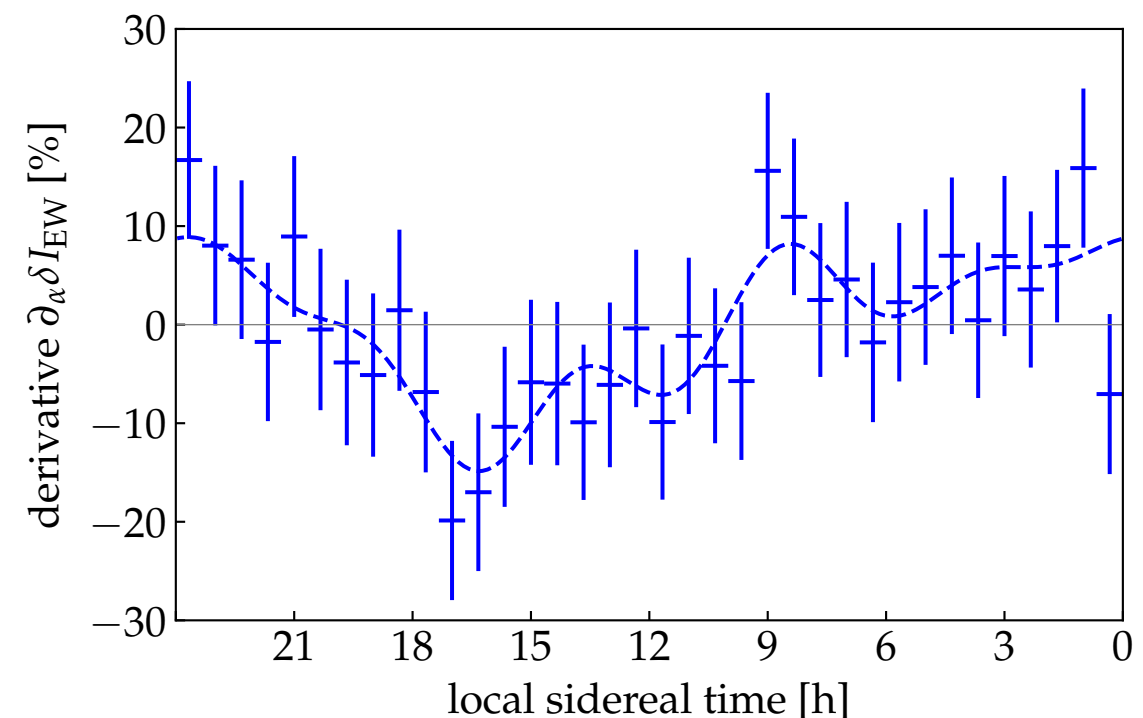
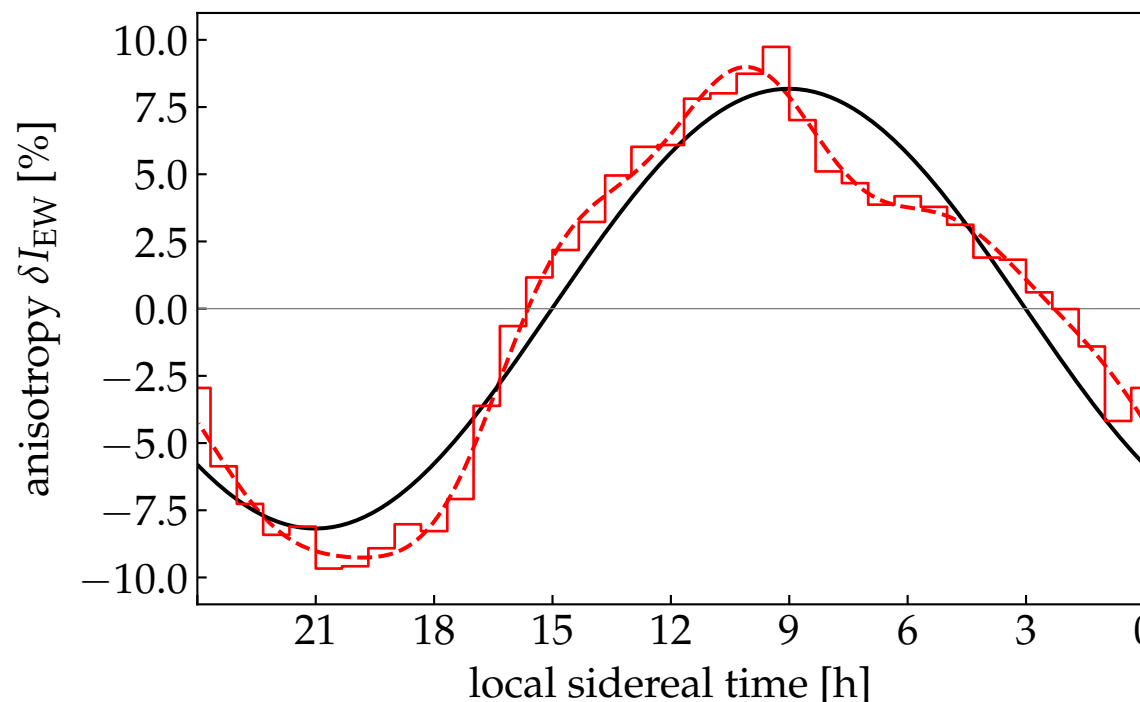
Field of View (FoV) of ground-based detector sweeps across the Sky over 24h (here shown for HAWC detector).

East-West Method

- Strong time variation of CR background level can be compensated by differential methods. [e.g. Bonino *et al.*'11]
- **East-West asymmetry:**

$$A_{\text{EW}}(t) \equiv \frac{N_{\text{E}}(t) - N_{\text{W}}(t)}{N_{\text{E}}(t) + N_{\text{W}}(t)} \simeq \underbrace{\Delta\alpha \frac{\partial}{\partial\alpha} \delta I(\alpha, 0)}_{\text{assuming dipole!}} + \underbrace{\text{const}}_{\text{local asym.}}$$

- For instance, Auger data > 8EeV:



Auger_EastWest_2017.ipynb

Likelihood Reconstruction

- East-West method introduces cross-talk between higher multipoles, regardless of the field of view.
- Alternatively, data can be analyzed to simultaneously reconstruct:
 - **relative acceptance** $\mathcal{A}(\varphi, \theta)$ (in local coordinates)
 - **relative intensity** $\mathcal{I}(\alpha, \delta)$ (in equatorial coordinates)
 - **background rate** $\mathcal{N}(t)$ (in sidereal time)
- expected number of CRs in sidereal time bin τ and local "pixel" i :

$$\mu_{\tau i} = \mu(\mathcal{I}_{\tau i}, \mathcal{N}_\tau, \mathcal{A}_i)$$

- reconstruction **likelihood**:

$$\mathcal{L}(\mathbf{n} | \mathcal{I}, \mathcal{N}, \mathcal{A}) = \prod_{\tau i} \frac{1}{n_{\tau i}!} (\mu_{\tau i})^{n_{\tau i}} e^{-\mu_{\tau i}}$$

- Maximum LH can be reconstructed by iterative methods.

[MA et al.'15]

Iterative Method

- Expected number of events:

$$\mu_{\tau i} = \mathcal{J}_{\tau i} \mathcal{N}_\tau \mathcal{A}_i$$

- Maximum LH values can be solved implicitly:

[MA et al.'15]

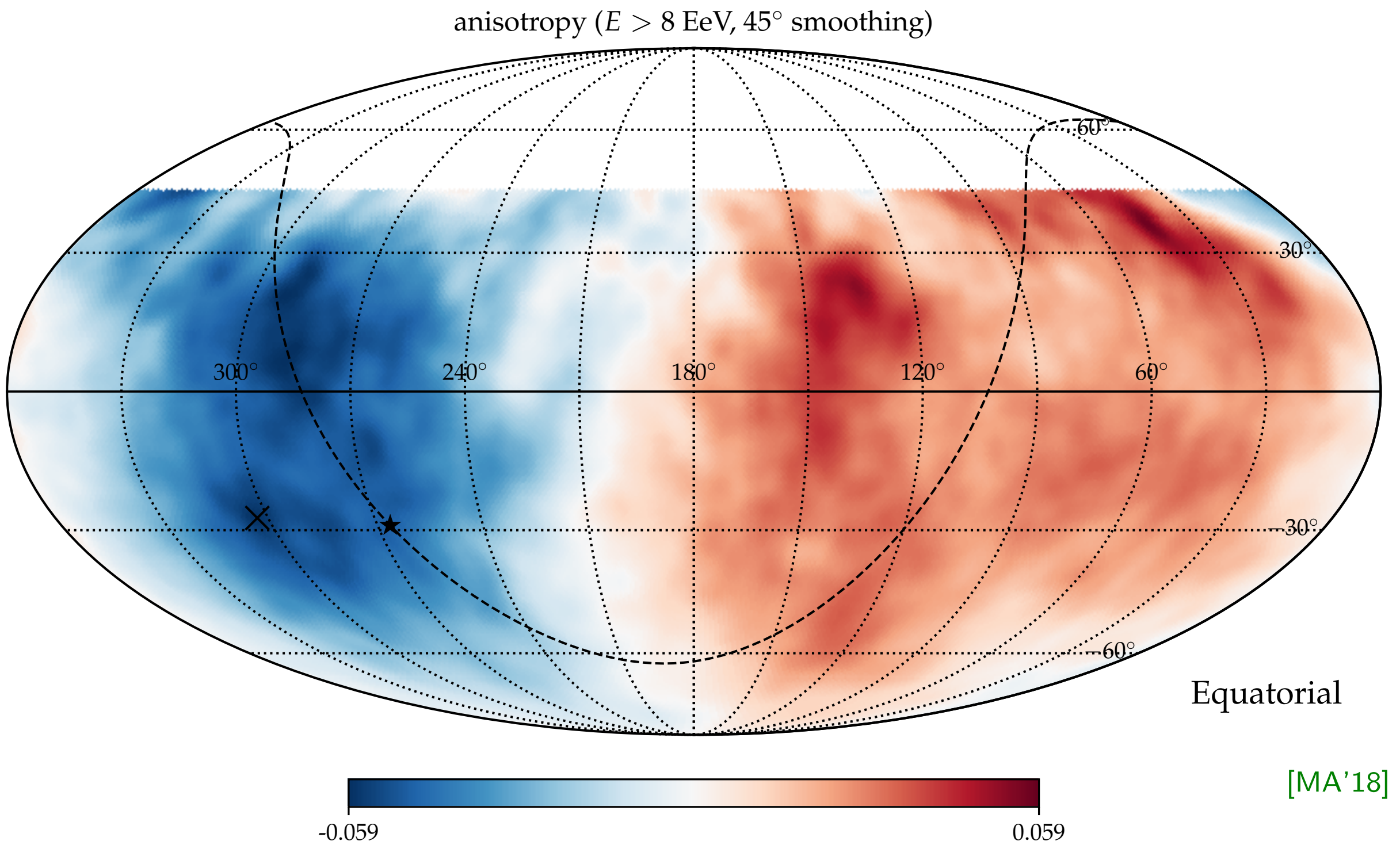
(a) $\hat{I}_\alpha = \sum_\tau n_{\tau\alpha} / \sum_\kappa \hat{\mathcal{A}}_{\kappa\alpha} \hat{\mathcal{N}}_\kappa$ (α : pixel EQ map)

(b) $\hat{\mathcal{N}}_\tau = \sum_i n_{\tau i} / \sum_j \hat{\mathcal{A}}_j \hat{I}_{\tau j}$ (τ : sidereal bin)

(c) $\hat{\mathcal{A}}_i = \sum_\tau n_{\tau i} / \sum_\kappa \hat{\mathcal{N}}_\kappa \hat{I}_{\kappa i}$ (i : pixel in local map)

- Start from $\hat{I}_\alpha = \text{const}$ and progressively iterate steps (a), (b) & (c).

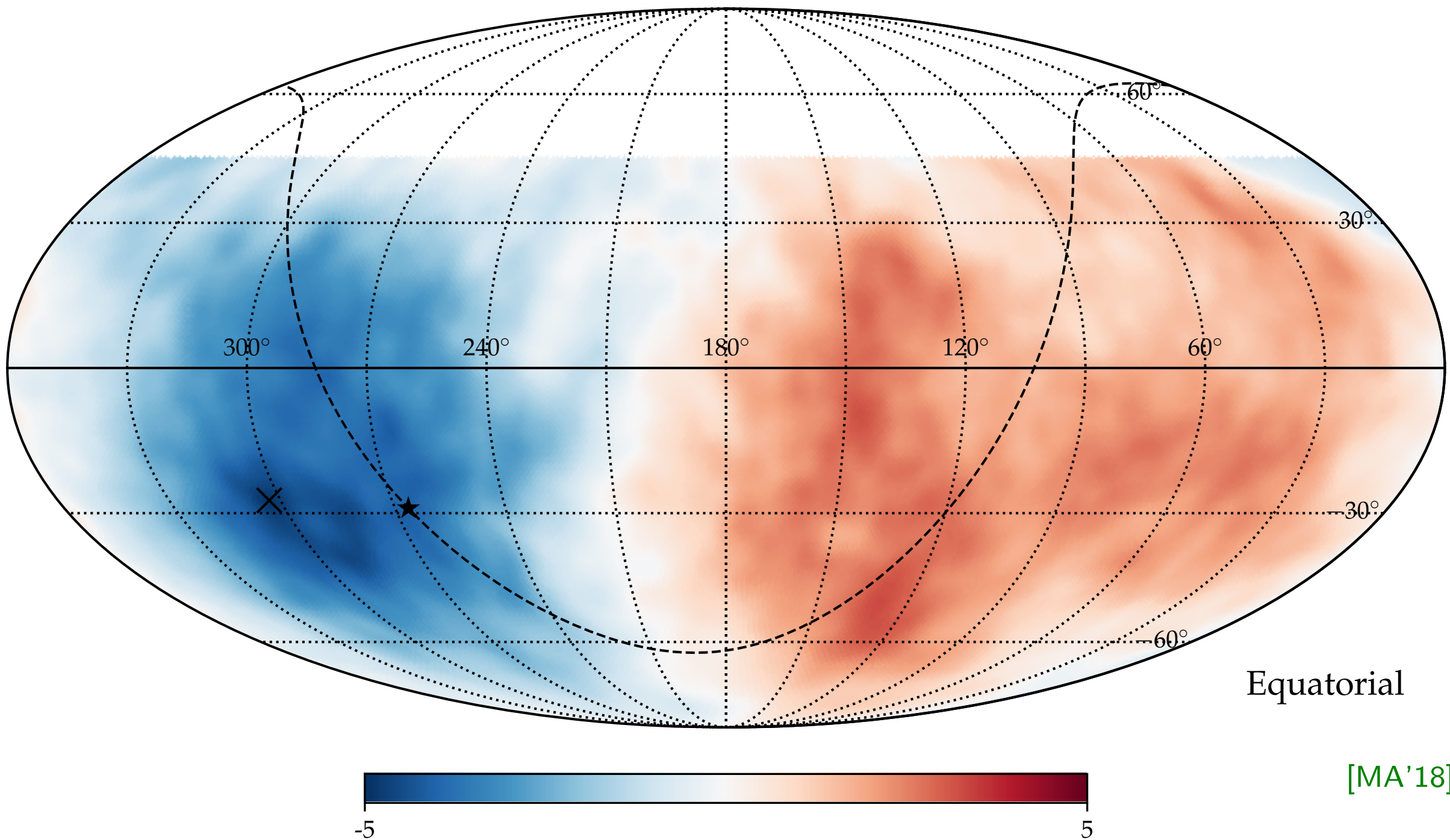
Likelihood Reconstruction



Auger_anisotropy_2017.ipynb

Likelihood Reconstruction

pre-trial significance ($E > 8$ EeV, 45° smoothing, $\sigma_{\max} = 4.86$)

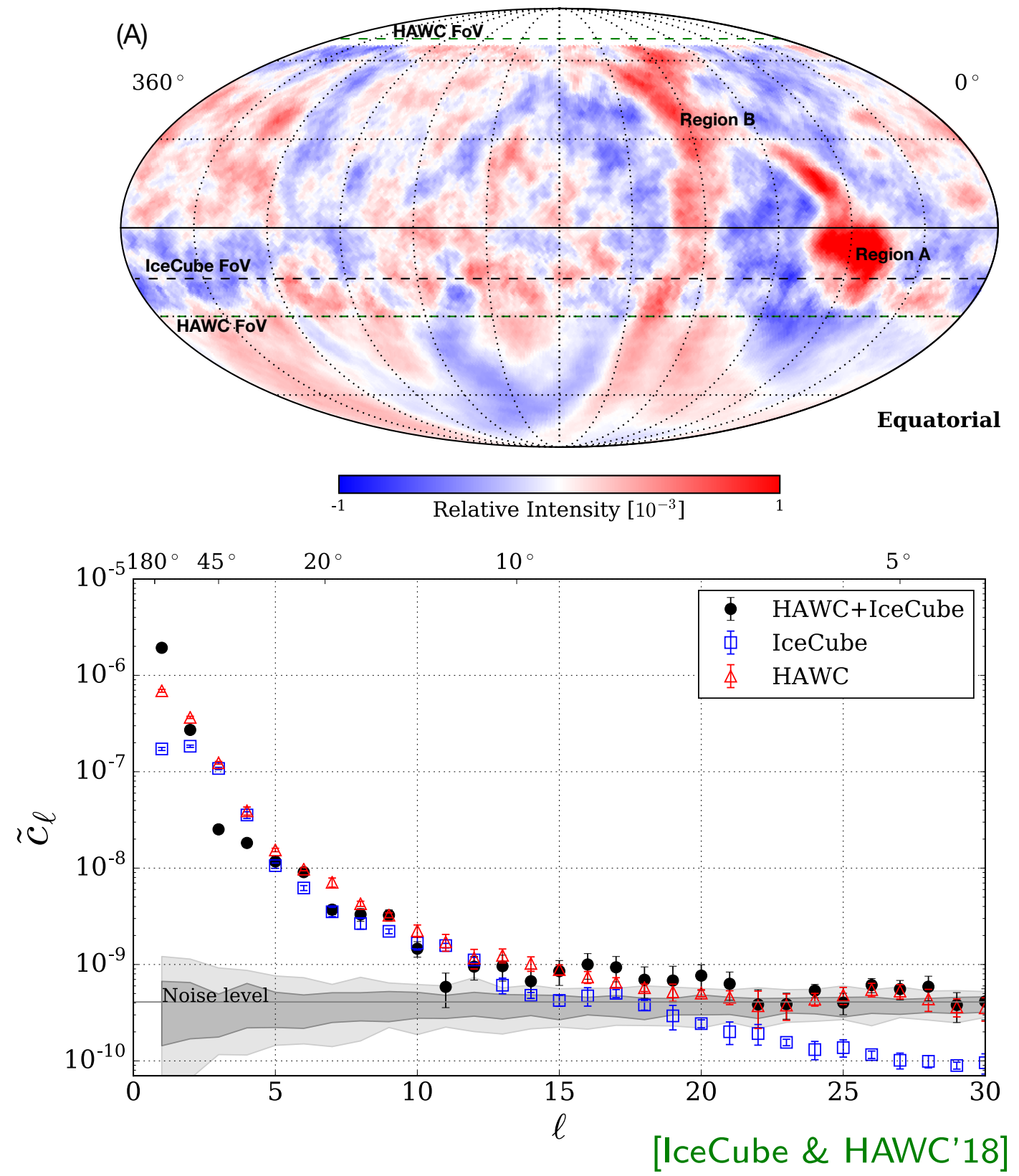


Auger_anisotropy_2017.ipynb

Small-Scale Anisotropy

- Significant TeV small-scale anisotropies down to angular scales of $\mathcal{O}(10^\circ)$.
- Strong local excess (*region A*) observed by Northern observatories.
[*Tibet-AS γ '06; Milagro'08]
[*ARGO-YBJ'13; HAWC'14*]*
- Angular power spectra of IceCube and HAWC data show excess compared to isotropic arrival directions. [*IC'11; HAWC'14*]

$$C_\ell = \frac{1}{2\ell + 1} \sum_{m=-\ell}^{\ell} |a_{\ell m}|^2$$



[IceCube & HAWC'18]